Supporting Information

1. Materials and methods for synthesis

The new compounds were fully characterized by NMR (^{1}H, ^{13}C), including the ^{1}H-^{13}C correlation spectra (HMQC and HMBC) using DMSO-d_6 as solvent, FT-IR, HR-mass and elemental analysis. Melting points were also determined. The NMR spectra were performed at room temperature on a Bruker Avance 3400 (^{1}H: 400 MHz, ^{13}C: 100 MHz). The data are reported by chemical shifts (ppm), multiplicity (s - singlet, brs - broad singlet, d - doublet, t - triplet, dd - doublet of doublets or m - multiplet), and the coupling constants (*J*) in hertz (Hz). IR spectra were recorded on a Spectrum Two FT-IR Spectrometer from PerkinElmer. The spectra were recorded at room temperature in the range of 4000-450 cm^{-1}, at the resolution of 8 cm^{-1}. The melting points were determined on a Stuart SMP3 melting 2 point apparatus. Elemental analyses were performed on a LECO CHNS-932 instrument (University of Minho). The halochromic properties of compounds were assessed by UV-Vis spectra recorded on the SHIMADZU UV-2501PC apparatus, using 1 cm wide quartz cells.

All commercial reagents were used without further purification. The reagents and solvents were purchased from Acros Organics, Sigma Aldrich, Chemlab, Fisher, Panreac, TCI and VWR chemicals BDH. Specifically, diaminomaleonitrile (DAMN), dimethylamine, 1,4-dioxane, triethyl orthoformate (TEOF), 1,8-diazabicyclo[5.4.0]undec-7-ene (DBU), trifluoroacetic acid (TFA) and triethylamine (Et_3N) were obtained from Acros Organics; acetonitrile, diatomaceus earth, *p*-fluoroaniline, *p*-chloroaniline, *m*-chloroaniline, *p*-bromoaniline, *m*-bromoaniline, *p*-toluidine or *p*-anisidine or aniline, anilinium chloride were acquired from Sigma Aldrich; acetic acid from Chemlab; piperidine from Riedel-de Haen; phenylhydrazine from Fisher; Diethyl ether, *n*-hexane, silica gel 60 were purchased from Panreac, deuterated DMSO from TCI and absolute ethanol from VWR chemicals BDH. Silica gel flash chromatography was achieved using silica gel 60 (0.015-0.040 mm) for column chromatography from Millipore. The reactions were monitored by thin layer chromatography (TLC) using Macherey-Nagel™ aluminum sheets UV254 that were observed directly and by UV light.

The synthetic precursors, 5-amino-4-(cyanoformimidoyl)-1*H*-imidazoles, were obtained in-house by a well-known method in a three step reaction (**SI Scheme 1**) starting from the following commercial reagents: DAMN, TEOF and a primary amine (*p*-fluoroaniline, *p*-chloroaniline, *m*-chloroaniline, *p*-bromoaniline, *m*-bromoaniline, *p*-toluidine or *p*-anisidine or aniline).[1] Then, the 5-aminoimidazole-4-carboxamidrazones **1** were prepared by the reaction of 5-amino-4-(cyanoformimidoyl)-1*H*-imidazoles with phenylhydrazine, accordingly to a previous method developed by the research group.[2] Compounds **1** were used as precursors to obtain the novel azoimidazoles **5**.

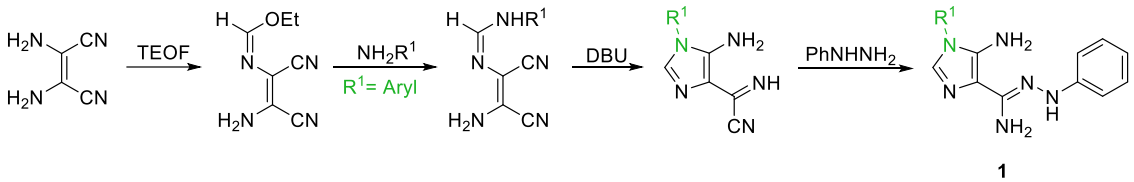

SI Scheme 1 – General procedure for the synthesis of amidrazone precursors **1**.

2. Colorimetric properties

Azoimidazoles **5** here described exhibit a vibrant green colour, so it was important to study their colorimetric properties through UV-Vis spectroscopy.

2.1. Solvatochromism

UV-Vis spectra of all the compounds of this new class of azoimidazoles were traced in the region of visible light (350 - 700 nm) in different solvents (ethanol, acetonitrile and 1,4-dioxane) (**SI-Figures 1 – 9**). The goal of this study was to understand how both solvent and structure influenced the absorption spectra. Maxima absorption wavelengths (λ_{max}) and molar absorption coefficients (ε) were determined in the same region (**SI-Table 1**). The Beer-Lambert Law (Equation 1) was used to determine the molar absorption coefficient (ε; M^{-1} cm^{-1}), considering "c" the concentration of the solution (M), "l" the cell width (cm) and "A" the absorbance.

$$A = \epsilon l c \qquad \text{Equation 1}$$

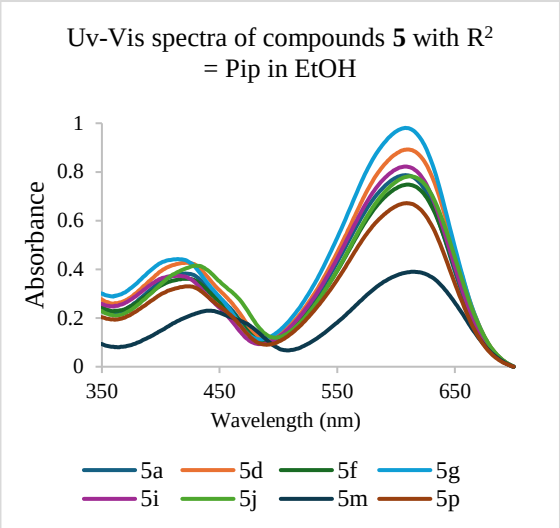

SI-Figure 1 - UV-Vis spectra of compounds **5** with R^2 = Pip in ethanol. The concentration for all compounds is 3.33 x 10^{-5} M.

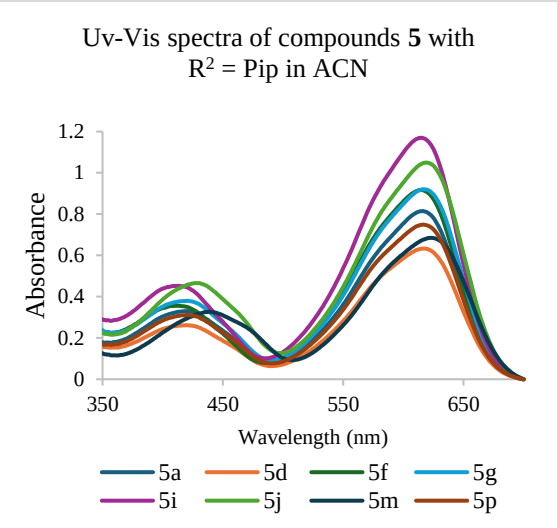

SI-Figure 2 - UV-Vis spectra of compounds **5** with R^2 = Pip in acetonitrile. The concentration for all compounds is 3.33 x 10^{-5} M.

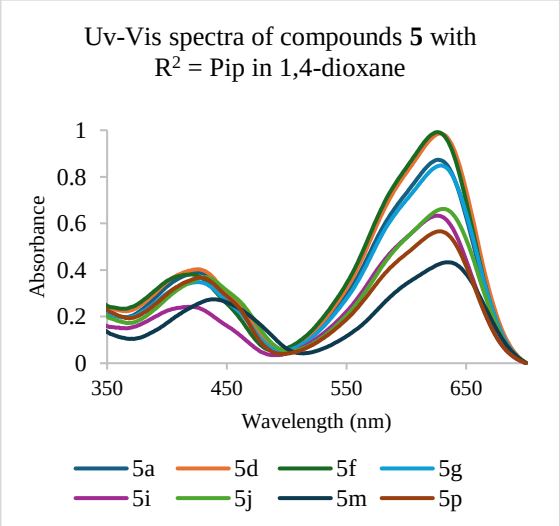

SI-Figure 3 - UV-Vis spectra of compounds **5** with R^2 = Pip in 1,4-dioxane. The concentration for all compounds is 3.33 x 10^{-5} M.

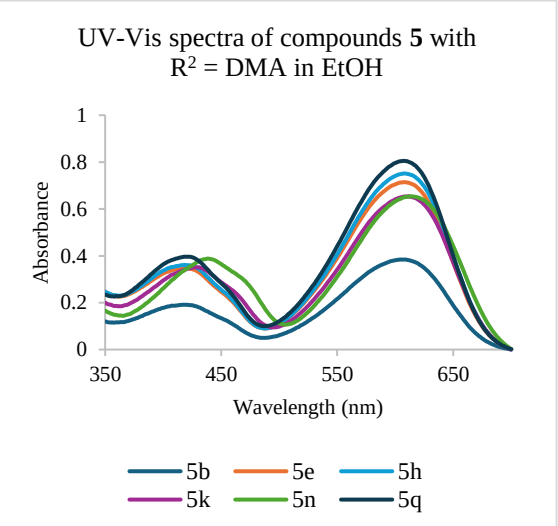

SI-Figure 4 - UV-Vis spectra of compounds **5** with R^2 = DMA in ethanol. The concentration for all compounds is 3.33 x 10^{-5} M.

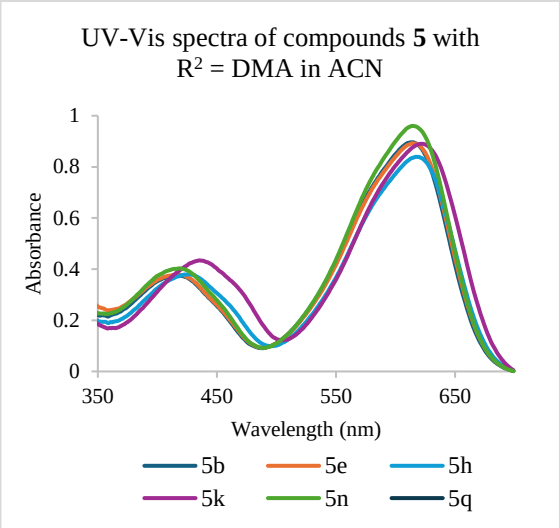

SI-Figure 5 - UV-Vis spectra of compounds **5** with R^2 = DMA in acetonitrile. The concentration for all compounds is 3.33 x 10^{-5} M.

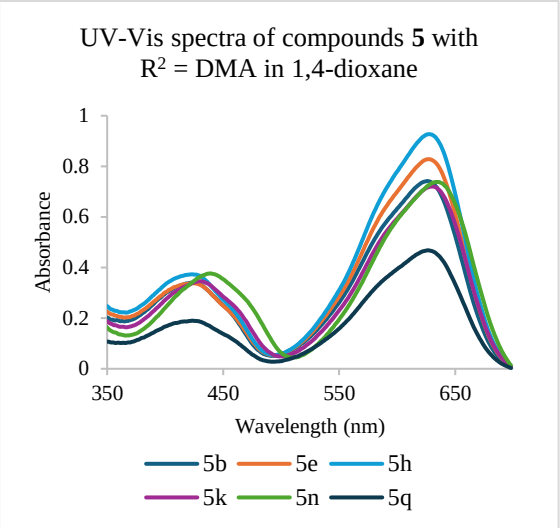

SI-Figure 6 - UV-Vis spectra of compounds **5** with R^2 = DMA in 1,4-dioxane. The concentration for compounds **5a**, **5d**, **5f** and **5g** is 3.33 x 10^{-5} M, and for **5b** and **5h** it is 1.67 x 10^{-5} M.

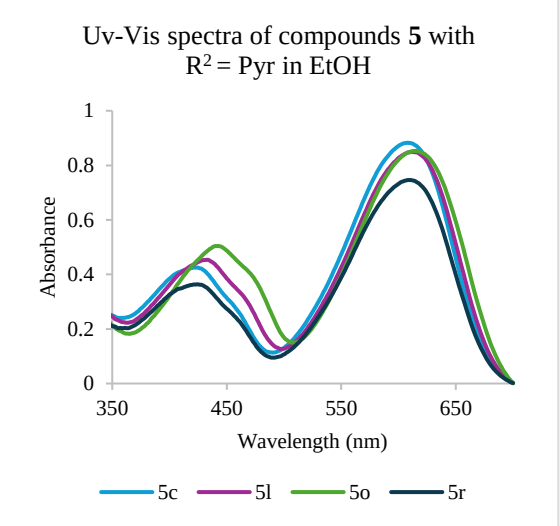

SI-Figure 7 - UV-Vis spectra of compounds **5** with R^2 = Pyr in ethanol. The concentration for compounds **5a** and **5h** is 3.33 x 10^{-5} M, and for **5f** and **5g** it is 1.67 x 10^{-5} M.

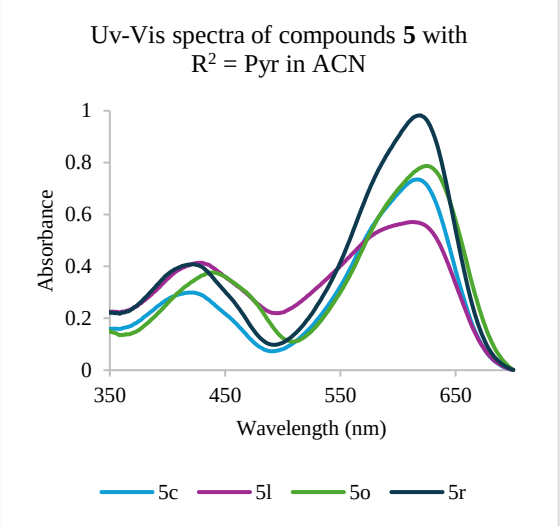

SI-Figure 8 - UV-Vis spectra of compounds **5** with R^2 = Pyr in acetonitrile. The concentration for compounds **5f**, **5g** and **5h** is 3.33 x 10^{-5} M, and for **5a** it is 2.22 x 10^{-5} M.

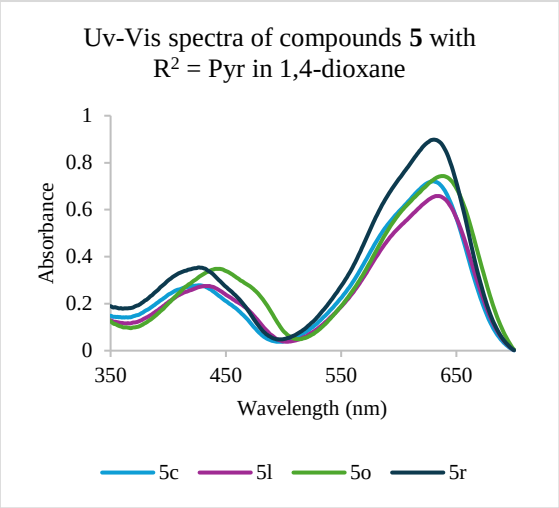

SI-Figure 9 - UV-Vis spectra of compounds **5** with R^2 = Pyr in 1,4-dioxane. The concentration for compounds **5g** and **5h** is 3,33 x 10^{-5} M, for **5a** it is 2.22 x 10^{-5} M and for **5f** it is 1.67 x 10^{-5} M.

SI-Table 1 - Maximum absorption wavelengths (λ_{max}) and molar absorption coefficients (ϵ) of azoimidazoles **5**.

		Ethanol		Acetonitrile		1,4-dioxane	
Comp.	**R^1**	**λ_{max}**	**ϵ (M^{-1} cm^{-1})**	**λ_{max}**	**ϵ (M^{-1} cm^{-1})**	**λ_{max}**	**ϵ (M^{-1} cm^{-1})**
5a	C_6H_4(*p*)F	421, 608	1.15 x 10^4, 2.36 x 10^4	418, 616	9.90 x 10^3, 2.45 x 10^4	424, 619	1.17 x 10^4, 2.62 x 10^4
5b	C_6H_4(*p*)F	416, 604	5.73 x 10^3, 1.15 x 10^4	416, 613	1.13 x 10^4, 2.69 x 10^4	422, 626	1.02 x 10^4, 2.23 x 10^4
5c	C_6H_4(*p*)F	421, 608	1.42 x 10^3, 2.65 x 10^4	418, 616	1.35 x 10^4, 3.31 x 10^4	426, 630	1.25 x 10^4, 3.24 x 10^4
5d	C_6H_4(*p*)Cl	421, 609	1.28 x 10^4, 2.68 x 10^4	419, 615	7.86 x 10^3, 1.90 x 10^4	425, 620	1.21 x 10^4, 2.96 x 10^4
5e	C_6H_4(*p*)Cl	418, 607	1.04 x 10^4, 2.14 x 10^4	415, 614	1.13 x 10^4, 2.68 x 10^4	423, 626	2.03 x 10^4, 4.97 x 10^4
5f	C_6H_4(*m*)Cl	418, 609	1.08 x 10^4, 2.24 x 10^4	410, 614	1.07 x 10^4, 2.75 x 10^4	420, 617	1.14 x 10^4, 2.98 x 10^4
5g	C_6H_4(*p*)Br	414, 608	1.33 x 10^4, 2.94 x 10^4	420, 617	1.14 x 10^4, 2.76 x 10^4	424, 622	1.04 x 10^4, 2.55 x 10^4
5h	C_6H_4(*p*)Br	418, 607	1.08 x 10^4, 2.25 x 10^4	414, 615	1.28 x 10^4, 3.03 x 10^4	422, 627	1.12 x 10^4, 2.78 x 10^4
5i	C_6H_4(*m*)Br	414, 607	1.12 x 10^4, 2.47 x 10^4	413, 615	1.36 x 10^4, 3.51 x 10^4	417, 618	1.45 x 10^4, 3.80 x 10^4
5j	C_6H_4(*p*)CH_3	429, 611	1.25 x 10^4, 2.35 x 10^4	427, 619	1.40 x 10^4, 3.15 x 10^4	432, 624	1.11 x 10^4, 1.99 x 10^4
5k	C_6H_4(*p*)CH_3	428, 611	1.05 x 10^4, 1.96 x 10^4	426, 617	1.14 x 10^4, 2.52 x 10^4	429, 629	1.04 x 10^4, 2.16 x 10^4
5l	C_6H_4(*p*)CH_3	433, 611	2.72 x 10^4, 5.09 x 10^4	427, 611	1.24 x 10^4, 1.71 x 10^4	431, 632	1.65 x 10^4, 3.95 x 10^4
5m	C_6H_4(*p*)OCH_3	439, 613	6.90 x 10^3, 1.17 x 10^4	438, 622	9.81 x 10^3, 2.06 x 10^4	437, 623	8.22 x 10^3, 1.30 x 10^4
5n	C_6H_4(*p*)OCH_3	438, 613	1.16 x 10^4, 1.96 x 10^4	435, 621	1.30 x 10^4, 2.67 x 10^4	439, 633	1.13 x 10^4, 2.21 x 10^4
5o	C_6H_4(*p*)OCH_3	440, 614	3.02 x 10^4, 5.12 x 10^4	439, 624	1.13 x 10^4, 2.36 x 10^4	441, 637	1.04 x 10^4, 2.23 x 10^4
5p	C_6H_5	421, 609	9.90 x 10^3, 2.02 x 10^4	420, 616	9.36 x 10^3, 2.25 x 10^4	427, 619	1.10 x 10^4, 1.70 x 10^4
5q	C_6H_5	418, 607	1.19 x 10^4, 2.42 x 10^4	418, 614	1.21 x 10^4, 2.88 x 10^4	423, 626	1.14 x 10^4, 2.81 x 10^4
5r	C_6H_5	424, 608	1.09 x 10^4, 2.24 x 10^4	421, 618	1.22 x 10^4, 2.95 x 10^4	426, 630	1.06 x 10^4, 2.69 x 10^4

2.2. Halochromism

Uv-Vis spectroscopy was also employed to assess the halochromic properties of compounds **5**. According to the method by *Ossowski et al.*[3], solutions of compound **5j** in a mixture of water/ethanol (60:40, v/v) were prepared. To obtain the different data points (**SI-Table 2**), successive amounts of a 4 M NaOH solution were added to provide pH values in the basic region, while sulfuric acid was added to study the acidic region of the pH spectrum. After each addition, a pH electrode was used to measure the pH of the solution, and the corresponding UV-Vis absorbance spectrum was acquired immediately. (**Figure 4**).

Moreover, pKa was determined by the graphical method of Salgado *et al.*[4]. The maximum absorbance wavelength was determined at minimum and maximum pH values and a graph of absorbance *vs.* pH was plotted at these wavelengths. The pKa corresponds to the point of intersection of the two series, which is determined by equalling the absorbance in the linear equations of the two points closest to the crossing at each curve. The pKa value obtained with this method was 4.89.

SI-Table 2 - Absorption spectra data of **5j** at different pH values.

pH	Wavelength	Absorbance	Wavelength	Absorbance
2.91	422	0.113	552	0.120
3.64	419	0.113	552	0.120
5.61	422	0.101	585	0.139
6.40	433	0.101	600	0.182
8.33	432	0.104	600	0.181
9.40	424	0.105	600	0.183
10.04	430	0.108	597	0.190

2.3. ab initio molecular quantum mechanics calculations

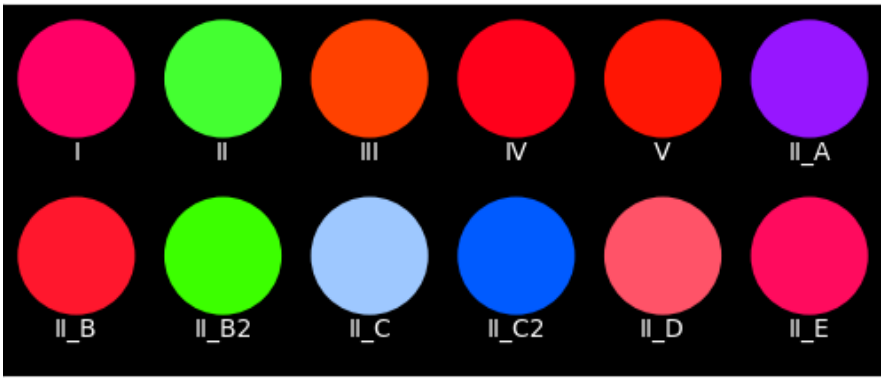

SI-Figure 10 - Expected colours of compound **5k** in considered tautomeric forms interacting with one water molecule (I-V) and selected protonated forms of tautomer II (II_A – II_E)

SI-Table 3 - ab initio calculations of selected tautomeric forms of compound **5k**.

Tautomeric form	Structure	ΔG (kcal/mol)	Vertical excitations energies for the first eight excited states in ground state geometry (nm) Corresponding oscillator strength (f_{osc})							
I	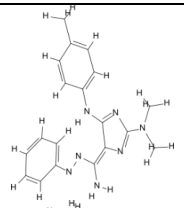	0	516	452	391	341	333	331	324	317
			0.587	0.0145	0.768	0.00155	0.0106	0.0225	0.0224	0.0482
II	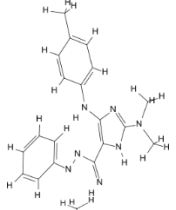	14.6	701	483	436	354	346	338	317	309
			0.187	0.0058	0.0839	0.00993	0.000544	0.127	0.347	0.00292
III	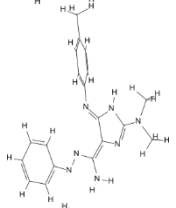	14.6	524	466	401	330	323	317	309	301
			0.0507	0.851	0.256	0.08	0.02	0.0869	0.026	0.016
IV	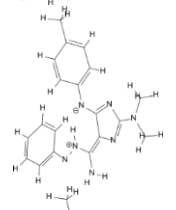	11.3	553	441	379	371	354	350	341	321
			0.483	0.527	0.0903	0.00409	0.000494	0.00461	0.037	0.0253
V	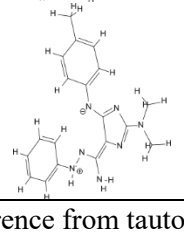	12.6	489	441	394	356	344	328	322	298
			0.458	0.123	0.384	0.0142	0.00294	0.0445	0.00796	0.00926

(*) Free energy difference from tautomer I

SI-Table 4 - ab initio calculations of selected tautomeric forms of compound **5k** in ethanol and in the presence of one water molecule.

Tautomeric form	Structure	ΔG (kcal/mol)	Vertical excitations energies for the first eight excited states in ground state geometry (nm) Corresponding oscillator strength (f_{osc})							
I	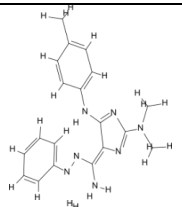		534	451	401	339	333	330	324	317
			0.494	0.0358	0.673	0.000428	0.0363	0.0111	0.0343	0.0677
II	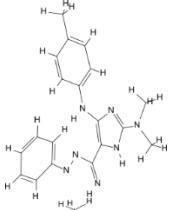	10.1	665	470	439	351	348	330	311	306
			0.247	0.0163	0.133	0.0127	0.000131	0.295	0.157	0.00543
III	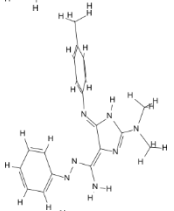	15.2	512	473	401	331	327	321	309	306
			0.0679	0.825	0.251	0.0629	0.00552	0.082	0.0369	0.067
IV	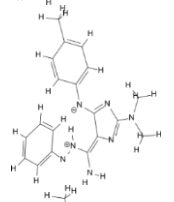	15.6	548	438	368	368	356	354	340	325
			0.512	0.59	0.0482	0.0199	0.000184	0.00467	0.0368	0.0217
V	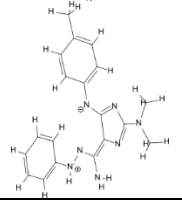	14.1	507	419	389	356	349	344	328	314
			0.473	0.357	0.17	0.0156	0.00166	0.0102	0.0416	0.0116

(*) Free energy difference from tautomer I

SI-Table 5 - ab initio calculations of selected protonated forms of tautomers I and II of compound **5k** in ethanol.

Protonated form	Structure	ΔG (*) (kcal/mol)	Vertical excitations energies for the first eight excited states in ground state geometry (nm) Corresponding oscillator strength (f_{osc})							
I_A	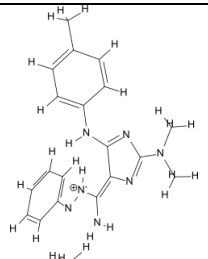	25.4	589	465	453	412	381	353	342	312
			0.361	0.105	1.27	0.0125	0.00755	0.0223	0.00447	0.419
I_A2	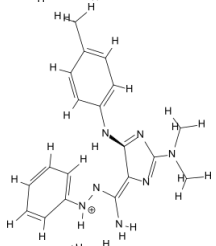	6.78	576	453	440	425	364	346	332	289
			0.0123	0.00523	0.00805	0.00345	0.00161	0.00455	0.00218	0.00308
I_B	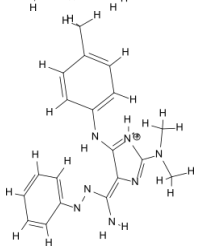	8.84	515	480	399	377	355	341	297	292
			0.771	0.0168	0.199	0.00835	0.00155	0.258	0.21	0.089
I_C	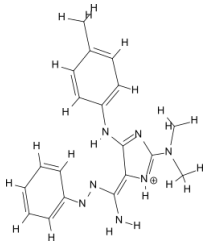	7.59	559	462	422	389	373	334	305	290
II_A		-6.98	0.287	0.0441	0.00152	0.816	0.0778	0.0899	0.0768	0.72

SI-Table 5 (cont.) - ab initio calculations of selected protonated forms of tautomers I and II of compound **5k** in ethanol.

Protonated form	Structure	ΔG (*) (kcal/mol)	Vertical excitations energies for the first eight excited states in ground state geometry (nm) Corresponding oscillator strength (f_{osc})							
I_D	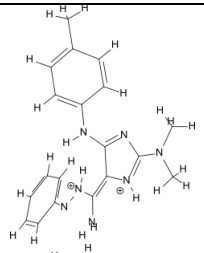	158	760	703	497	449	394	362	352	323
II_B		144	0.348	0.00067	1.08	0.0349	0.00781	0.322	0.0561	0.563
I_D2	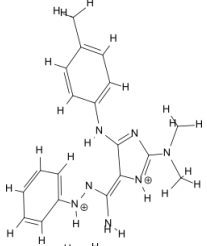	98.4	656	633	518	453	377	374	337	321
II_B2		83.8	0.499	0.00863	0.0118	1.03	0.0463	0.0103	0.014	1.06
I_E	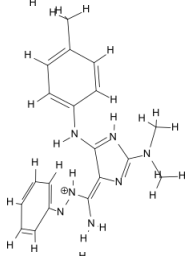	158	647	558	502	460	368	343	334	326
			0.325	0.00833	1.49	0.0224	0.126	0.0567	0.0673	0.0214
I_E2	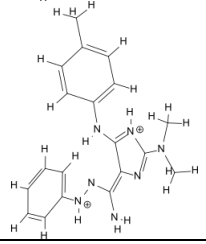	96.6	542	494	453	445	391	343	289	274
			0.161	0.0983	0.00135	0.013	0.926	0.199	0.173	0.0566

SI-Table 5 (cont.) - ab initio calculations of selected protonated forms of tautomers I and II of compound **5k** in ethanol.

Protonated form	Structure	ΔG (*) (kcal/mol)	Vertical excitations energies for the first eight excited states in ground state geometry (nm) Corresponding oscillator strength (f_{osc})							
II_C	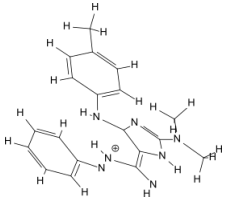	21.9	1160	727	556	424	391	380	362	347
			0.0364	0.302	0.0219	0.000425	0.00343	0.0199	0.581	0.00958
II_C2	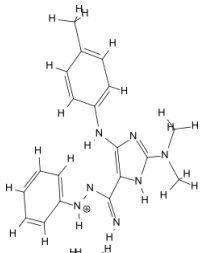	18.6	682	571	516	487	418	389	363	341
			0.547	0.225	0.00103	0.0136	0.0499	0.8	0.0261	0.000215
II_D	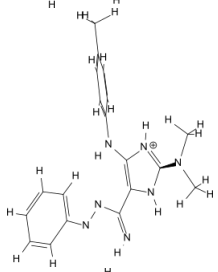	12.1	504	474	342	337	318	313	300	283
			0.0993	0.0383	0.0149	0.0299	0.541	0.00266	0.149	0.123
I_F	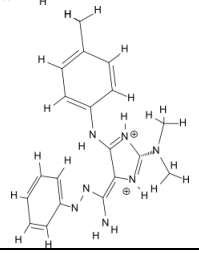	97	542	494	453	445	391	343	289	274
II_E		82.5	0.161	0.0983	0.00135	0.013	0.926	0.199	0.173	0.0566

3. Antimicrobial activity

3.1. Culture media and reagents

For fungus, the culture media/reagents used were: Sabouraud Dextrose Agar (SDA) (bio-Mérieux; Marcy L'Etoile, France); RPMI-1640 broth (Biochrom AG; Berlin, Germany) and 3-(N-morpholino) propanesulfonic acid (MOPS) (Sigma-Aldrich; St. Louis, MO, USA). For the tests, RPMI-1640 was buffered to pH 7.0 using MOPS. For bacteria Mueller-Hinton Agar (MHA) and broth (MHB) (Liofilchem;Téramo, Italy) were used.

3.2. Microorganisms

Two bacteria reference strains from American Type Culture Collection (ATCC) were used: *Escherichia coli* 25922 and *Staphylococcus aureus* 25923. For fungi, the reference strains from ATTC used in this work were: *Candida albicans* 10231, *C. krusei* 6258 and *A. fumigatus* 204305. A reference strain from Colección Española de Cultivos Tipo (CECT) was also used: *Cryptococcus neoformans* 1078. In the case of dermatophytes, a clinical strain was included: *Trichophyton rubrum* FF5.

3.3. Compounds solutions

All the compounds were previously dissolved in dimethyl sulfoxide (DMSO) (Sigma-Aldrich; St. Louis, MO, USA). Before each test, a series of 1:2 dilutions was prepared in the suitable culture medium (RPMI for fungi and MHB for bacteria), with concentrations ranging from 256 to 0.5 μg mL^{-1}.

3.4. Susceptibility tests

The susceptibility tests were carried out in accordance with the Clinical and Laboratory Standards. Institute (CLSI) with regard to the broth microdilution method for yeasts (reference document M27-A3), filamentous fungi (reference document M38-A2) and bacteria (reference document M07-A10). In resume, the yeasts were subcultured on SDA 24 hours before the test. On the day of the test, a yeast suspension was prepared, the final concentration of which was adjusted to 10^3 colony forming units (CFU) mL^{-1}. In the case of moulds, the procedure was similar, but the concentration of spores was adjusted to 0.4-5 x 10^4 spores mL^{-1} in the case of *A. fumigatus* or 1-3 x 10^3 spores mL^{-1} in the case of dermatophytes. In all cases, these suspensions were prepared in RPMI-1640. In 96-well flat-bottom plates, 100 μL of each of the prepared suspensions were mixed with 100 μL of different dilutions of the compounds. The plates containing yeast and *A. fumigatus* were incubated at 36 °C for 48h and those containing *T. rubrum* at 24 for 5 to 7 days. In the case of bacteria, a suspension with a concentration of 5 x 10^5 CFU mL^{-1} was prepared in MH broth. In 96-well flat-bottom plates, 50 μL of the bacterial suspension was mixed with 50 μL of each compound dilution. The plates were then incubated at 36 °C for 16 to 18h.

3.5. Controls and MIC/MLC determination

For all the experiments a positive control, consisting of microorganism growing in culture medium (representing 100% growth), a negative control, consisting in culture medium (corresponding to 0% growth), and a DMSO control consisting in microorganism cultured in culture medium supplemented with DMSO at the concentration of 1.0%; v/v (corresponding to the DMSO control) were included.

At the end of incubation, the growth of the different microorganisms was correlated with the turbidity of the medium. The Minimum Inhibitory Concentration (MIC) was determined by visual observation of the plates as the lowest concentration capable of completely inhibiting the growth of the microorganism when comparing with that of the positive control.

Having defined the MIC, 10 μL of the contents of all the wells in which no growth was observed were transferred to a culture plate containing SDA in the case of fungi or MHA in the case of bacteria. The plates were incubated under the temperature and incubation time conditions described previously for each of the microorganisms. The minimum lethal concentration corresponded to the lowest concentration at which no growth was observed.

The MIC and CML results are shown in **SI-Table 6**.

SI-Table 6 - Antimicrobial activity (MIC and MLC) of compounds **5** against fungi (yeasts and filamentous fungi) and bacteria (Gram-positive and Gram-negative).

	MIC (MLC) μg mL^{-1}							
	5a	**5b**	**5c**	**5d**	**5e**	**5f**	**5g**	**5h**
C. albicans ATCC 10231	213.3±42.7 (≥256)	192±37.0 (213.3±42.7)	256±0.0 (256±0.0)	192.0±52.3 (≥256)	256±0.0 (256±0.0)	>256 (>256)	>256 (>256)	>256 (>256)
C. krusei ATCC 6258	16.0±0.0 (21.3±5.3)	13.3±2.7 (13.3±2.7)	16±0.0 (16±0.0)	26.7±5.3 (37.3±14.1)	24±4.6 (24±4.6)	32.0±0.0 (32.0±0.0)	32.0±0.0 (53.3±10.7)	36±10.1 (52±12.0)
C. neoformans CECT 1078	13.3 ± 2.7 (13.3 ± 2.7)	8.0±0.0 (13.3±2.7)	10.7±2.7 (10.7±2.7)	32.0±0.0 (42.7±10.7)	10±3.1 (18.7±7.1)	24.0±8.0 (34.7±16.2)	53.3±10.7 (53.3±10.7)	19.1±6.7 (42.7±10.7)
A. fumigatus ATCC 204305	>256 (>256)	256±0.0 (≥256)	256±0.0 (≥256)	>256 (>256)	256±0.0 (256±0.0)	>256 (>256)	>256 (>256)	>256 (>256)
T. rubrum FF5	170.7±42.7 (>256)	128±0.0 (128±0.0)	128±0.0 (128±0.0)	149.3±56.4 (213.3±42.7)	128±0.0 (128±0.0)	≥256 (>256)	>256 (>256)	≥256 (>256)
E. coli ATCC 25922	>256 (>256)	>256 (>256)	>256 (>256)	>256 (>256)	>256 (>256)	>256 (>256)	>256 (>256)	>256 (>256)
S. aureus ATCC 25923	213.3±42.7 (>256)	64±18.5 (>256)	>256 (>256)	106.7±21.3 (≥256)	≥256 (>256)	>256 (>256)	>256 (>256)	>256 (>256)

MIC, minimum inhibitory concentration; MLC, minimum lethal concentration; The results are presented as mean ± SEM.

SI-Table 6 (cont.) - Antimicrobial activity (MIC and MLC) of compounds **5** against fungi (yeasts and filamentous fungi) and bacteria (Gram-positive and Gram-negative).

	MIC (MLC) μg mL^{-1}									
	5i	**5j**	**5k**	**5l**	**5m**	**5n**	**5o**	**5p**	**5q**	**5r**
C. albicans ATCC 10231	>256 (>256)	89.6±15.7 (≥256)	256±0.0 (256±0.0)	>256 (>256)	128.0±0.0 (256.0±0.0)	>256 (>256)	>256 (>256)	128.0±0.0 (256.0±0.0)	>256 (>256)	>256 (>256)
C. krusei ATCC 6258	32.0±0.0 (53.3±10.7)	4.0±0.0 (5.3±1.3)	16±0.0 (16±0.0)	40±8.0 (80±27.7)	16.0±0.0 (16.0±0.0)	104±15.3 (112±16.0)	128±0.0 (256±0.0)	16.0±0.0 (16.0±0.0)	53.3±10.7(85.3±21.3)	44±7.7 (64±22.6)
C. neoformans CECT 1078	26.7±5.3 (26.7±5.3)	2.0±0.0 (3.3±0.7)	7.3±0.7 (13.3±2.7)	14.7±1.3 (21.3±5.3)	13.3±2.7 (13.3±2.7)	56±8.0 (96±18.5)	96±32.0 (256±0.0)	13.3±2.7 (18.7±7.1)	16±3.3 (20±4.0)	13.3±2.7 (18.7±7.1)
A. fumigatus ATCC 204305	>256 (>256)	≥256 (≥256)	256±0.0 (≥256)	>256 (>256)	>256 (>256)	>256 (>256)	>256 (>256)	>256 (>256)	>256 (>256)	>256 (>256)
T. rubrum FF5	341.3±85.3 (>256)	44.0±7.7 (48.0±9.2)	128±0.0 (128±0.0)	256±0.0 (256±0.0)	128.0±0.0 (213.3±42.7)	>256 (>256)	≥256 (>256)	128.0±0.0 (256±0.0)	>256 (>256)	>256 (>256)
E. coli ATCC 25922	>256 (>256)	>256 (>256)	>256 (>256)	>256 (>256)	>256 (>256)	>256 (>256)	>256 (>256)	>256 (>256)	>256 (>256)	>256 (>256)
S. aureus ATCC 25923	64.0±0.0 (170.7±42.7)	10.7±1.3 (≥256)	>256 (>256)	>256 (>256)	85.3±21.3 (170.7±42.7)	>256 (>256)	>256 (>256)	128.0±0.0 (170.7±42.7)	>256 (>256)	>256 (>256)

MIC, minimum inhibitory concentration; MLC, minimum lethal concentration; The results are presented as mean ± SEM.

4. NMR spectra

4.1. 1H and 13C NMR spectra

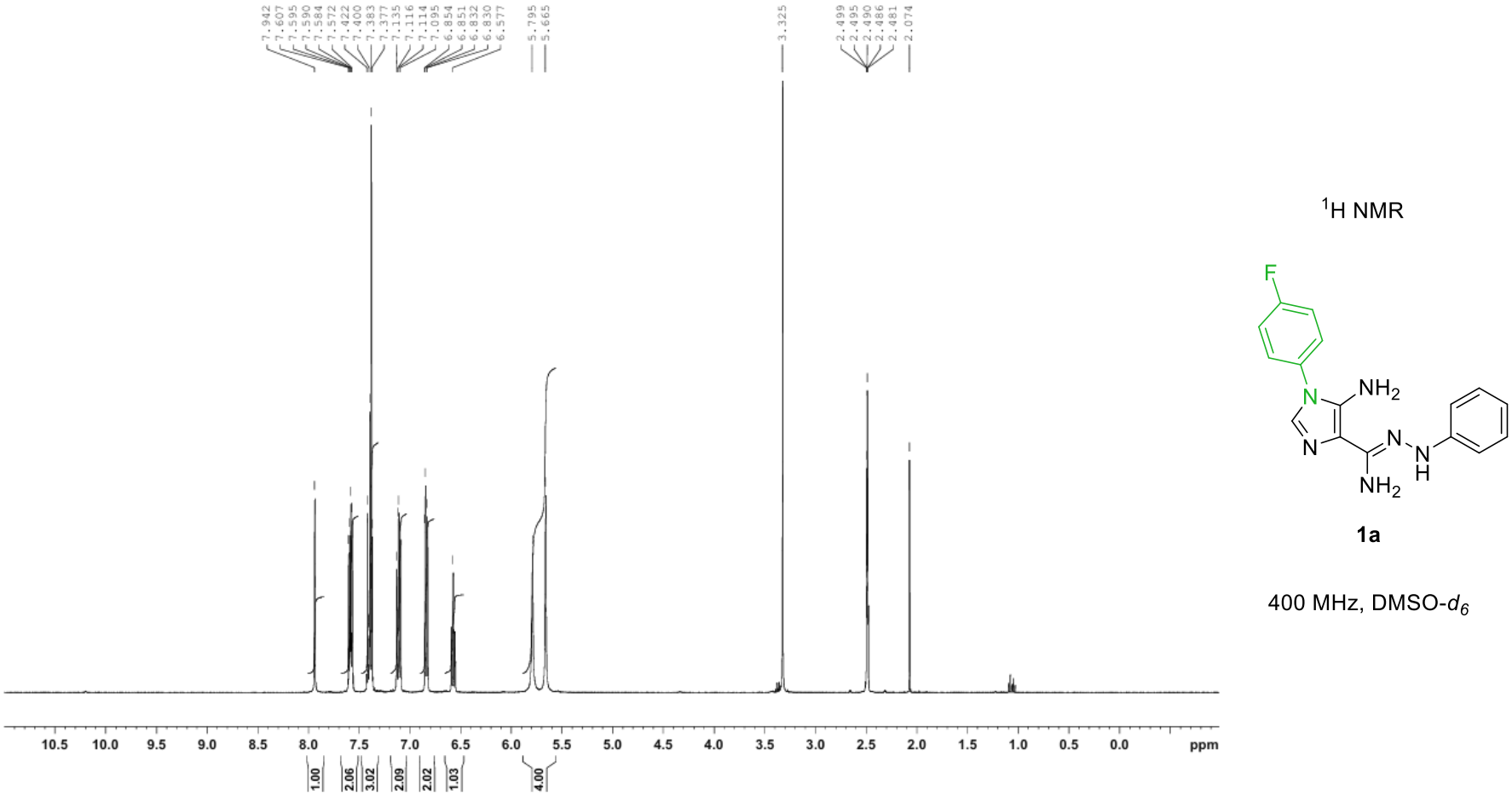

SI-Figure 11 - ^{1}H NMR spectrum of (*Z*)-5-amino-1-(4-fluorophenyl)-*N*'-phenyl-1*H*-imidazole-4-carbohydrazonamide (**1a**).

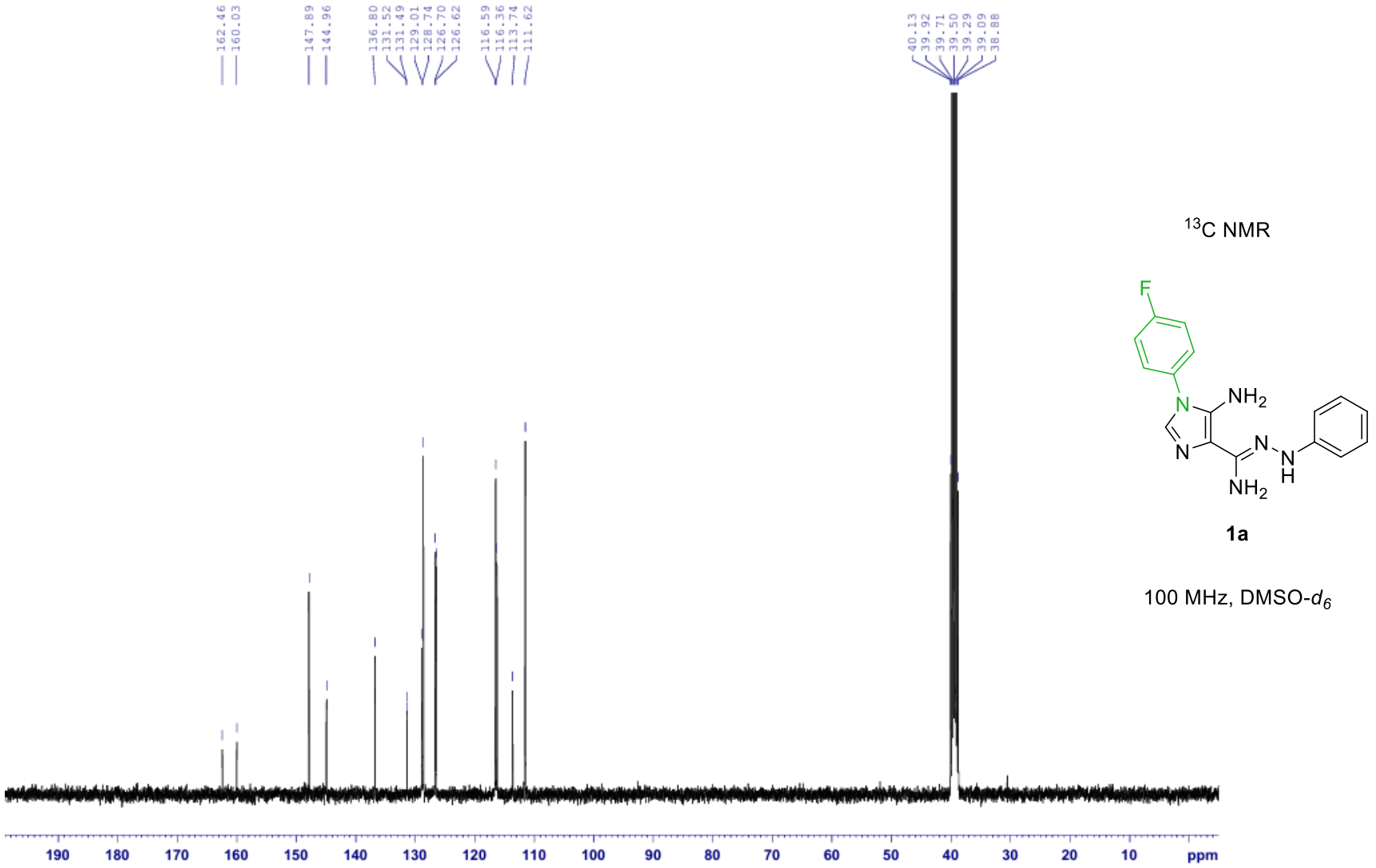

SI-Figure 12 - ^{13}C NMR spectrum of (*Z*)-5-amino-1-(4-fluorophenyl)-*N*'-phenyl-1*H*-imidazole-4-carbohydrazonamide (**1a**).

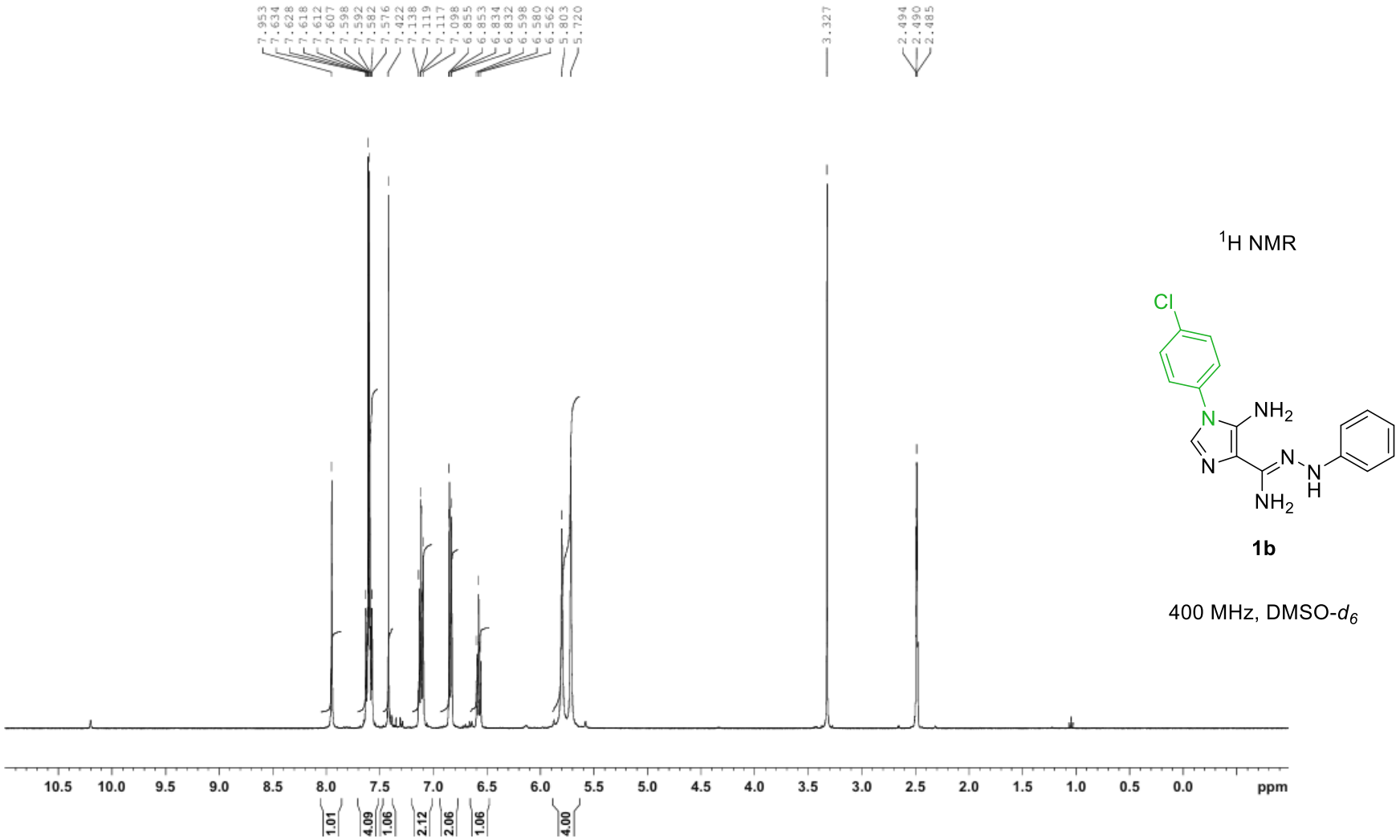

SI-Figure 13 - ^{1}H NMR spectrum of (*Z*)-5-amino-1-(4-chlorophenyl)-*N*'-phenyl-1*H*-imidazole-4-carbohydrazonamide (**1b**).

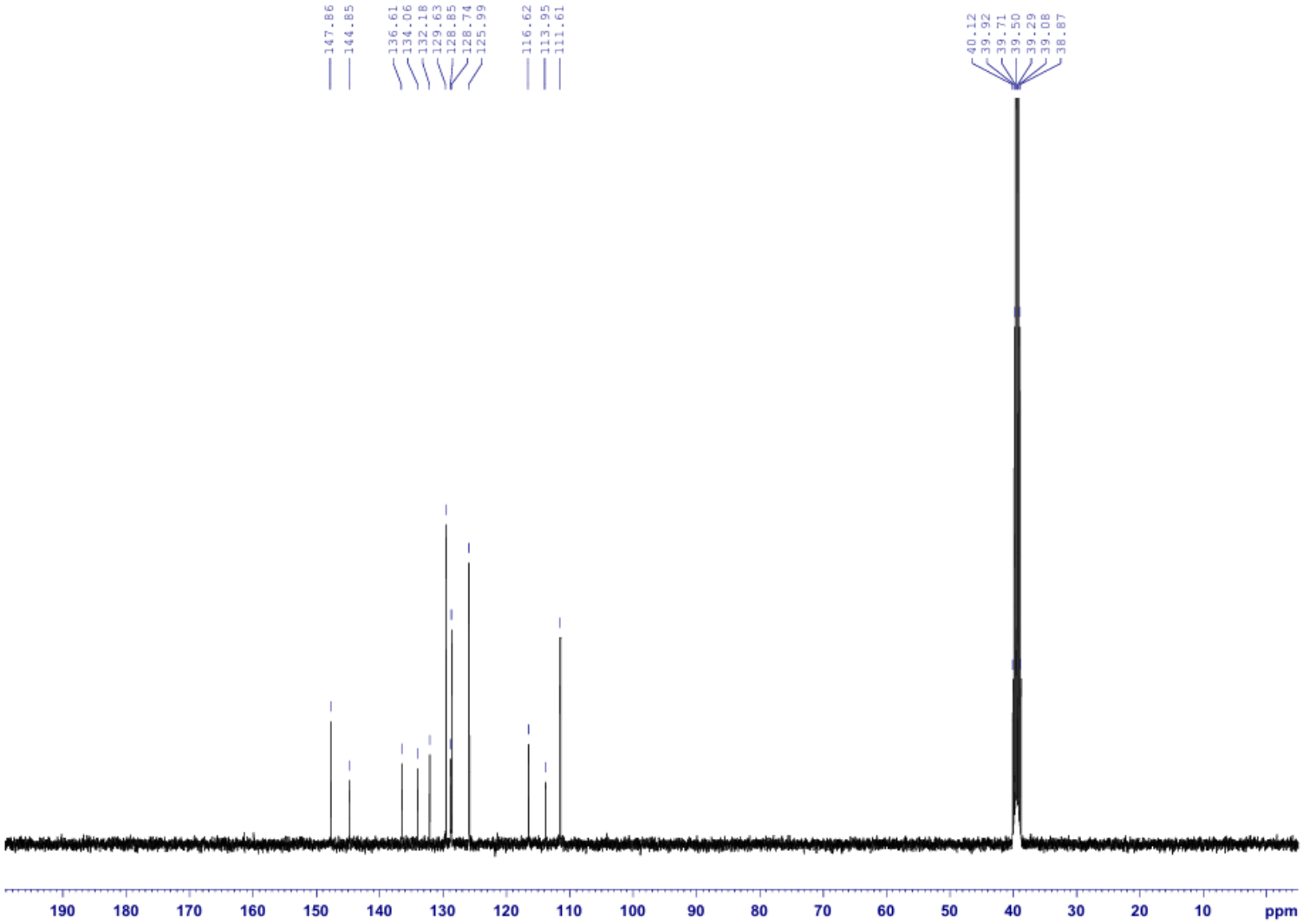

^{13}C NMR

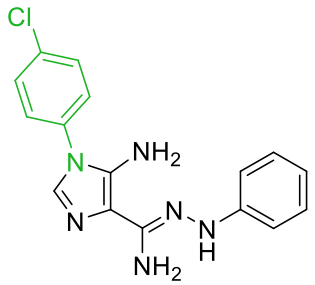

1b

100 MHz, DMSO-d_6

SI-Figure 14 - ^{13}C NMR spectrum of (*Z*)-5-amino-1-(4-chlorophenyl)-*N*'-phenyl-1*H*-imidazole-4-carbohydrazonamide (**1b**).

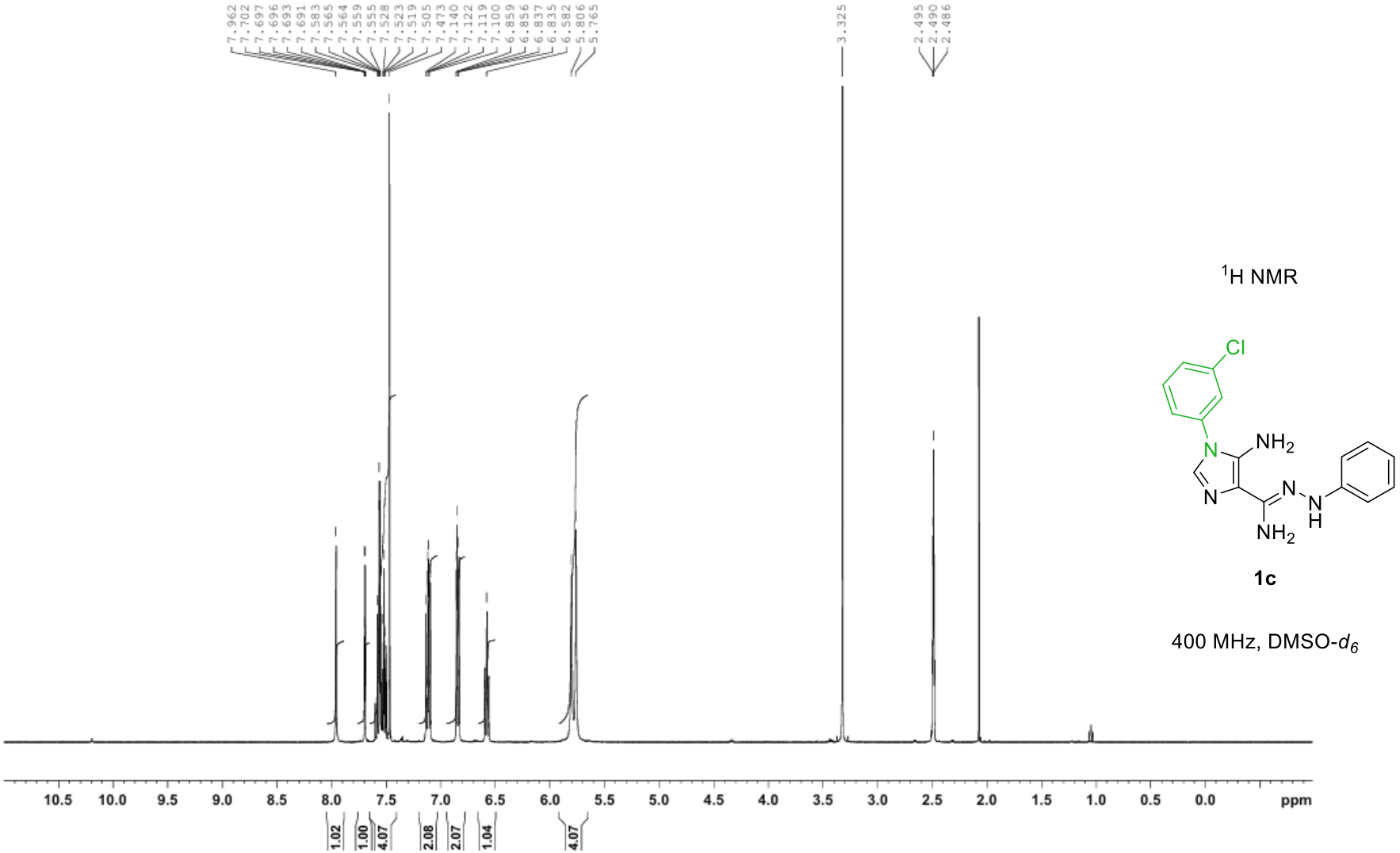

SI-Figure 15 - ^{1}H NMR spectrum of (*Z*)-5-amino-1-(3-chlorophenyl)-*N*'-phenyl-1*H*-imidazole-4-carbohydrazonamide (**1c**).

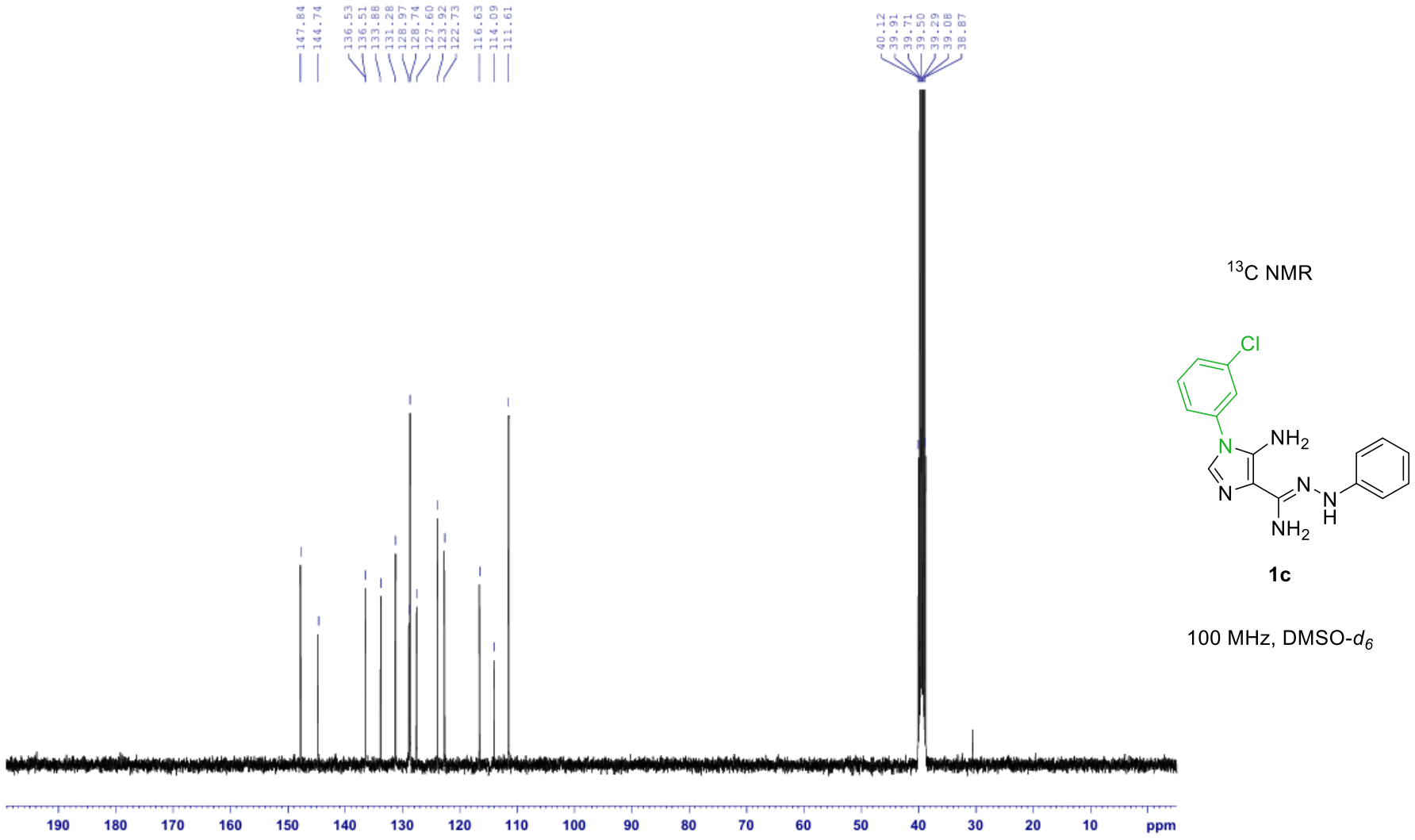

SI-Figure 16 - ^{13}C NMR spectrum of (*Z*)-5-amino-1-(3-chlorophenyl)-*N*'-phenyl-1*H*-imidazole-4-carbohydrazonamide (**1c**).

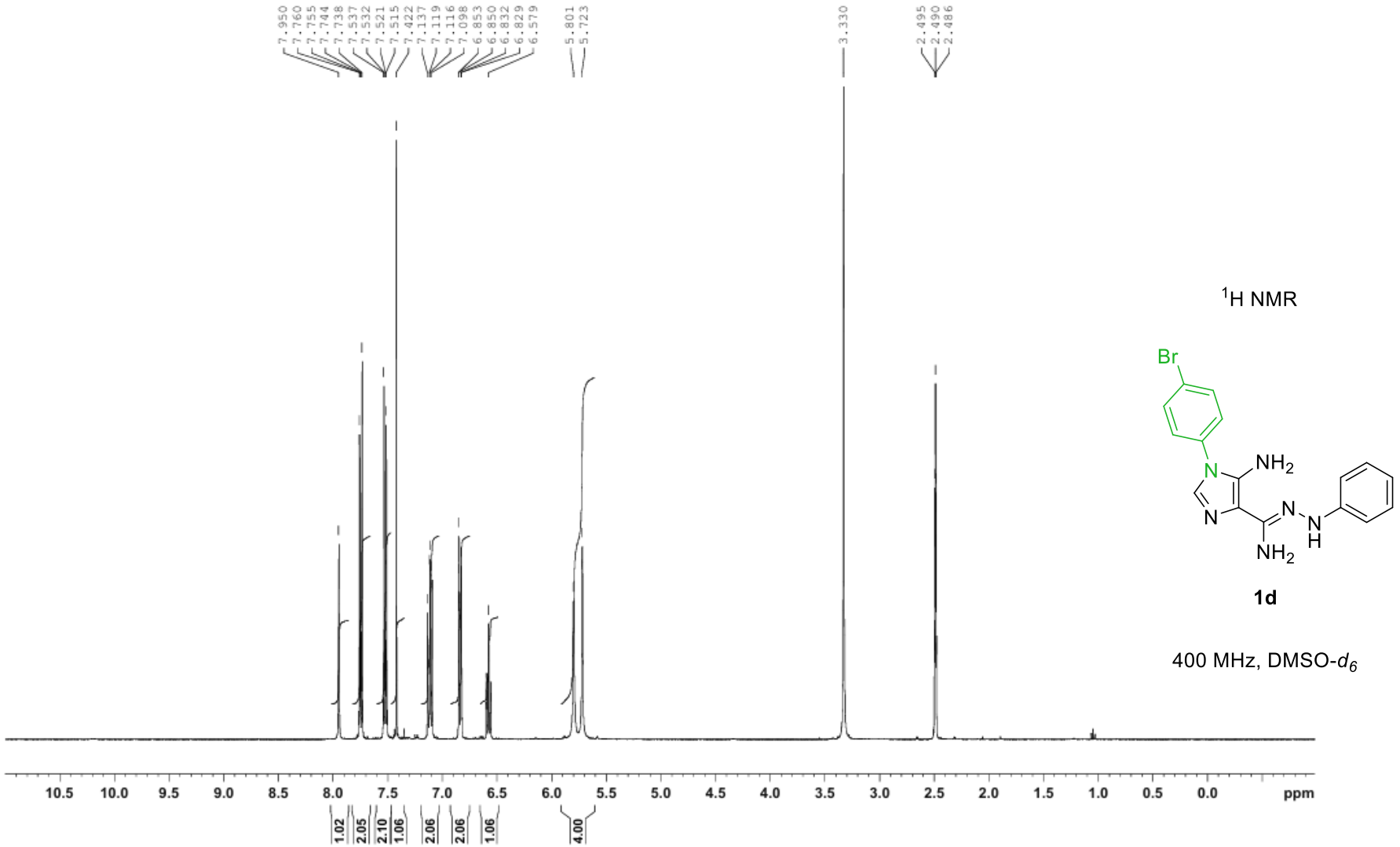

SI-Figure 17 - ^{1}H NMR spectrum of (*Z*)-5-amino-1-(4-bromophenyl)-*N*'-phenyl-1*H*-imidazole-4-carbohydrazonamide (**1d**).

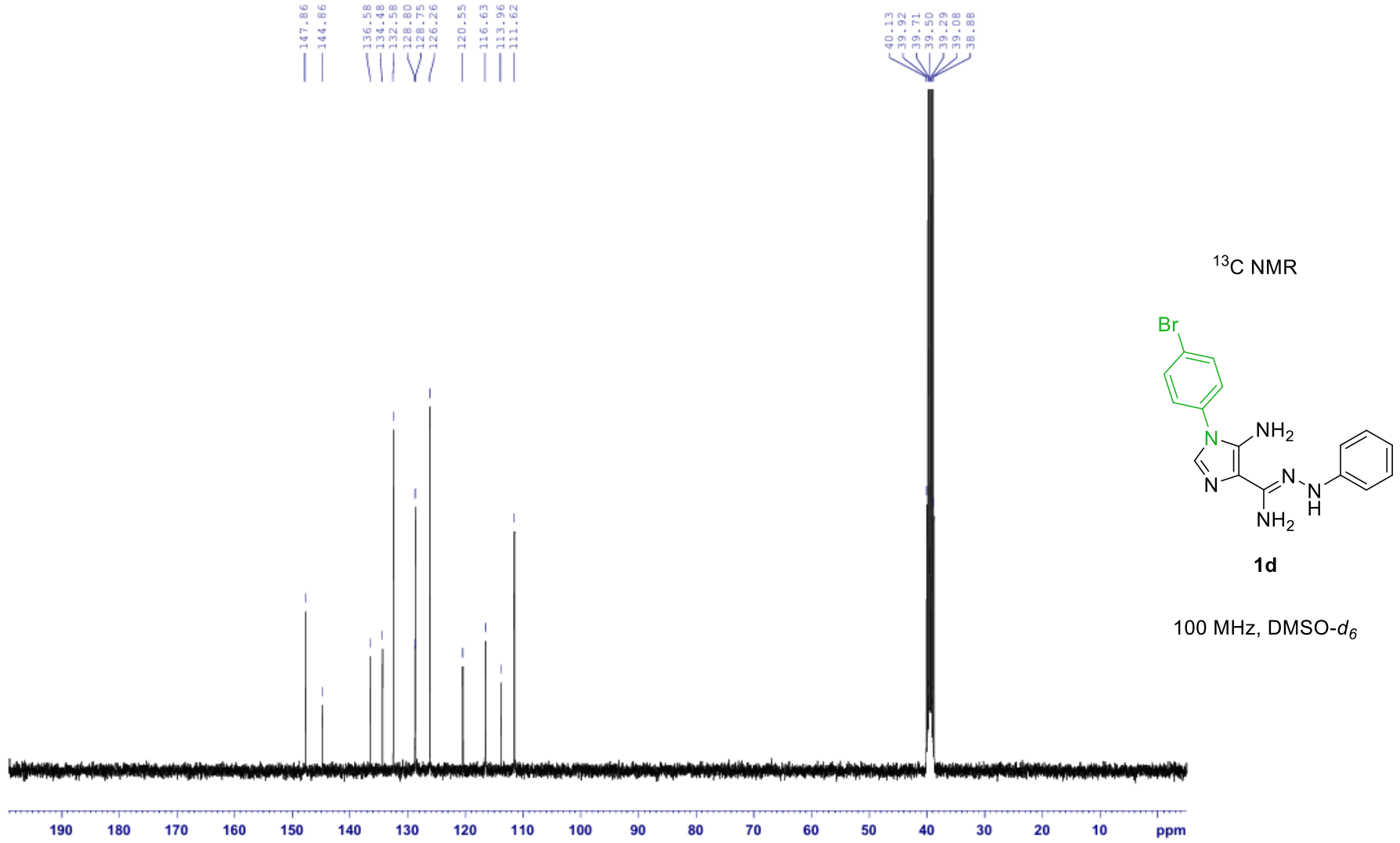

SI-Figure 18 - ^{13}C NMR spectrum of (*Z*)-5-amino-1-(4-bromophenyl)-*N*'-phenyl-1*H*-imidazole-4-carbohydrazonamide (**1d**).

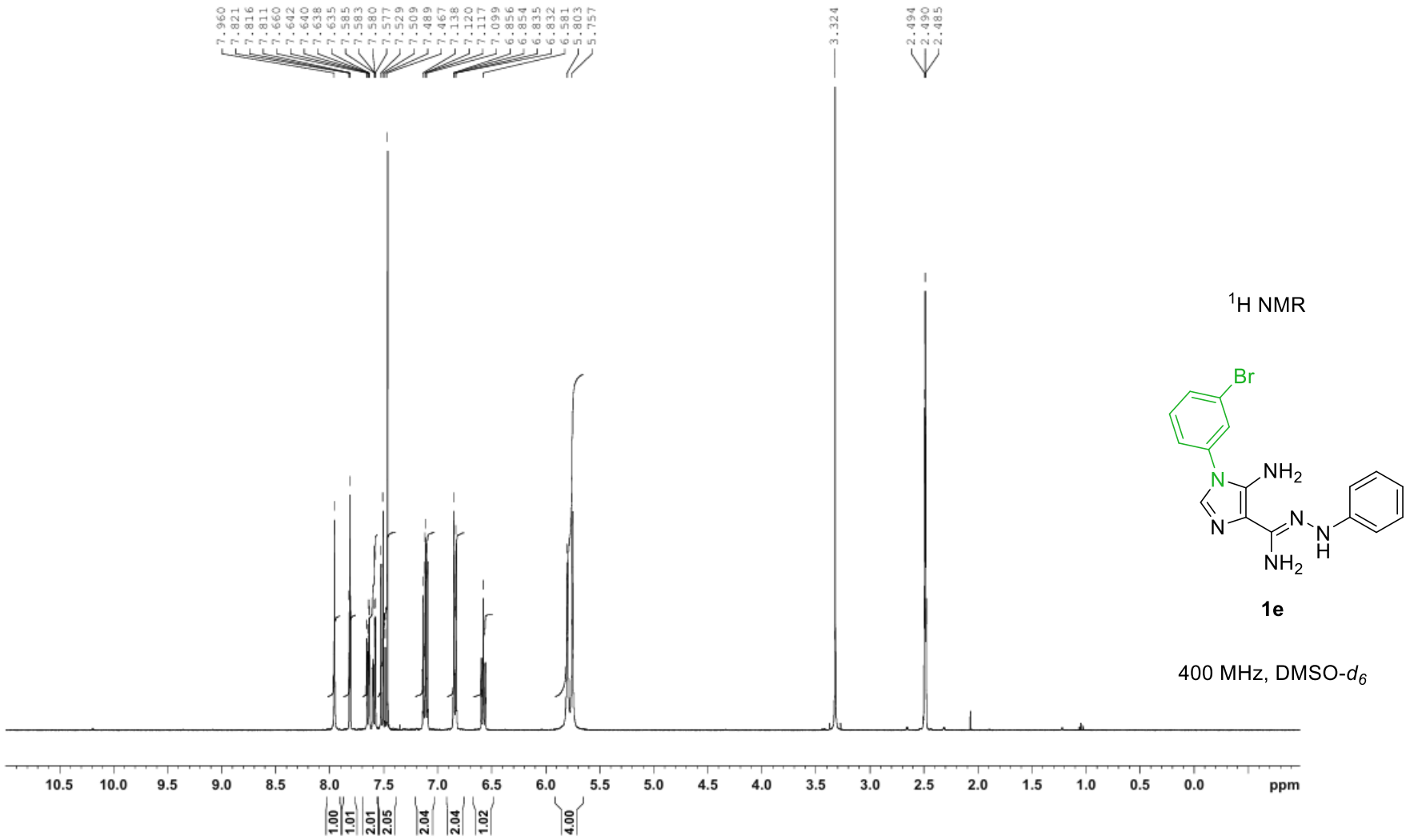

SI-Figure 19 - ^{1}H NMR spectrum of (*Z*)-5-amino-1-(3-bromophenyl)-*N*'-phenyl-1*H*-imidazole-4-carbohydrazonamide (**1e**).

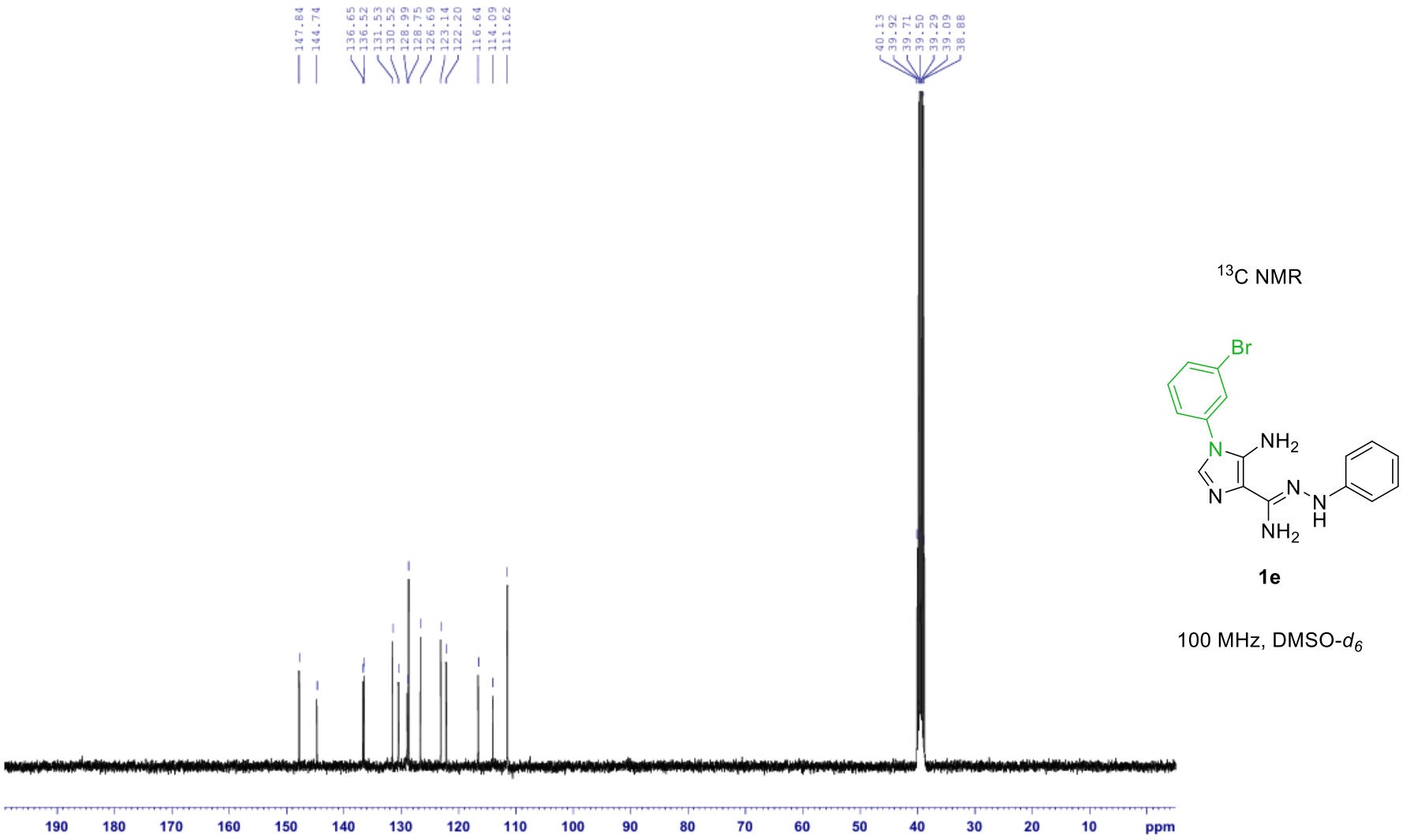

SI-Figure 20 - ^{13}C NMR spectrum of (*Z*)-5-amino-1-(3-bromophenyl)-*N*'-phenyl-1*H*-imidazole-4-carbohydrazonamide (**1e**).

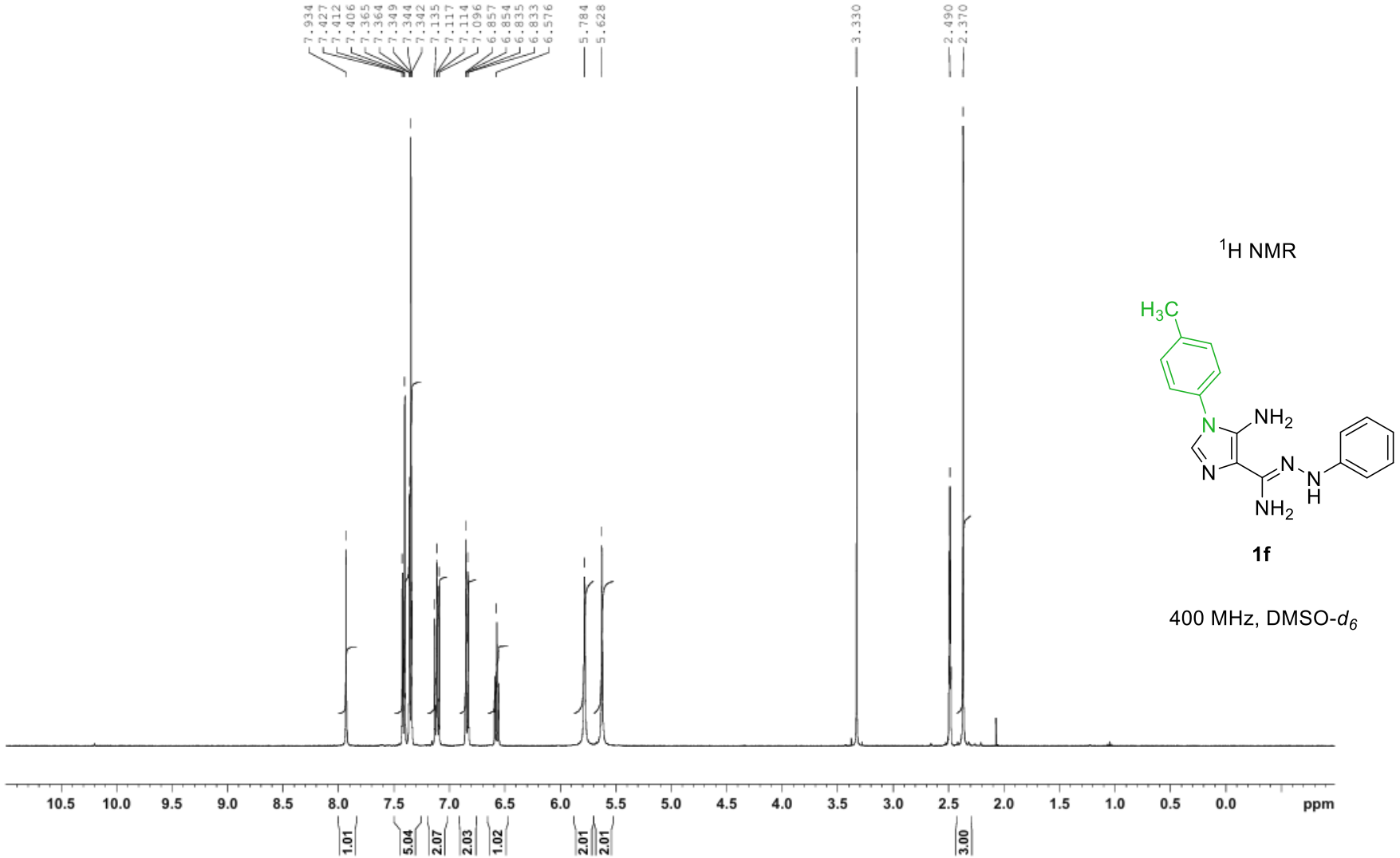

SI-Figure 21 - ^{1}H NMR spectrum of (*Z*)-5-amino-1-(*p*-tolyl)-*N*'-phenyl-1*H*-imidazole-4-carbohydrazonamide (**1f**).

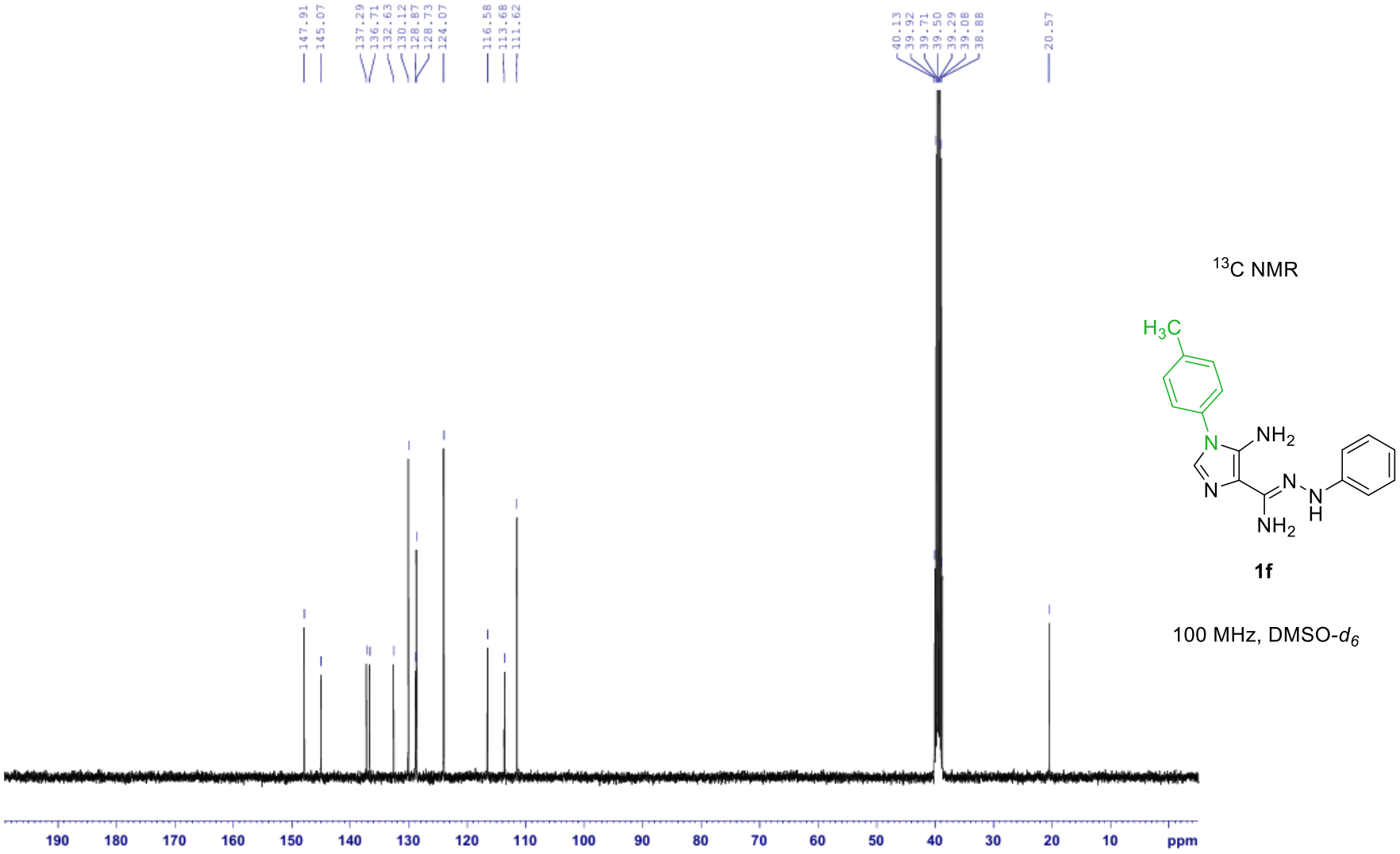

SI-Figure 22 - ^{13}C NMR spectrum of (*Z*)-5-amino-1-(*p*-tolyl)-*N*'-phenyl-1*H*-imidazole-4-carbohydrazonamide (**1f**).

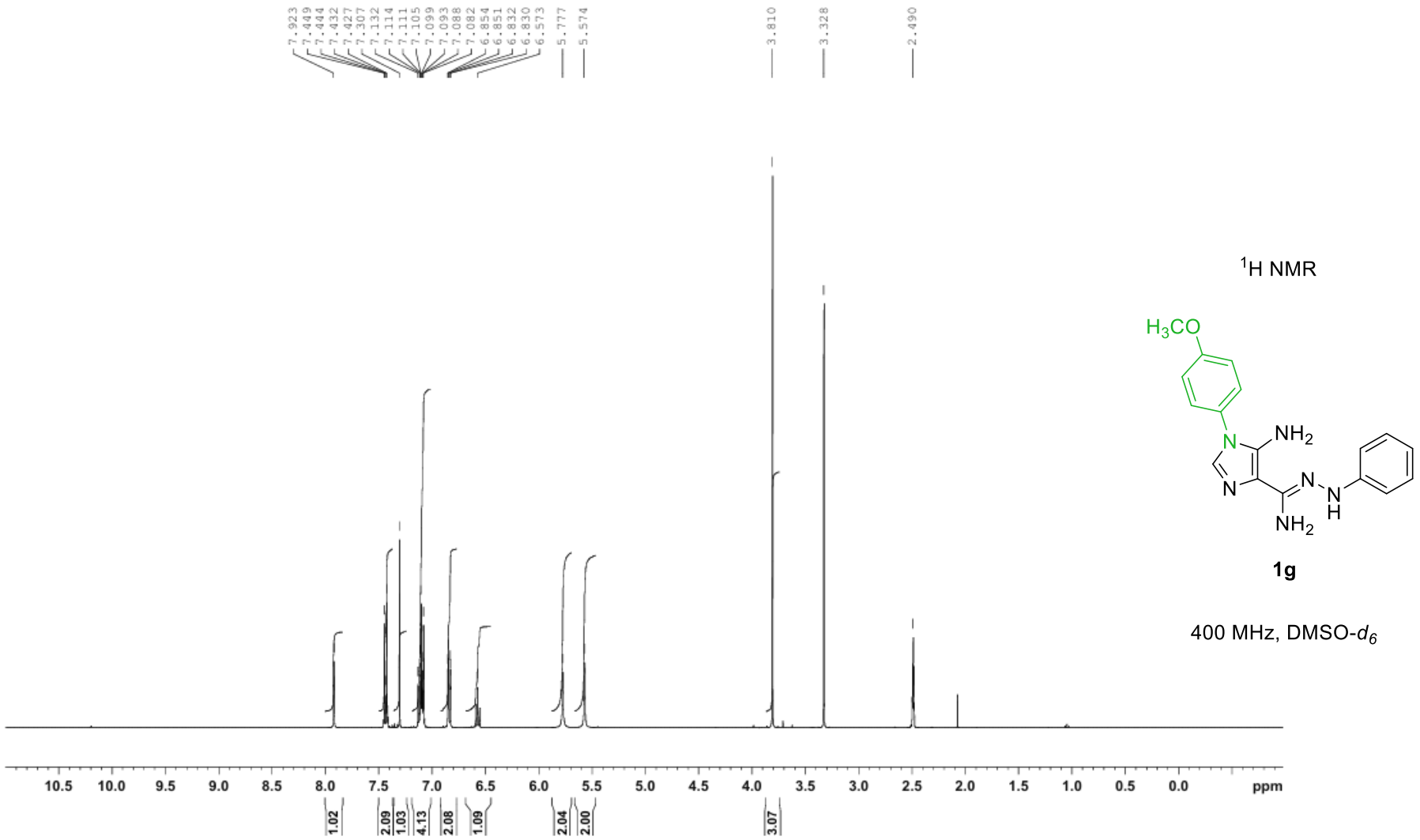

SI-Figure 23 - ^{1}H NMR spectrum of (*Z*)-5-amino-1-(4-methoxyphenyl)-*N*'-phenyl-1*H*-imidazole-4-carbohydrazonamide (**1g**).

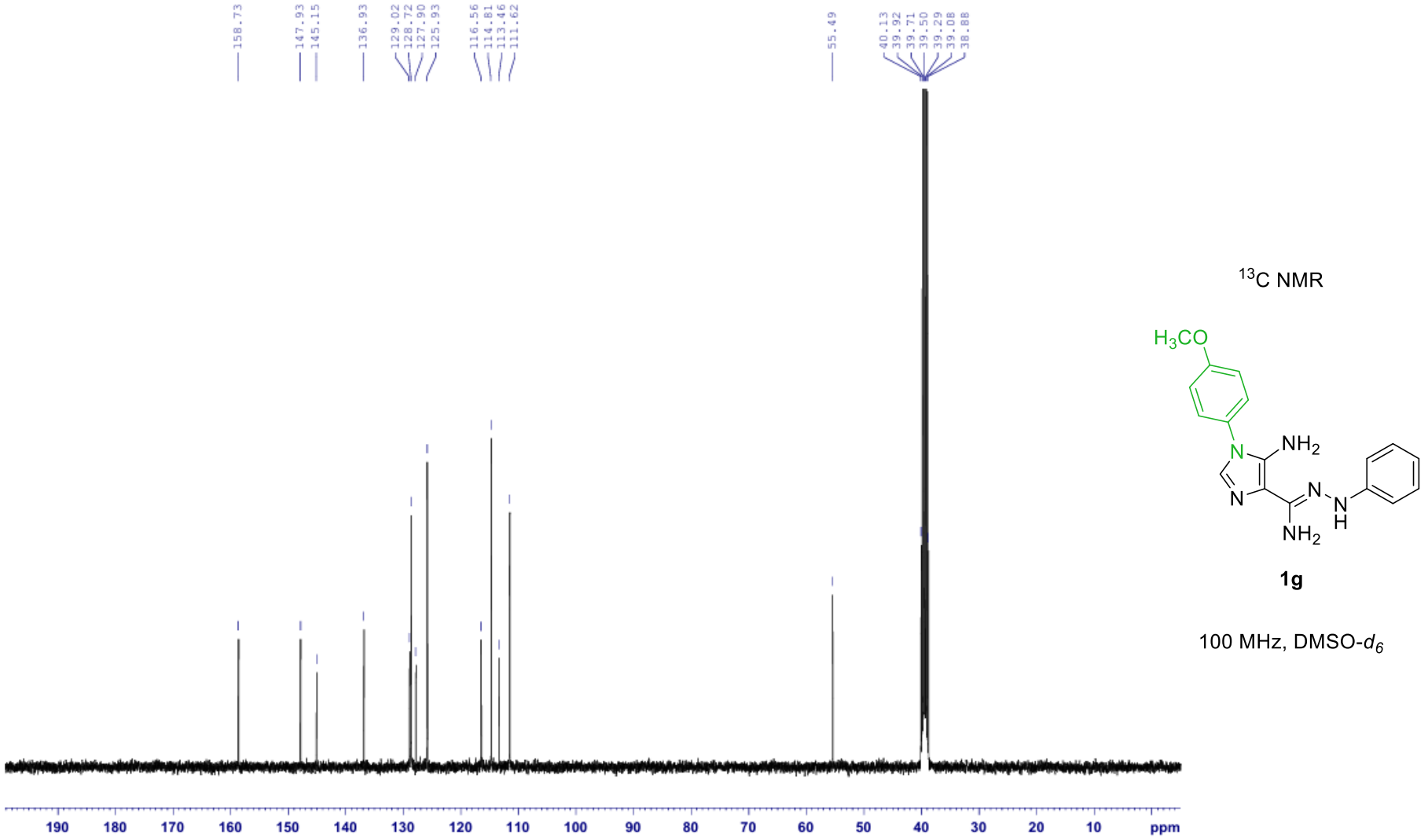

SI-Figure 24 - ^{13}C NMR spectrum of (*Z*)-5-amino-1-(4-methoxyphenyl)-*N*'-phenyl-1*H*-imidazole-4-carbohydrazonamide (**1g**).

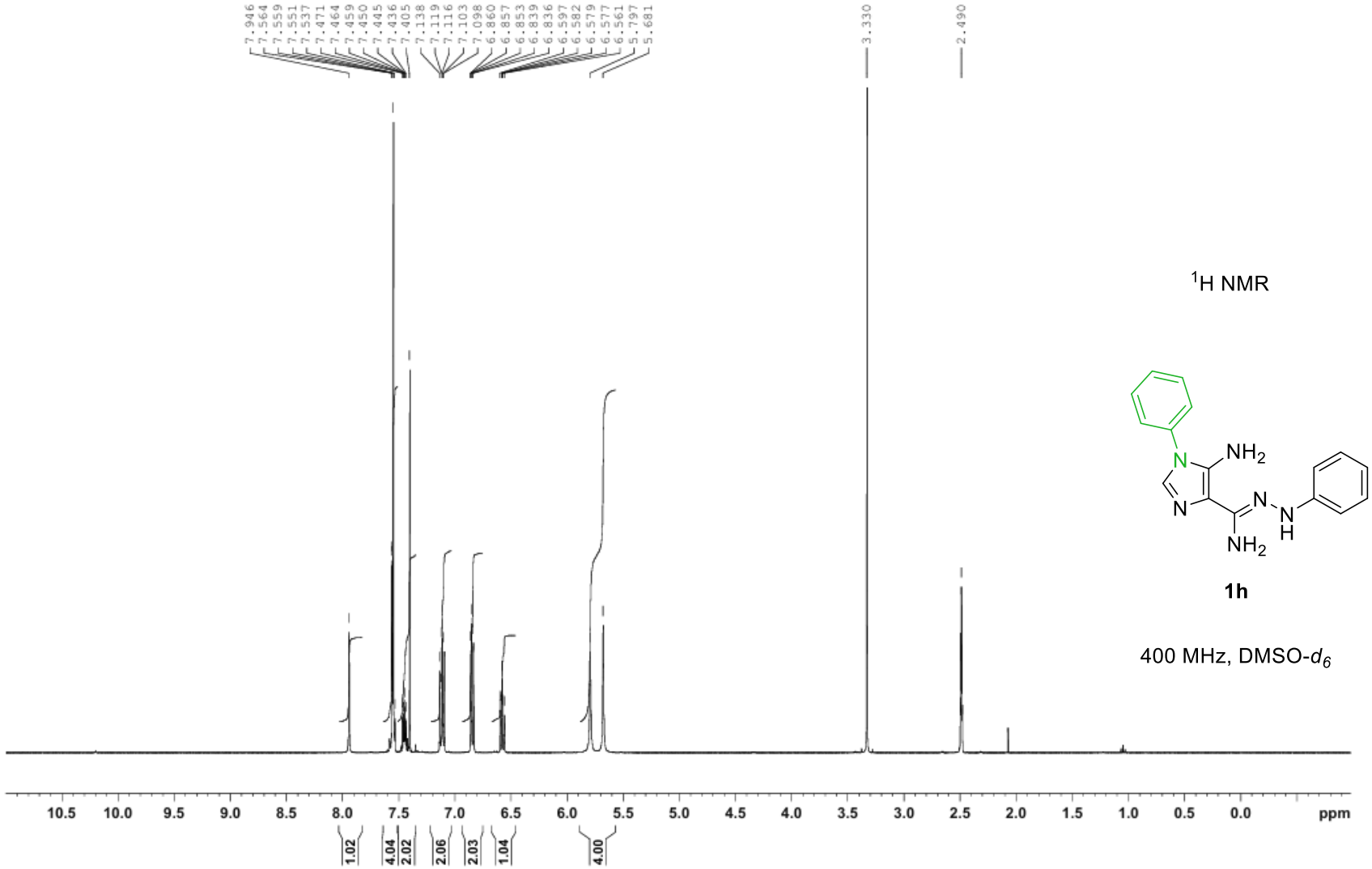

SI-Figure 25 - ^{1}H NMR spectrum of (*Z*)-5-amino-N',1-diphenyl-1*H*-imidazole-4-carbohydrazonamide (**1h**).

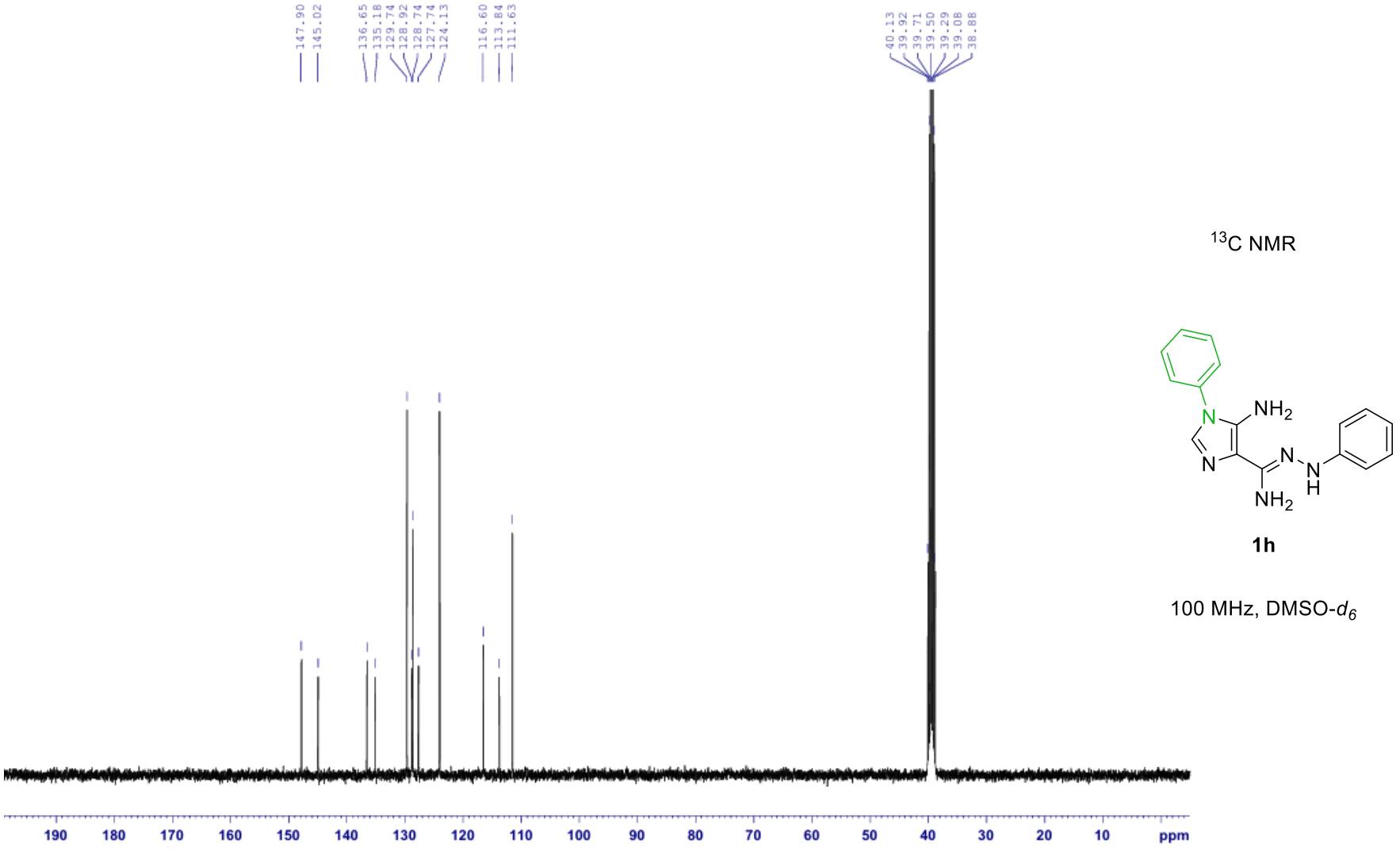

SI-Figure 26 - ^{13}C NMR spectrum of (*Z*)-5-amino-N',1-diphenyl-1*H*-imidazole-4-carbohydrazonamide (**1h**).

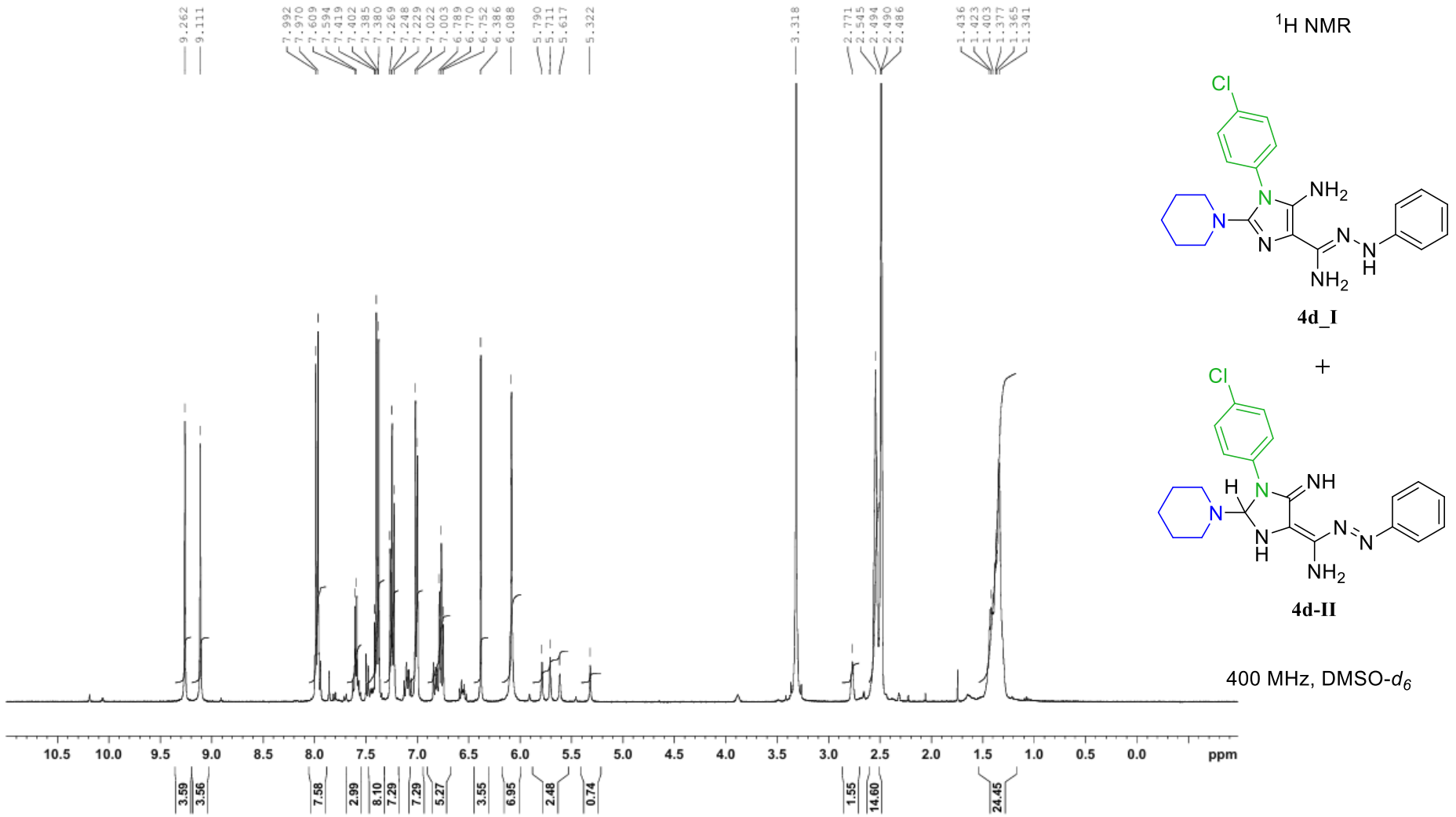

SI-Figure 27 - ^{1}H NMR spectrum of (*Z*)-5-amino-1-(4-chlorophenyl)-*N*'-phenyl-2-(piperidin-1-yl)-1*H*-imidazole-4-carbohydrazonamide (**4d_I**) and (*E*)-(1-(4-chlorophenyl)-5-imino-2-(piperidin-1-yl)imidazolidin-4-ylidene)((*E*)-phenyldiazenyl)methanamine (**4d_II**).

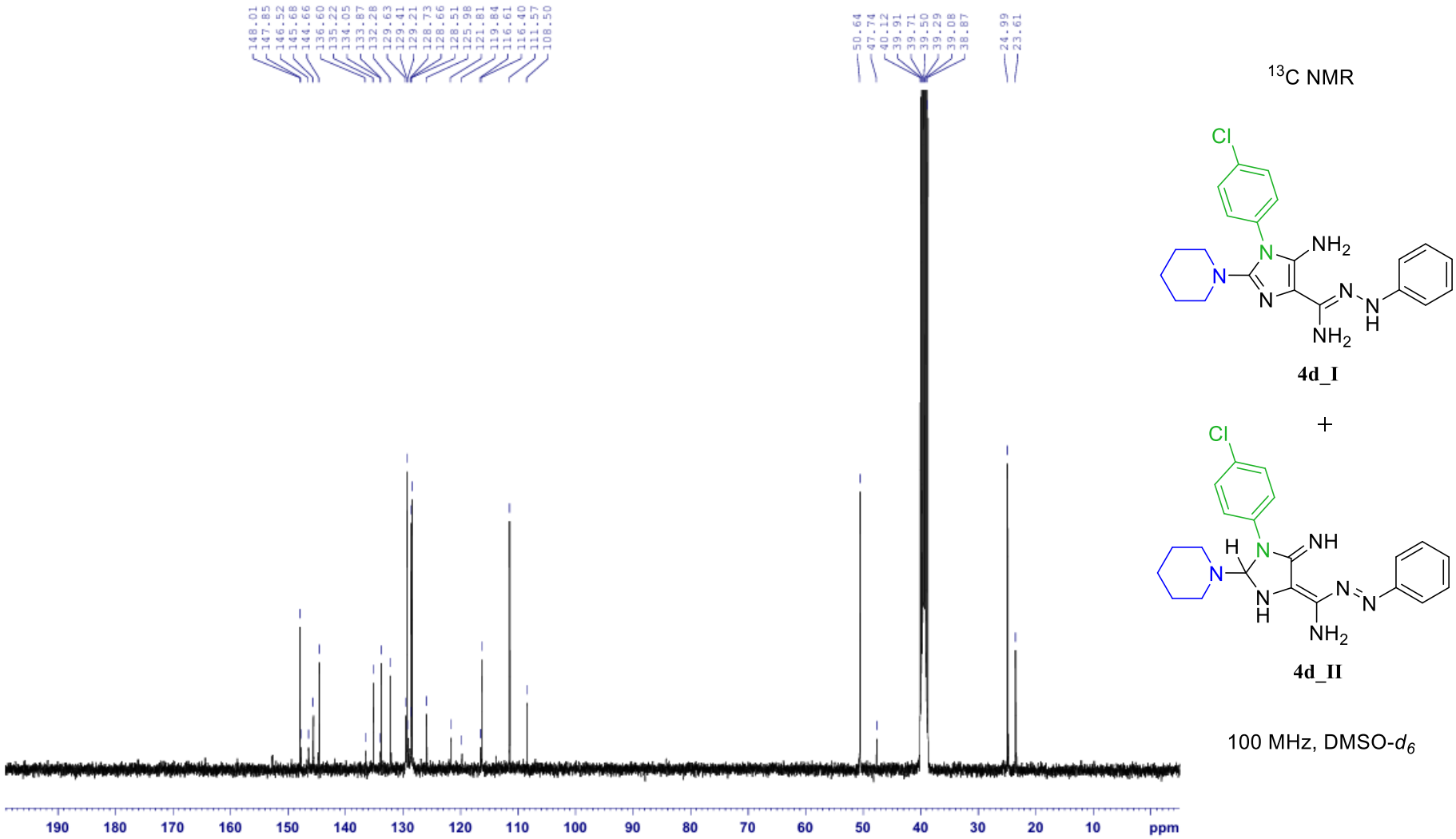

SI-Figure 28 - ^{13}C NMR spectrum of (*Z*)-5-amino-1-(4-chlorophenyl)-*N*'-phenyl-2-(piperidin-1-yl)-1*H*-imidazole-4-carbohydrazonamide (**4d_I**) and (*E*)-(1-(4-chlorophenyl)-5-imino-2-(piperidin-1-yl)imidazolidin-4-ylidene)((*E*)-phenyldiazenyl)methanamine (**4d_II**).

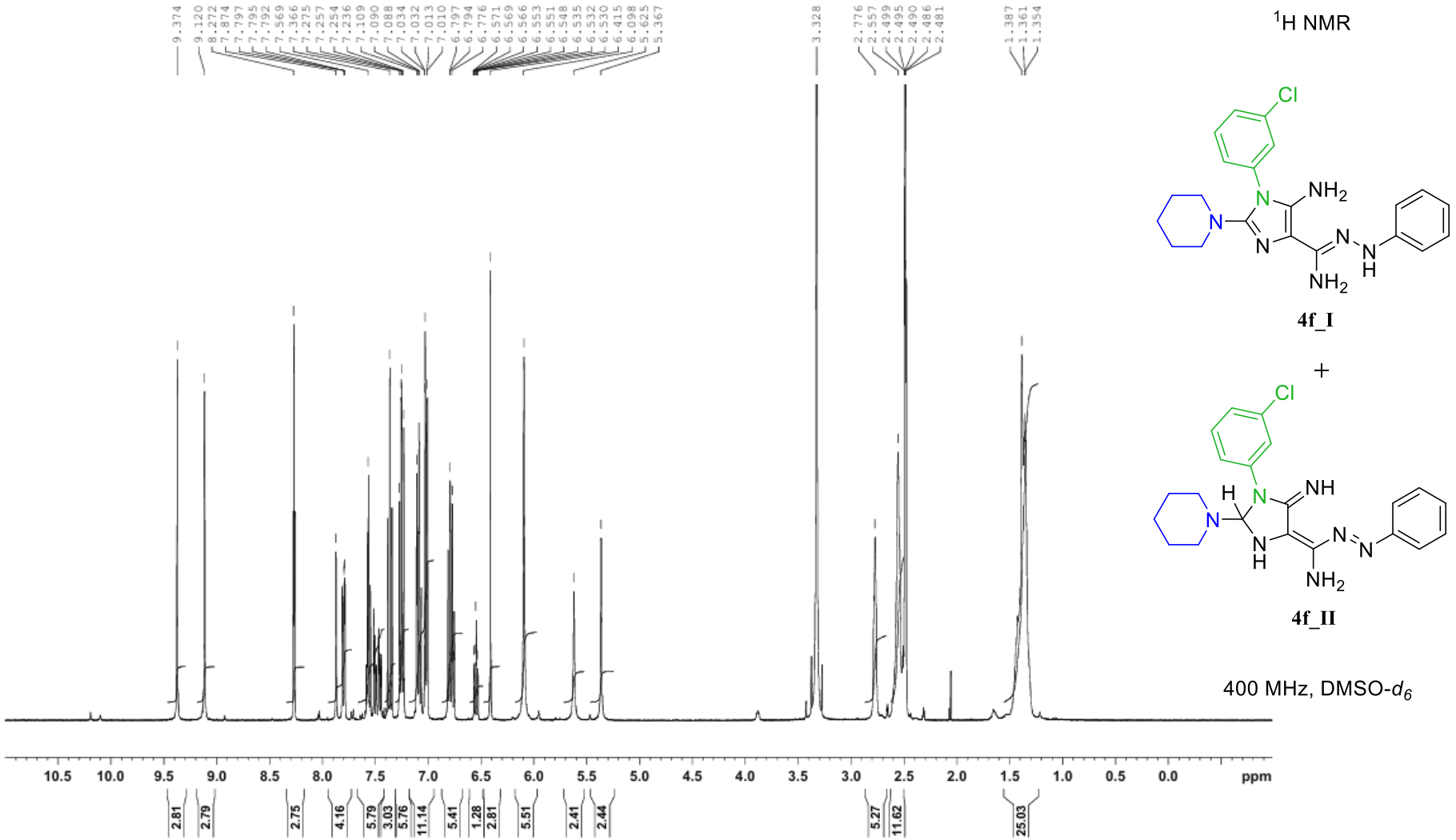

SI-Figure 29 - ^{1}H NMR spectrum of (*Z*)-5-amino-1-(3-chlorophenyl)-*N*'-phenyl-2-(piperidin-1-yl)-1*H*-imidazole-4-carbohydrazonamide (**4f_I**) and (*E*)-(1-(3-chlorophenyl)-5-imino-2-(piperidin-1-yl)imidazolidin-4-ylidene)((*E*)-phenyldiazenyl)methanamine (**4f_II**).

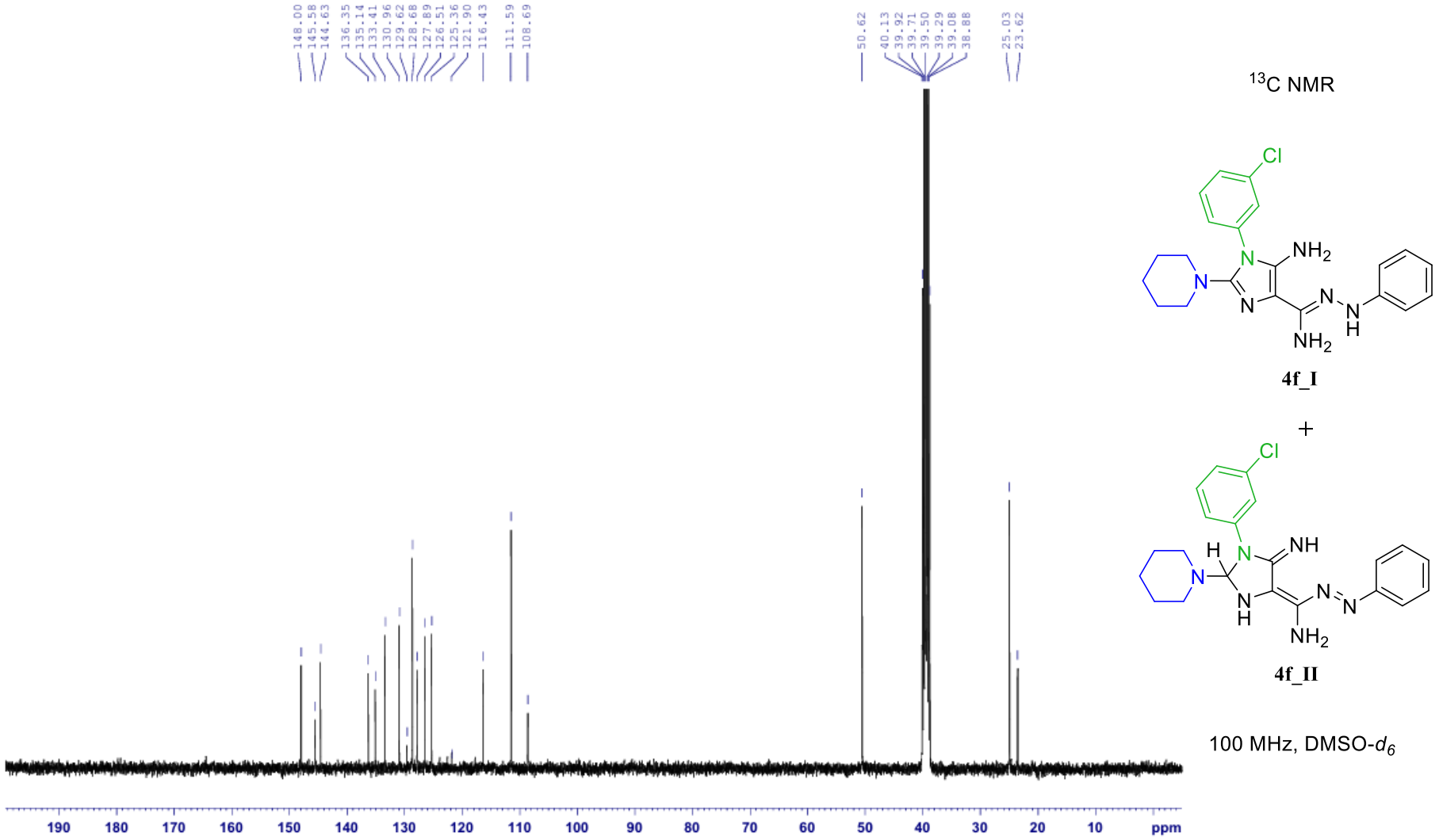

SI-Figure 30 - ^{13}C NMR spectrum of (*Z*)-5-amino-1-(3-chlorophenyl)-*N*'-phenyl-2-(piperidin-1-yl)-1*H*-imidazole-4-carbohydrazonamide (**4f_I**) and (*E*)-(1-(3-chlorophenyl)-5-imino-2-(piperidin-1-yl)imidazolidin-4-ylidene)((*E*)-phenyldiazenyl)methanamine (**4f_II**).

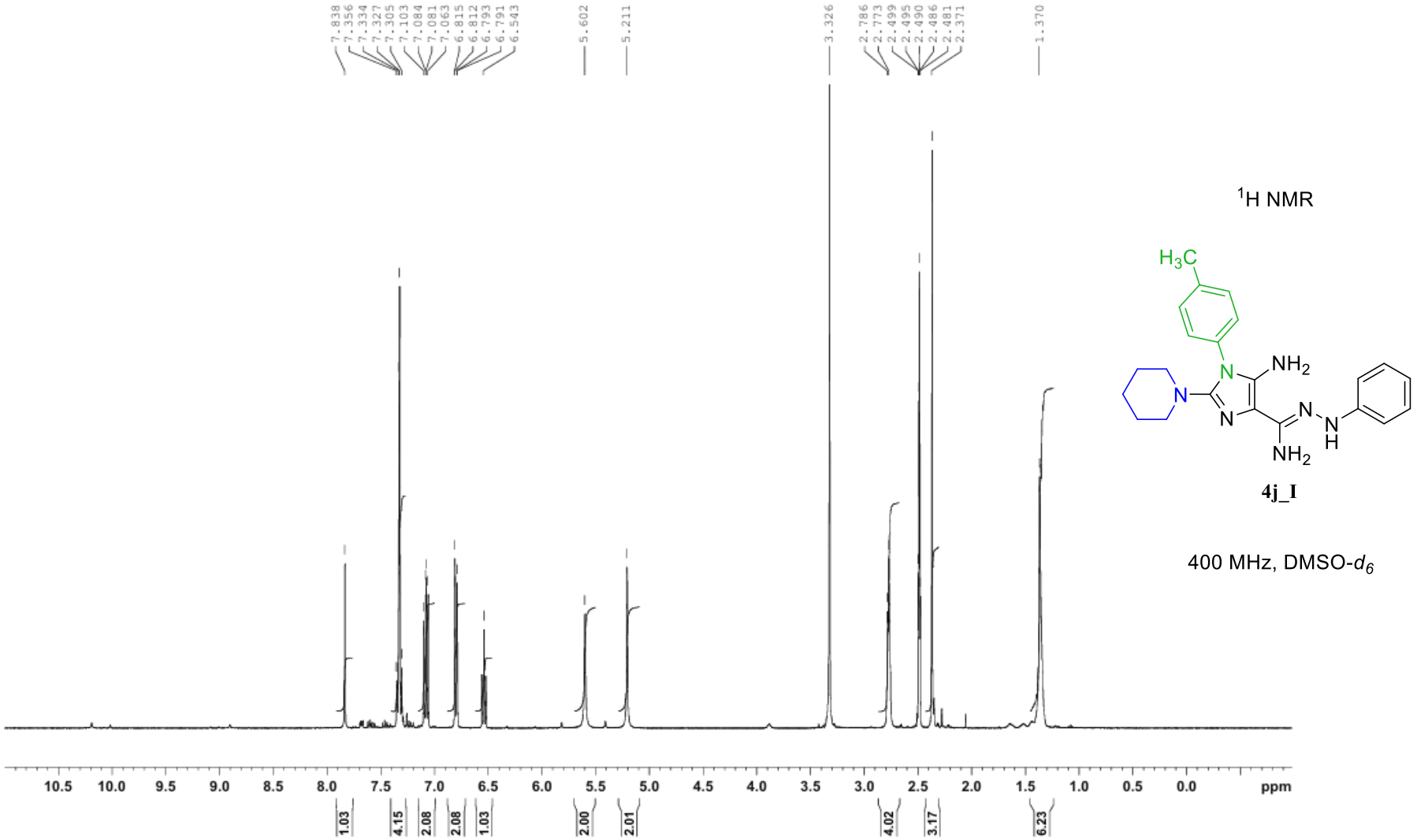

SI-Figure 31 - ^{1}H NMR spectrum of (*Z*)-5-amino-1-(*p*-tolyl)-*N*'-phenyl-2-(piperidin-1-yl)-1*H*-imidazole-4-carbohydrazonamide (**4j_I**)

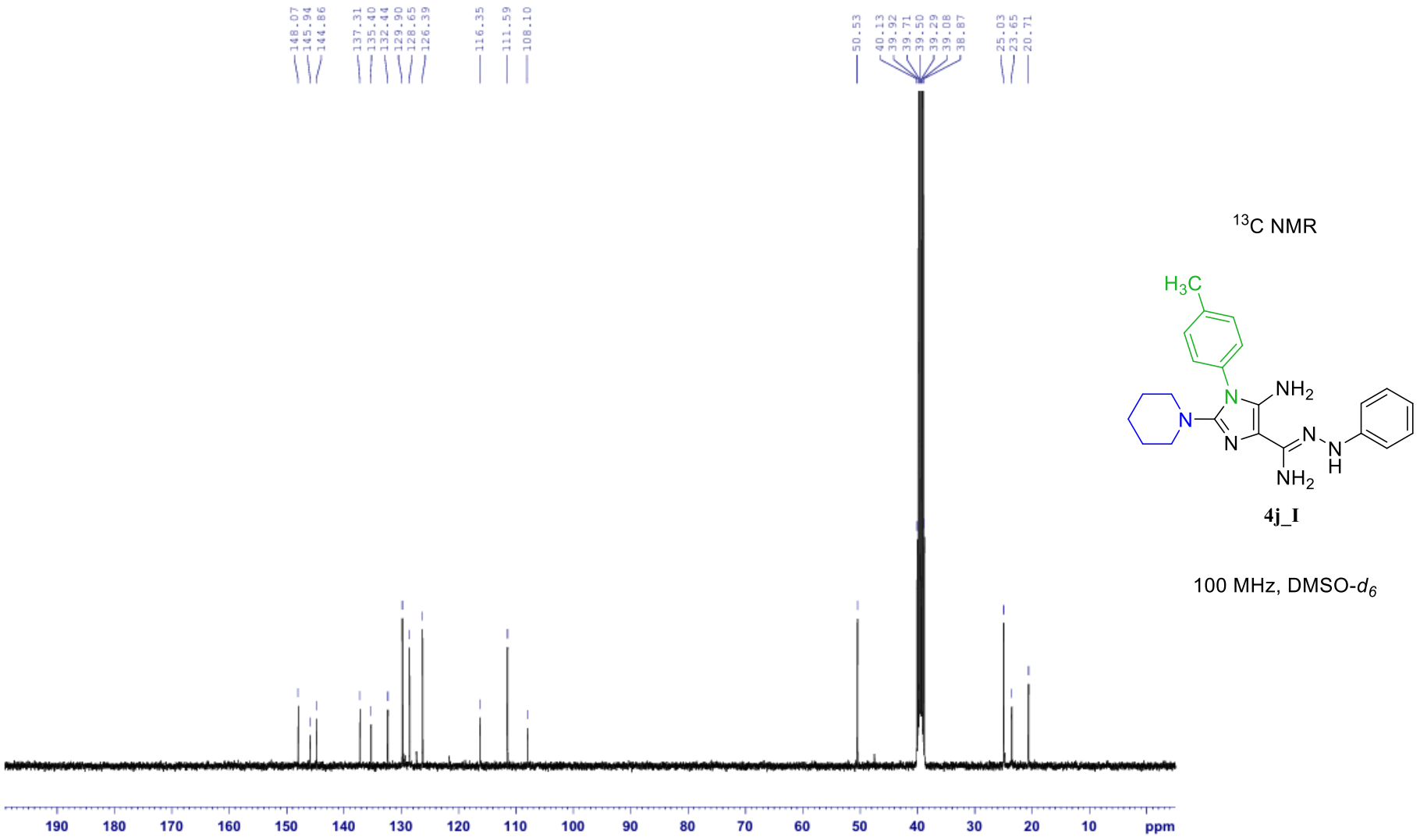

SI-Figure 32 - ^{13}C NMR spectrum of (*Z*)-5-amino-1-(*p*-tolyl)-*N*'-phenyl-2-(piperidin-1-yl)-1*H*-imidazole-4-carbohydrazonamide (**4j_I**)

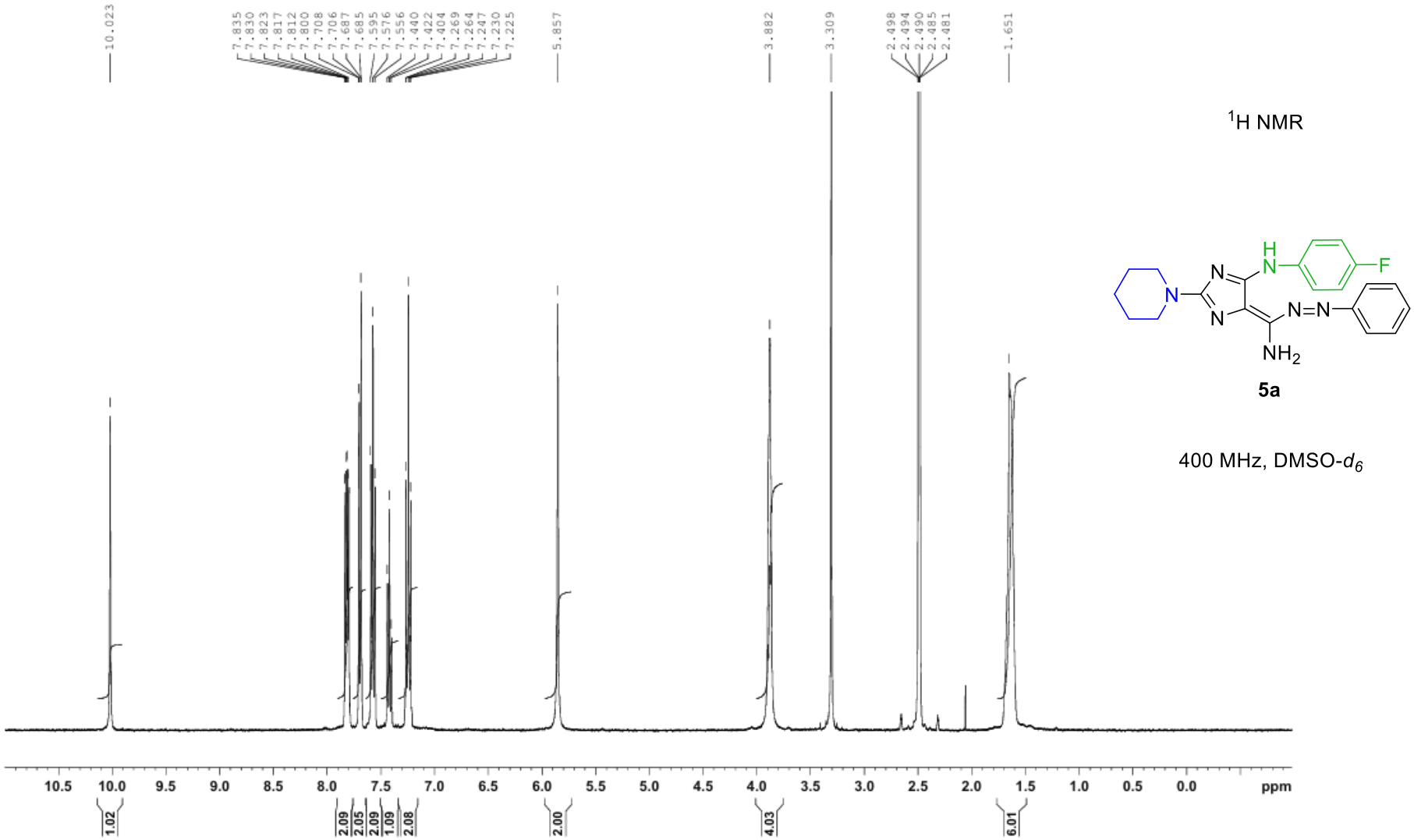

^{1}H NMR

5a

400 MHz, DMSO-d_6

SI-Figure 33 - ^{1}H NMR spectrum of (4*E*)-4-(amino(phenyldiazenyl)methylene)-*N*-(4-fluorophenyl)-2-(piperidin-1-yl)-4*H*-imidazol-5-amine (**5a**).

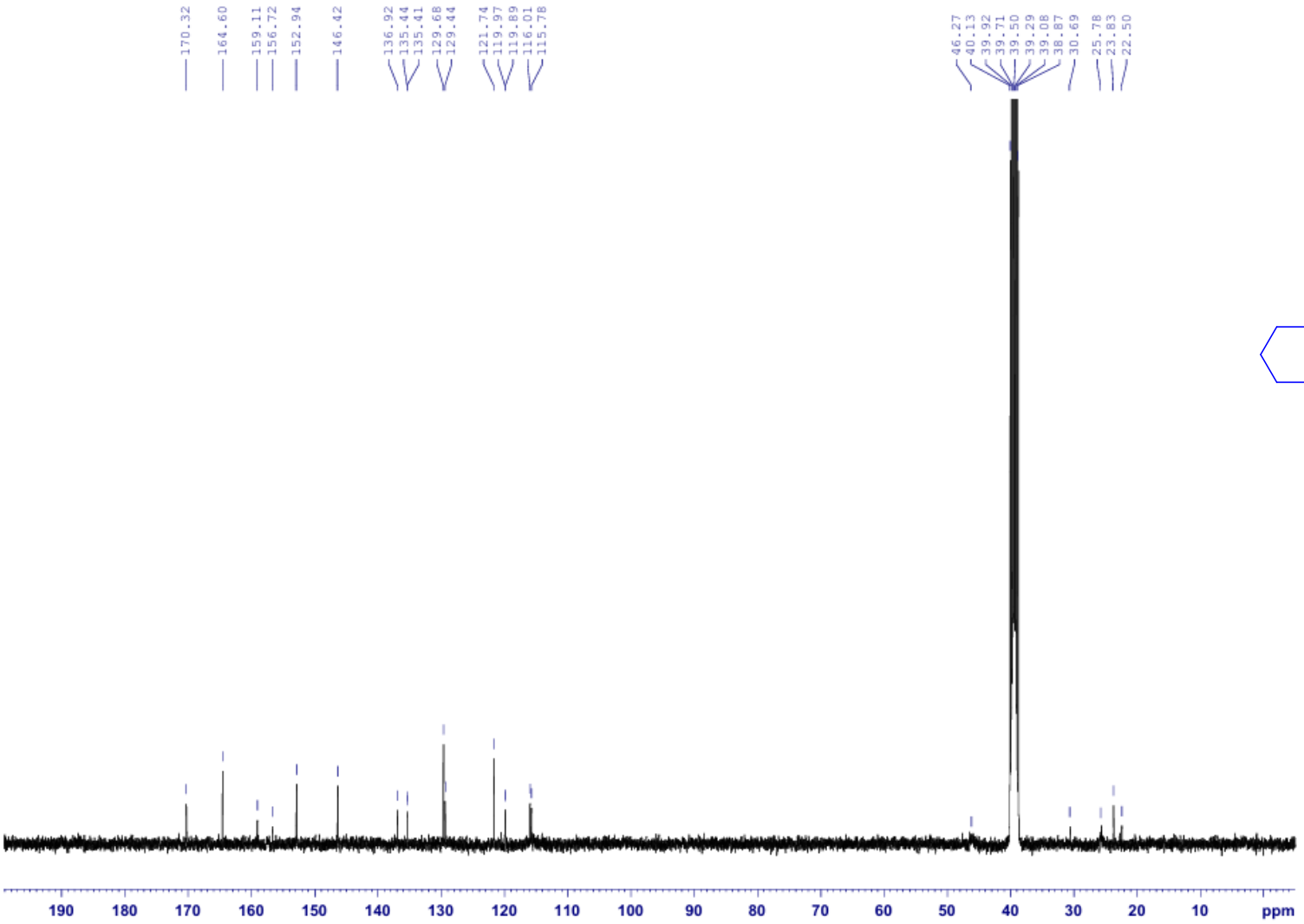

^{13}C NMR

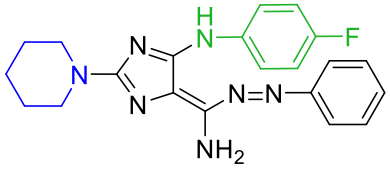

5a

100 MHz, DMSO-d_6

SI-Figure 34 - ^{13}C NMR spectrum of (4*E*)-4-(amino(phenyldiazenyl)methylene)-*N*-(4-fluorophenyl)-2-(piperidin-1-yl)-4*H*-imidazol-5-amine (**5a**).

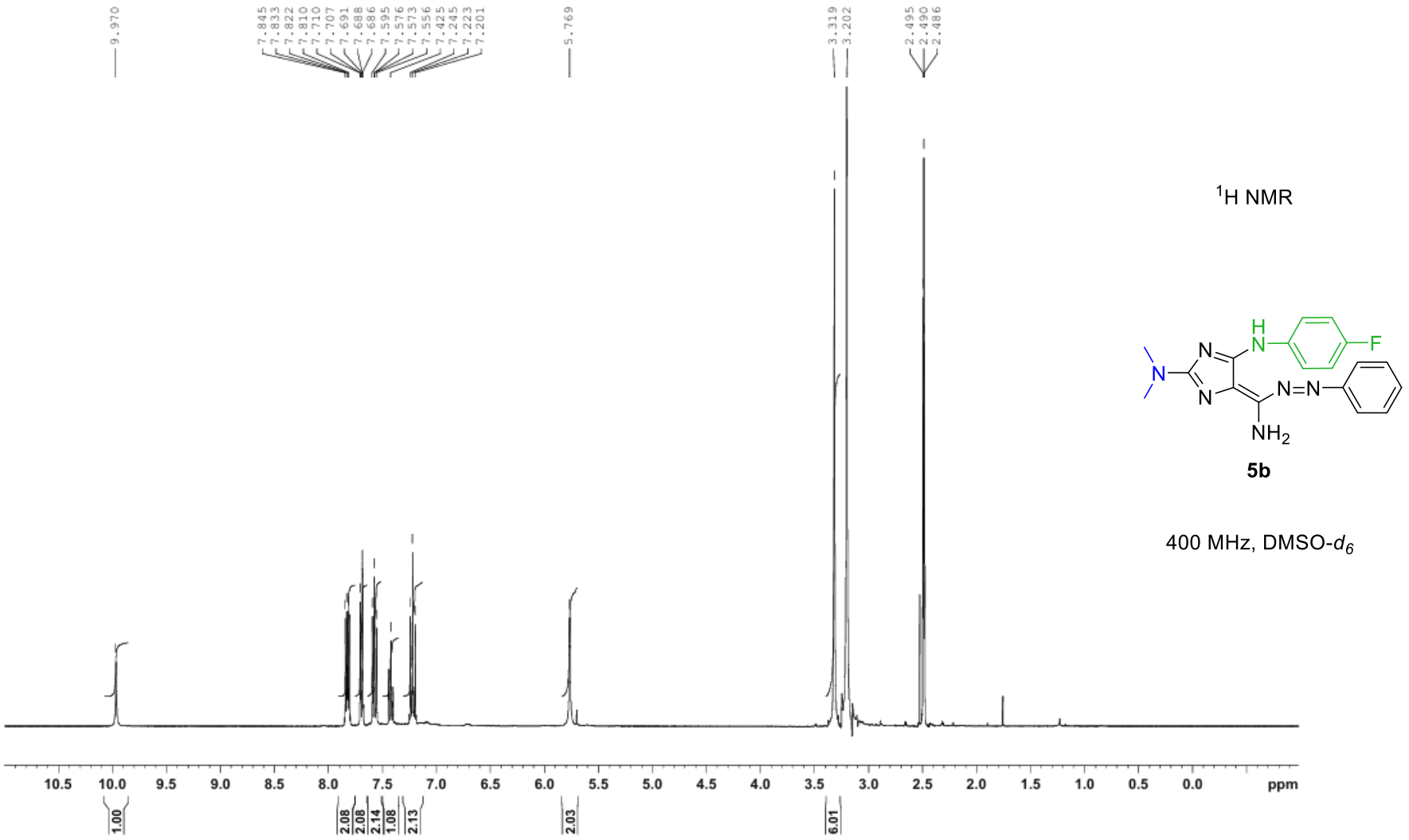

SI-Figure 35 - ^{1}H NMR spectrum of (4*E*)-4-(amino(phenyldiazenyl)methylene)-*N*5-(4-fluorophenyl)-N^2,N^2-dimethyl-4*H*-imidazole-2,5-diamine (**5b**).

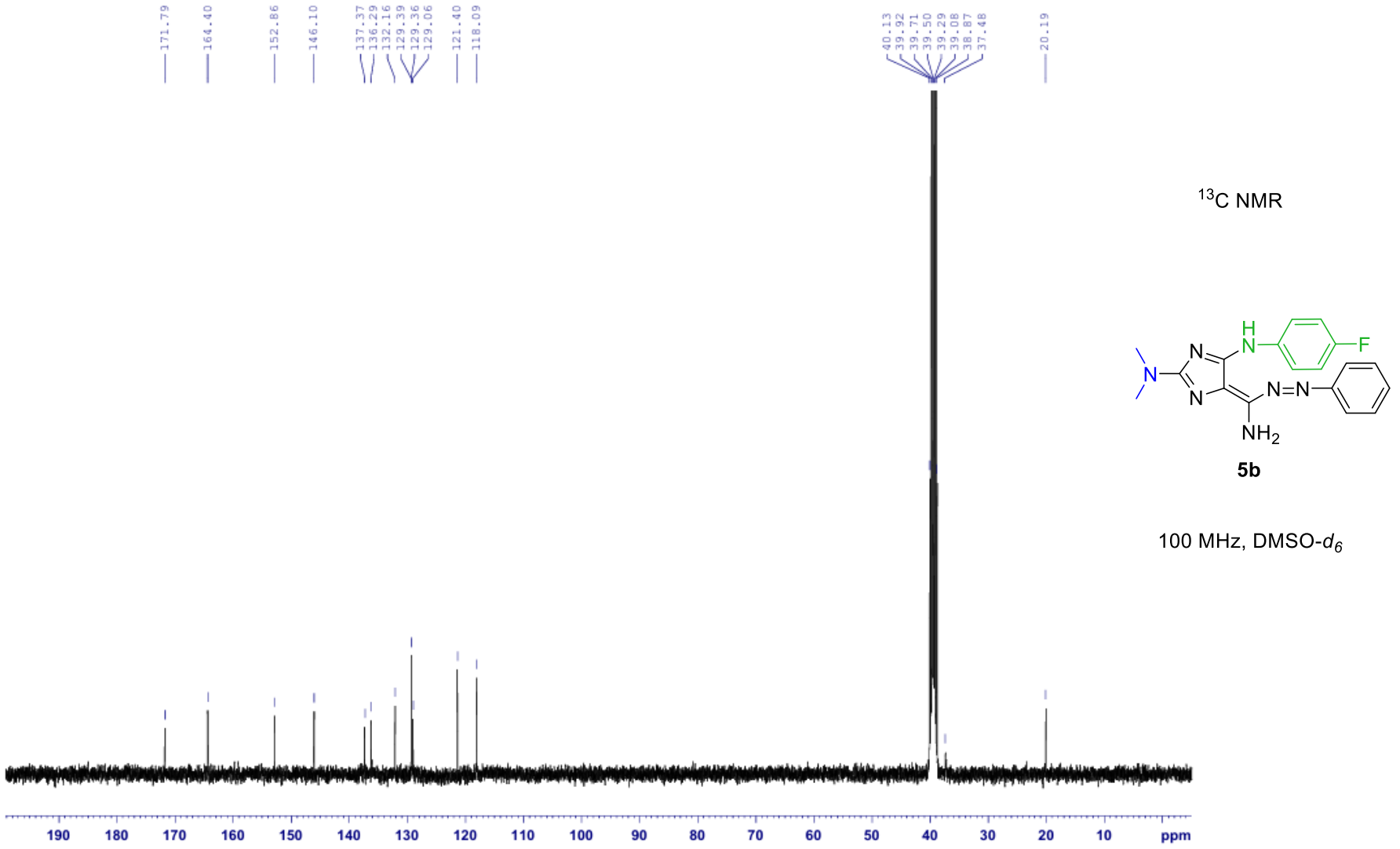

^{13}C NMR

5b

100 MHz, DMSO-d_6

SI-Figure 36 - - ^{13}C NMR spectrum of (4*E*)-4-(amino(phenyldiazenyl)methylene)-*N*5-(4-fluorophenyl)-N^2,N^2-dimethyl-4*H*-imidazole-2,5-diamine (**5b**).

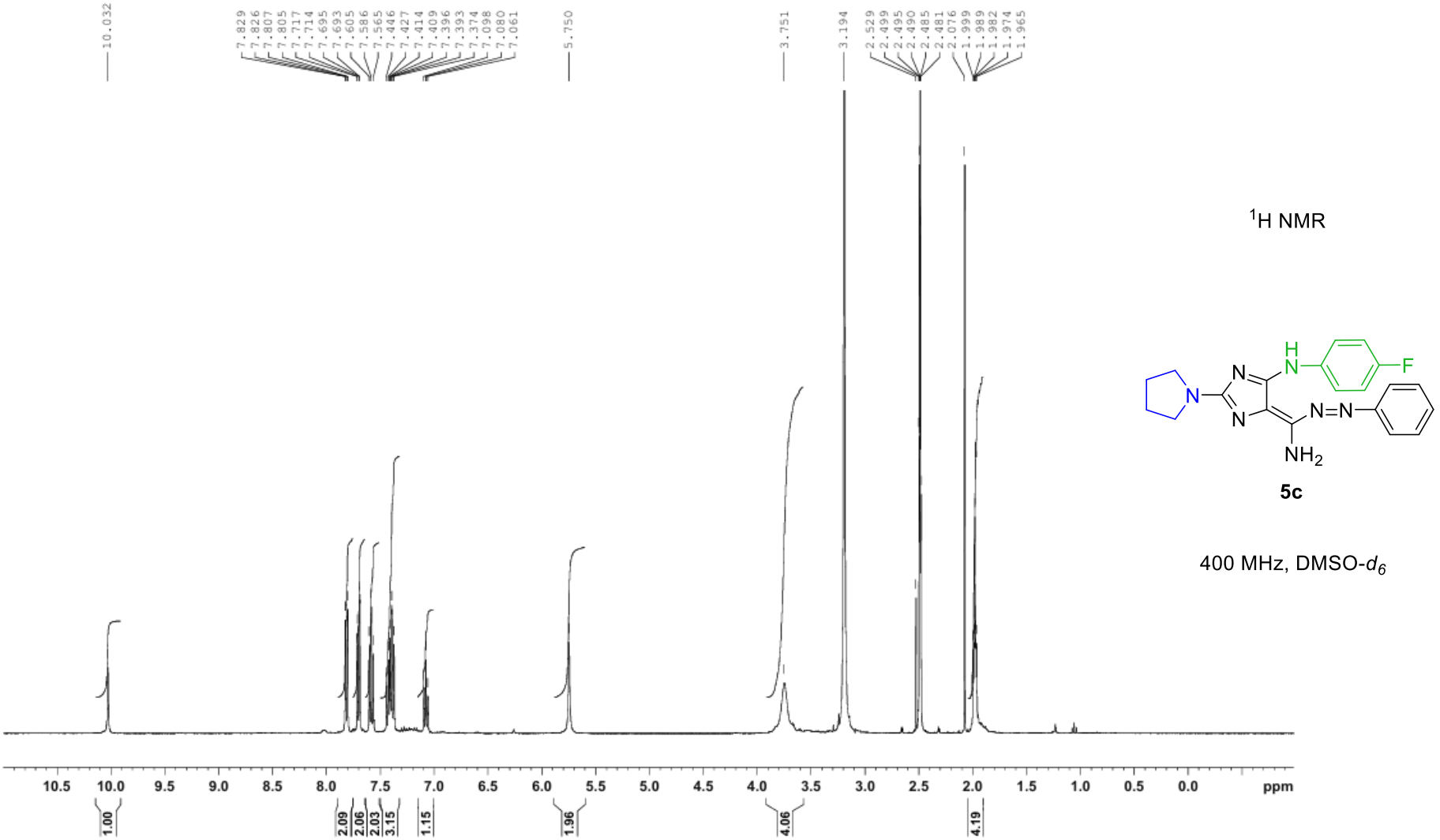

SI-Figure 37 - ^{1}H NMR spectrum of (4*E*)-4-(amino(phenyldiazenyl)methylene)-*N*-(4-fluorophenyl)-2-(pyrrolidin-1-yl)-4*H*-imidazol-5-amine (**5c**).

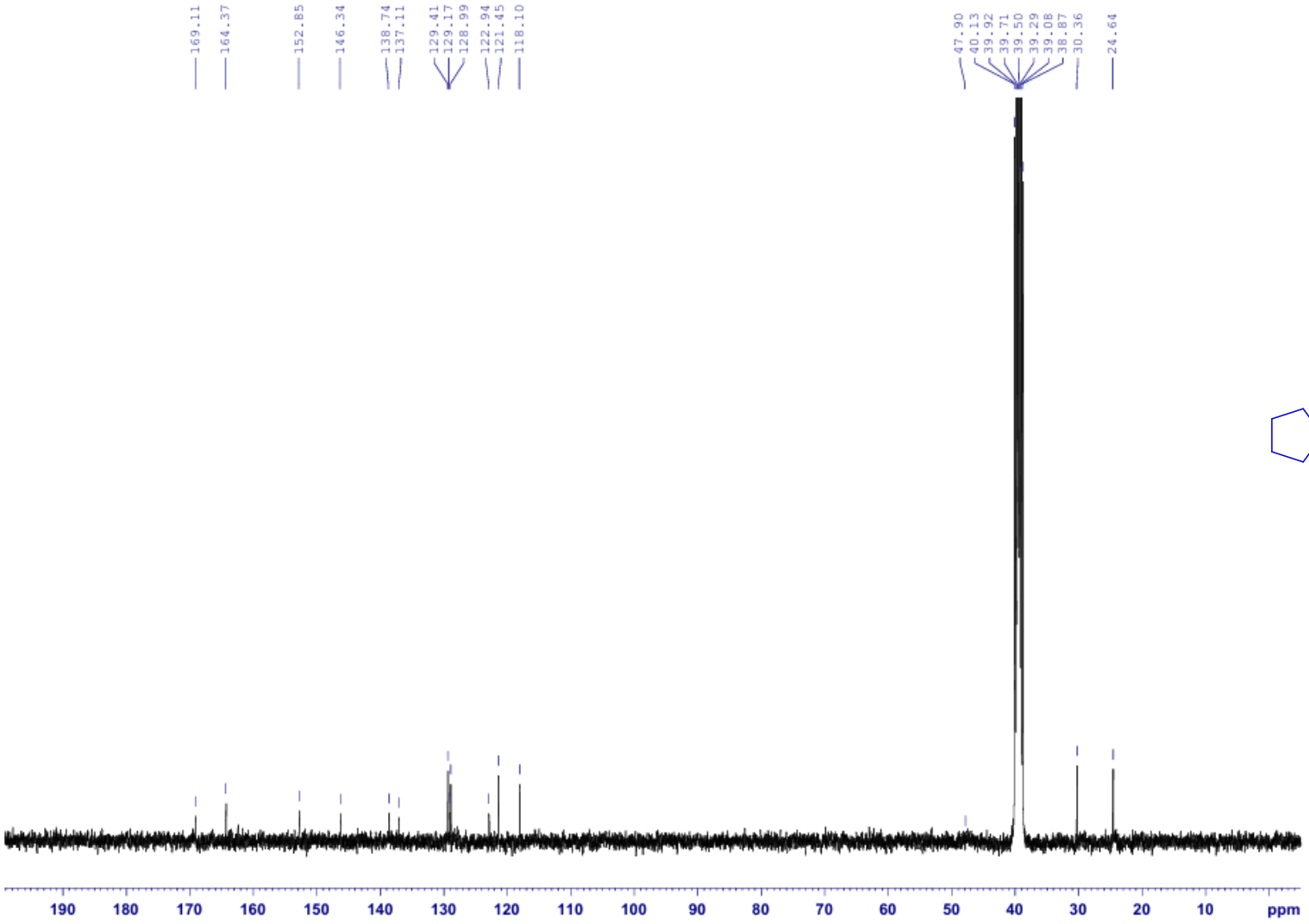

^{13}C NMR

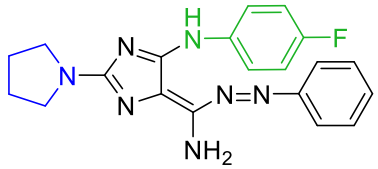

5c

100 MHz, DMSO-d_6

SI-Figure 38 – ^{13}C NMR spectrum of (4*E*)-4-(amino(phenyldiazenyl)methylene)-*N*-(4-fluorophenyl)-2-(pyrrolidin-1-yl)-4*H*-imidazol-5-amine (**5c**).

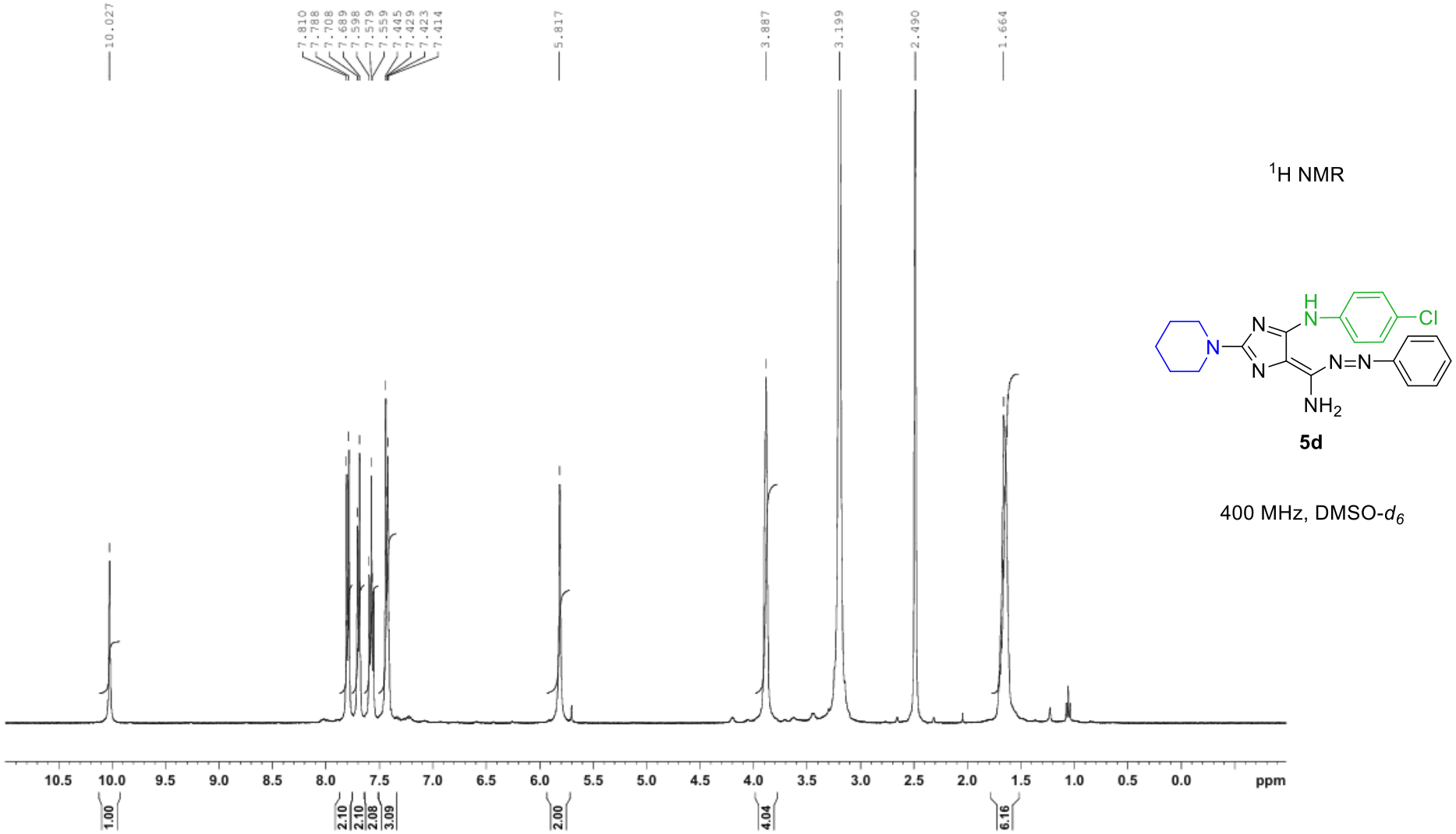

SI-Figure 39 - ^{1}H NMR spectrum of (4*E*)-4-(amino(phenyldiazenyl)methylene)-*N*-(4-chlorophenyl)-2-(piperidin-1-yl)-4*H*-imidazol-5-amine (**5d**).

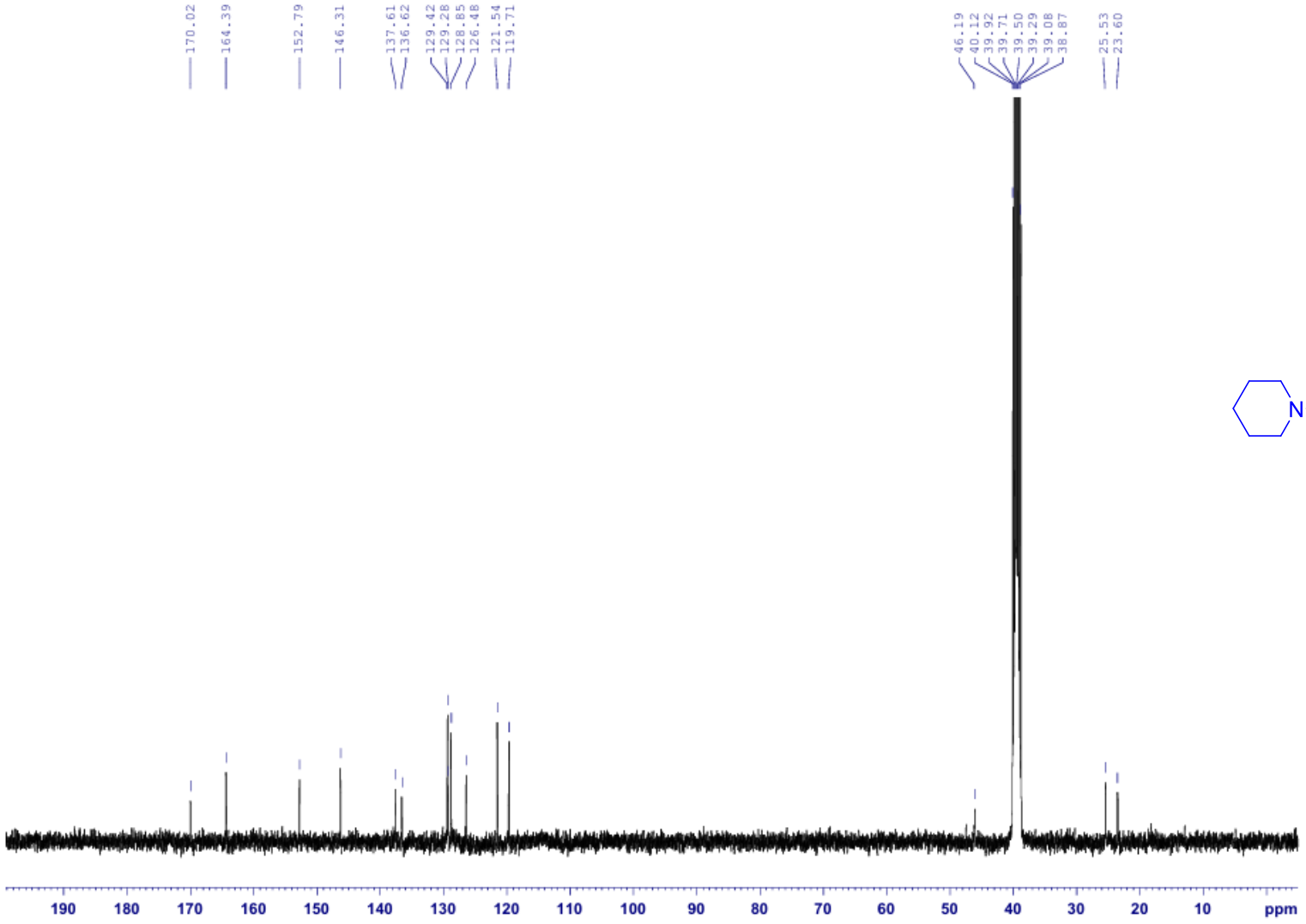

^{13}C NMR

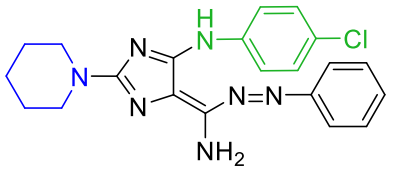

5d

100 MHz, DMSO-d_6

SI-Figure 40 - ^{13}C NMR spectrum of (4*E*)-4-(amino(phenyldiazenyl)methylene)-*N*-(4-chlorophenyl)-2-(piperidin-1-yl)-4*H*-imidazol-5-amine (**5d**).

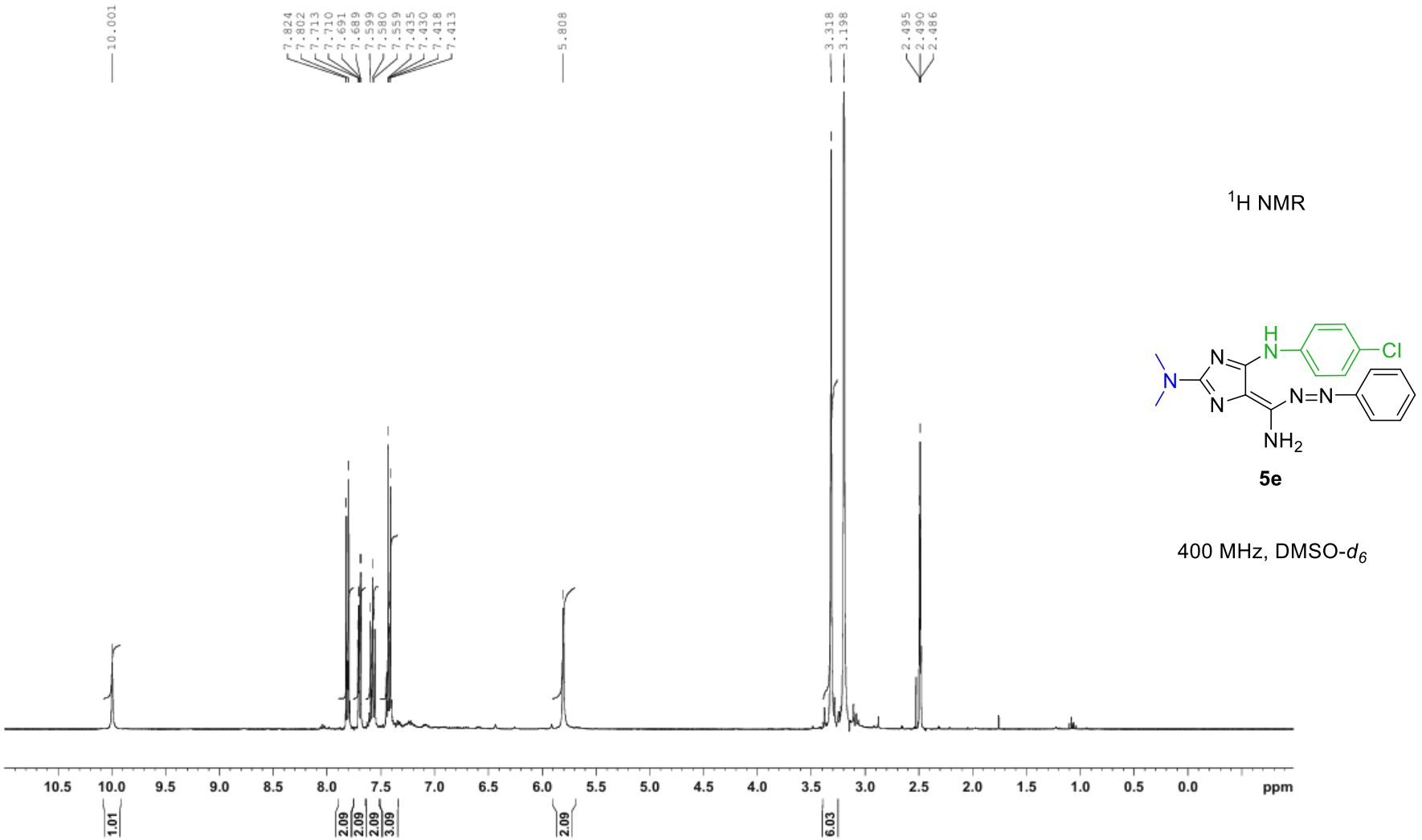

^{1}H NMR

5e

400 MHz, DMSO-d_6

SI-Figure 41 - ^{1}H NMR spectrum of (4*E*)-4-(amino(phenyldiazenyl)methylene)-*N*5-(4-chlorophenyl)-N^2,N^2-dimethyl-4*H*-imidazole-2,5-diamine (**5e**).

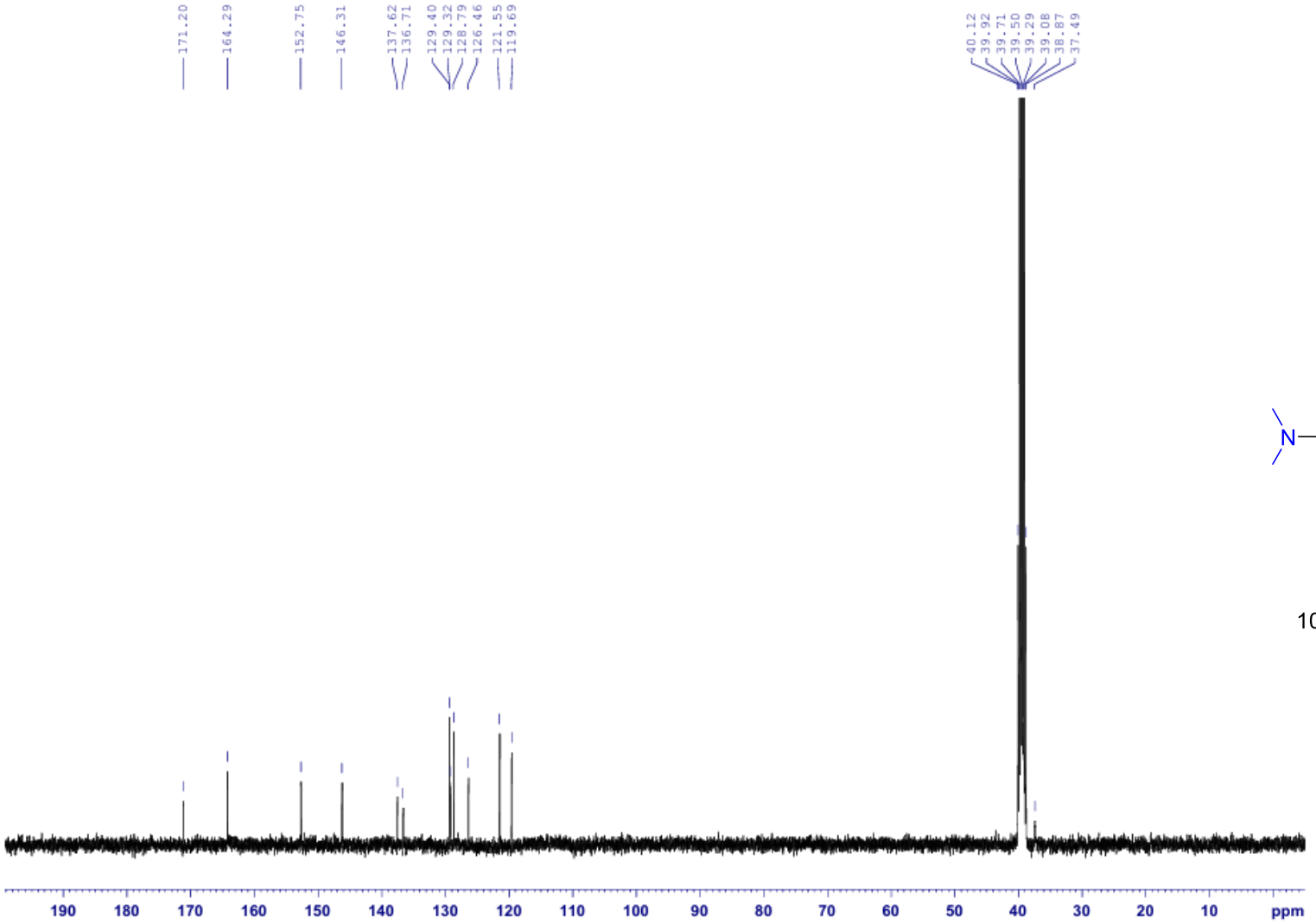

^{13}C NMR

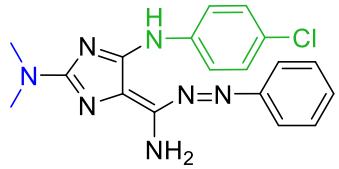

5e

100 MHz, DMSO-d_6

SI-Figure 42 - ^{13}C NMR spectrum of (4*E*)-4-(amino(phenyldiazenyl)methylene)-*N*5-(4-chlorophenyl)-N^2,N^2-dimethyl-4*H*-imidazole-2,5-diamine (**5e**).

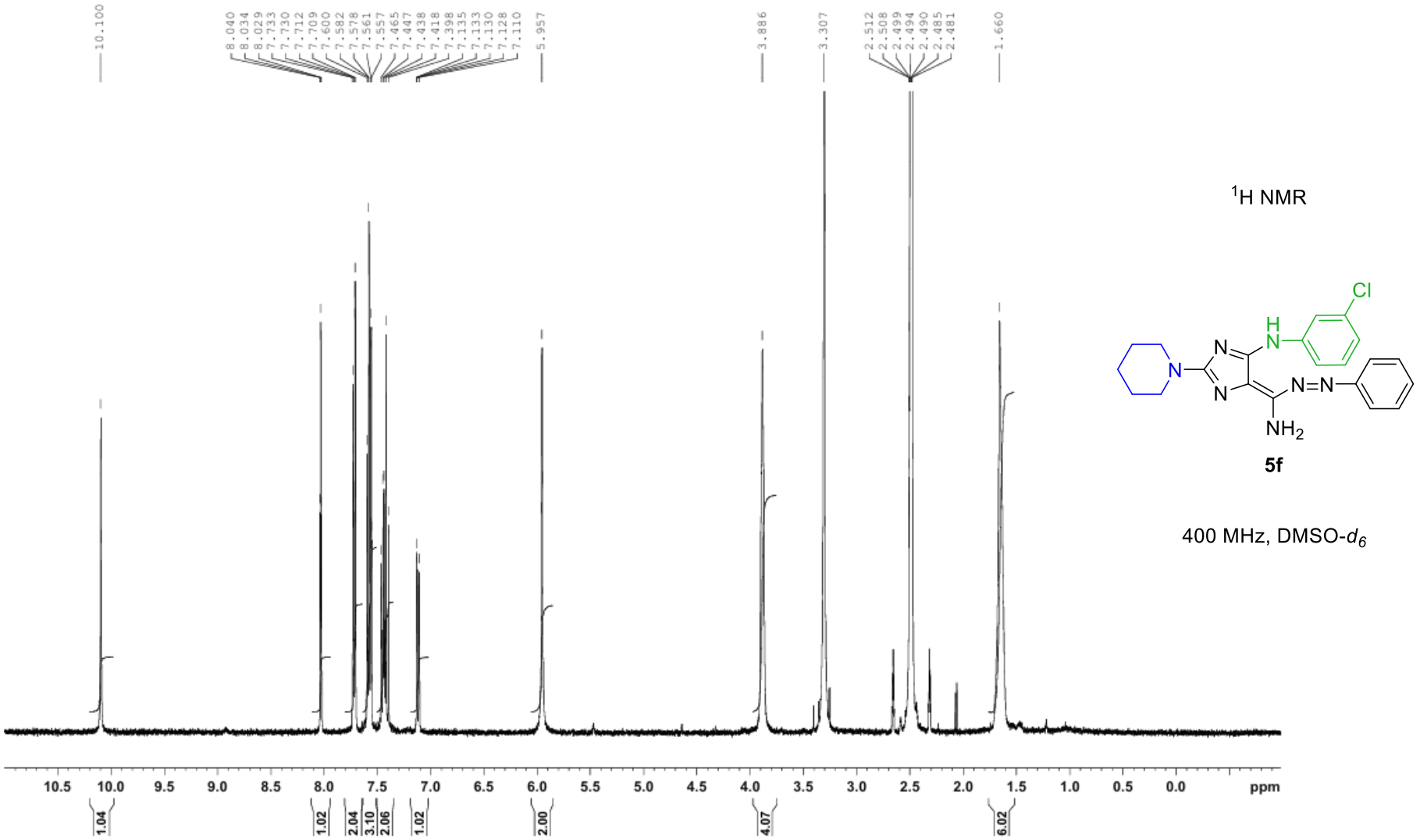

SI-Figure 43 - ^{1}H NMR spectrum of (4*E*)-4-(amino(phenyldiazenyl)methylene)-*N*-(3-chlorophenyl)-2-(piperidin-1-yl)-4*H*-imidazol-5-amine (**5f**).

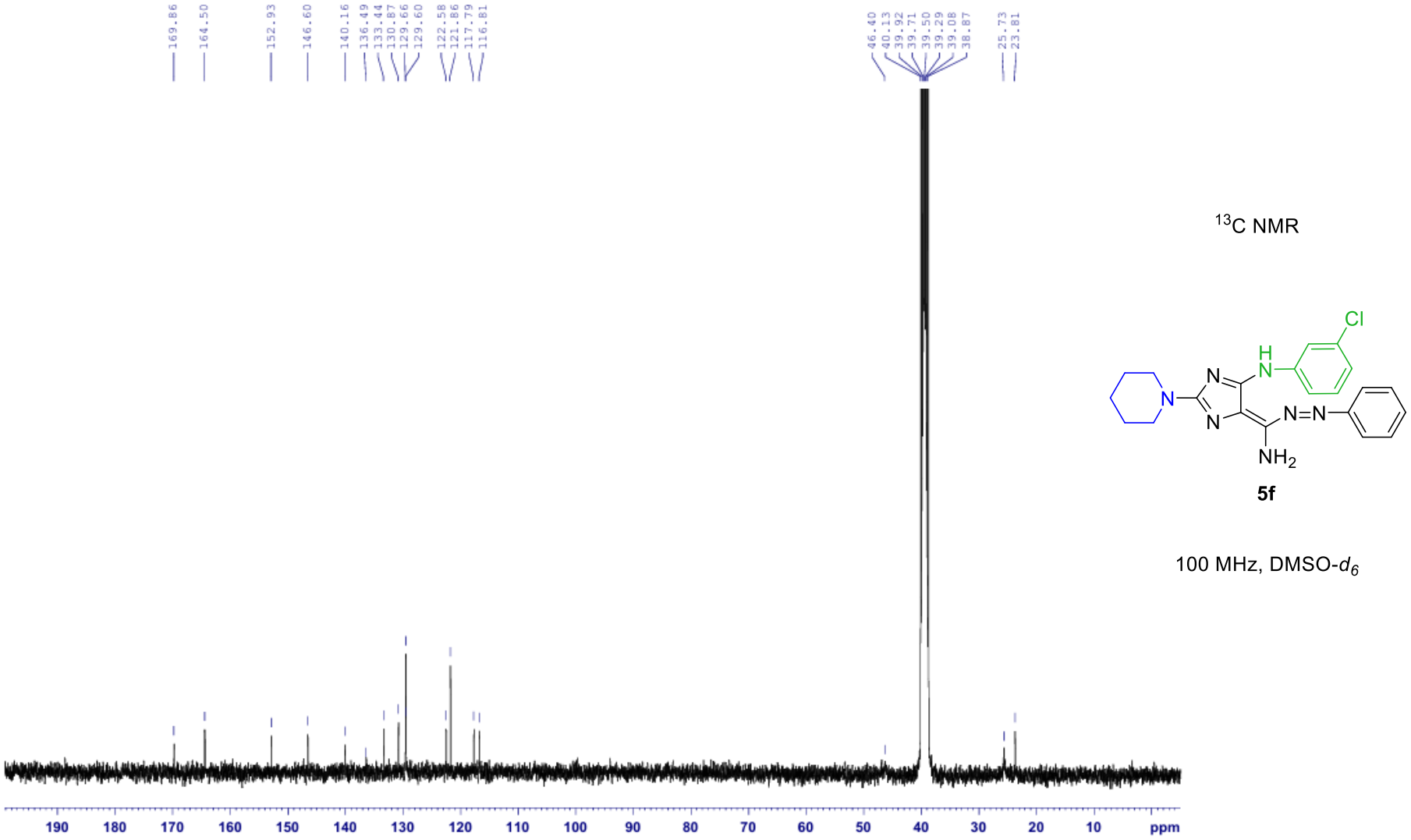

SI-Figure 44 - ^{13}C NMR spectrum of (4*E*)-4-(amino(phenyldiazenyl)methylene)-*N*-(3-chlorophenyl)-2-(piperidin-1-yl)-4*H*-imidazol-5-amine (**5f**).

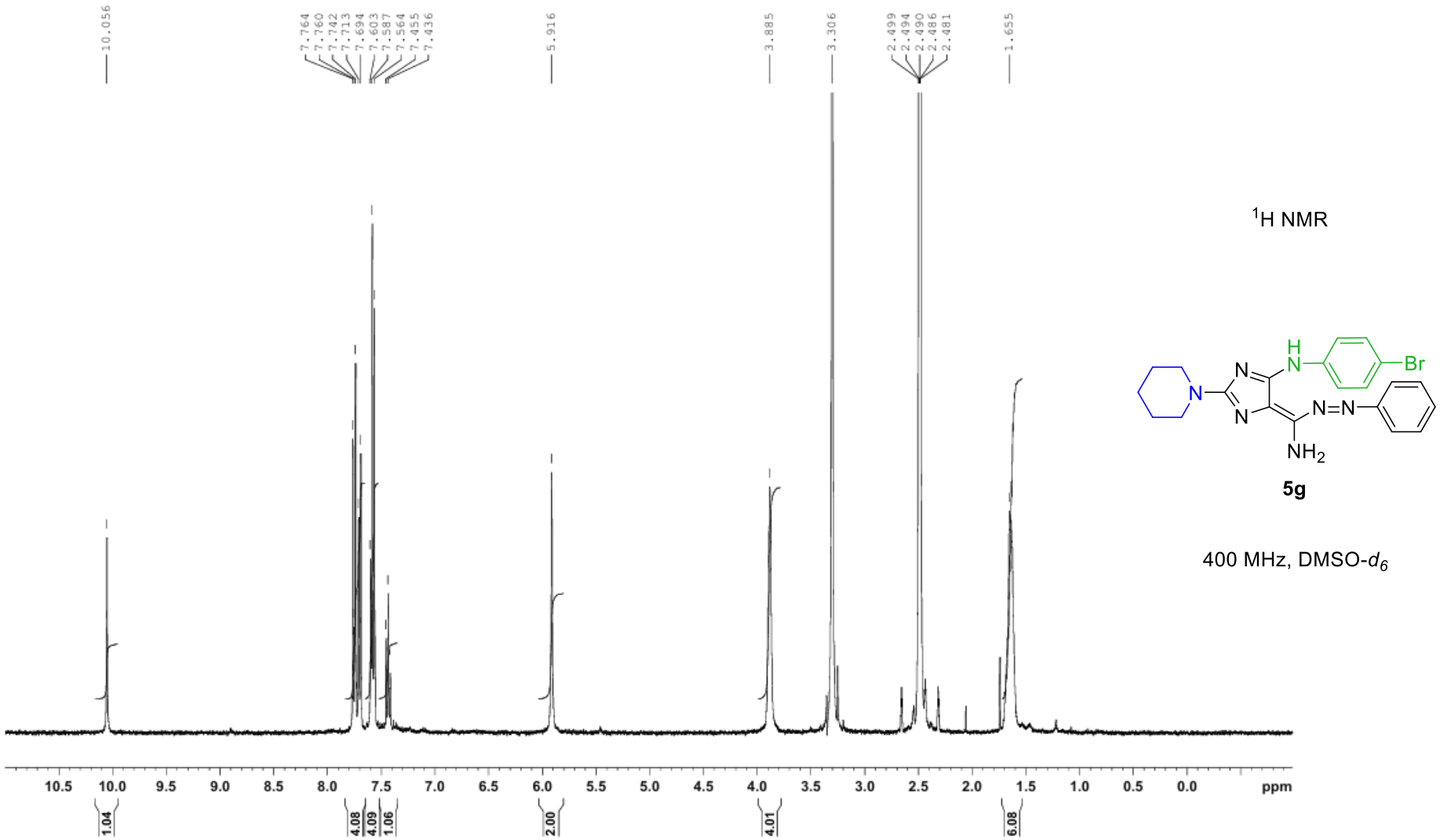

SI-Figure 45 - ^{1}H NMR spectrum of (4*E*)-4-(amino(phenyldiazenyl)methylene)-*N*-(4-bromophenyl)-2-(piperidin-1-yl)-4*H*-imidazol-5-amine (**5g**).

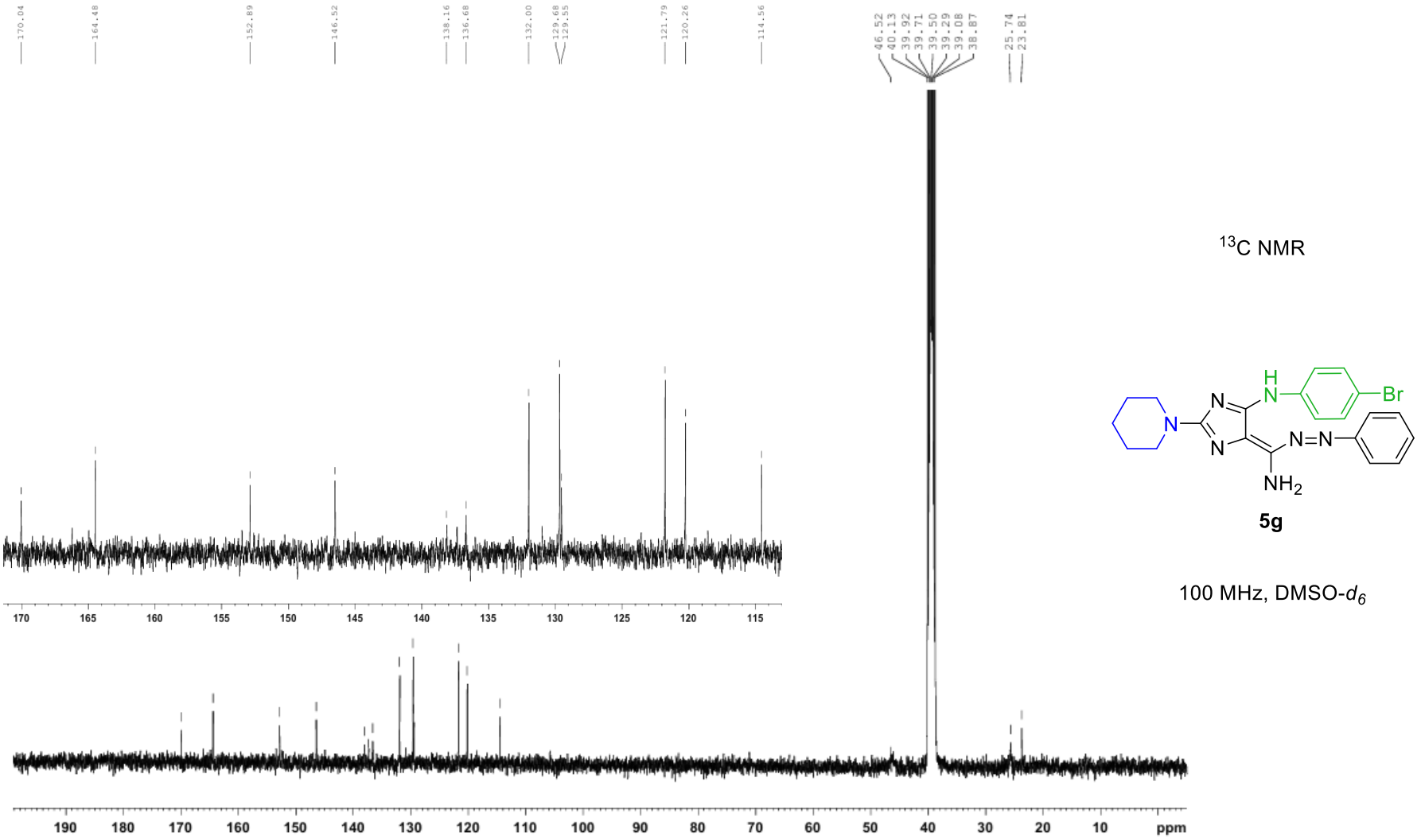

SI-Figure 46 - ^{13}C NMR spectrum of (4*E*)-4-(amino(phenyldiazenyl)methylene)-*N*-(4-bromophenyl)-2-(piperidin-1-yl)-4*H*-imidazol-5-amine (**5g**).

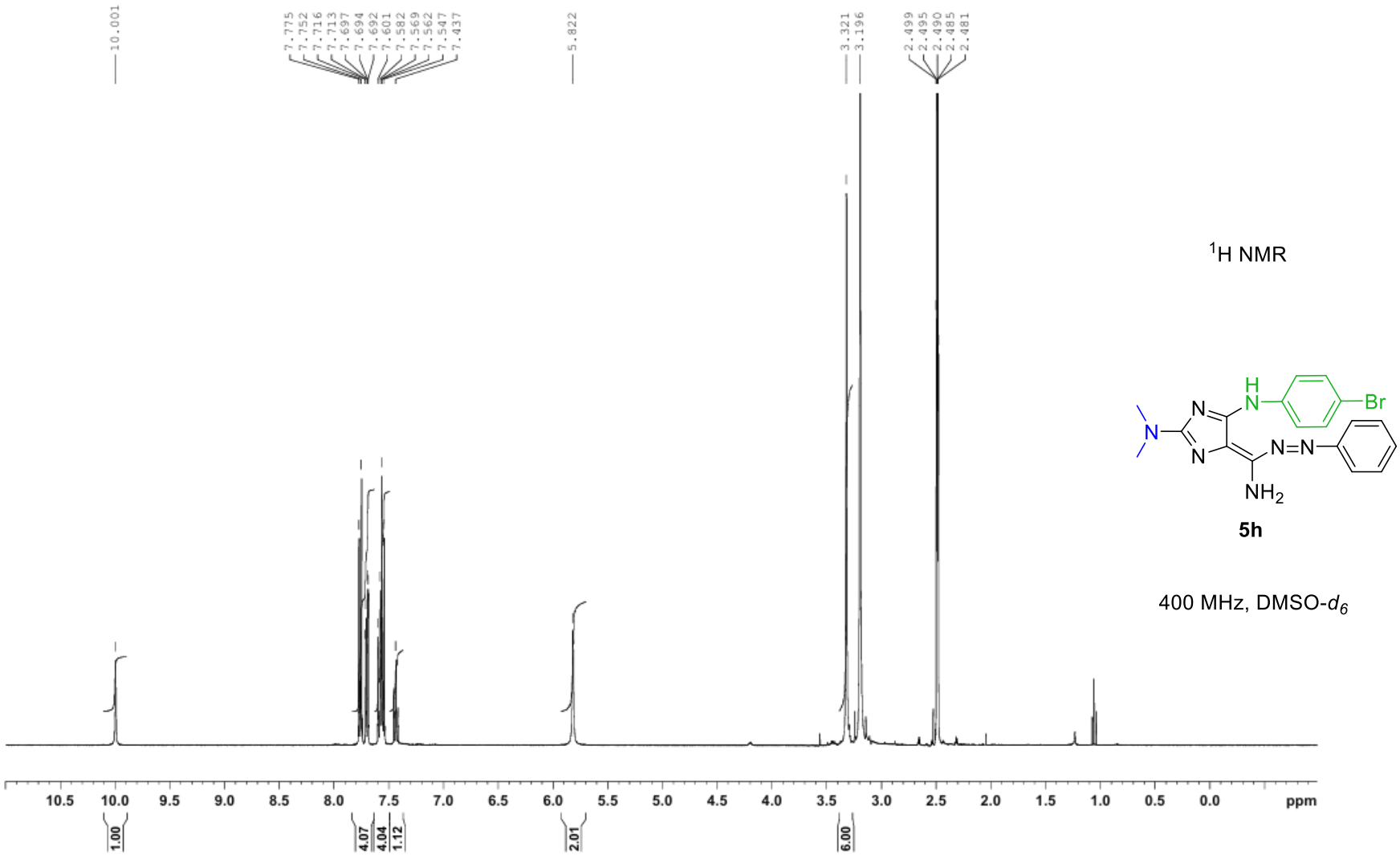

SI-Figure 47 - ^{1}H NMR spectrum of (4*E*)-4-(amino(phenyldiazenyl)methylene)-*N*5-(4-bromophenyl)-N^2,N^2-dimethyl-4*H*-imidazole-2,5-diamine (**5h**).

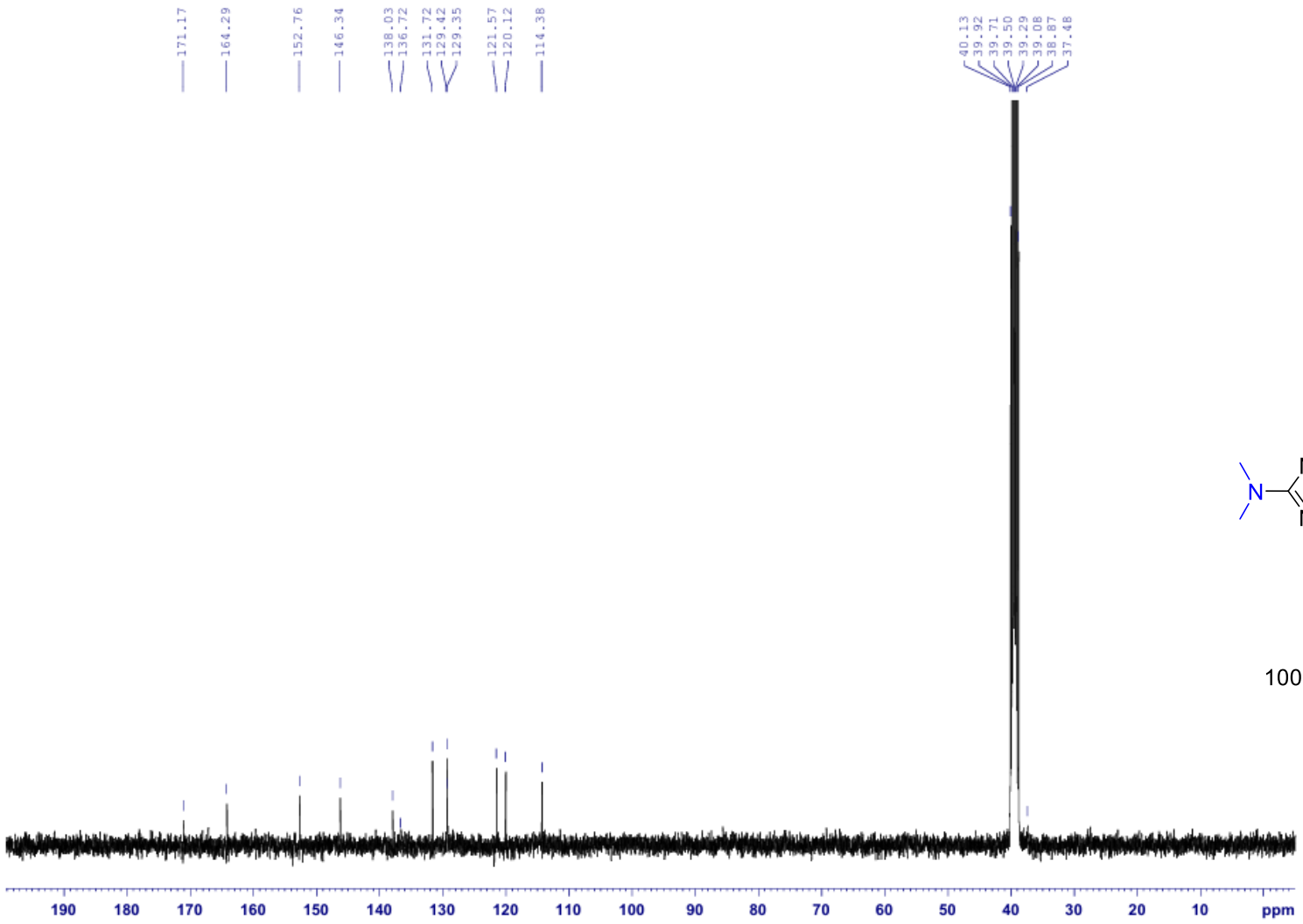

^{13}C NMR

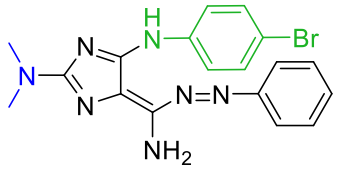

5h

100 MHz, DMSO-d_6

SI-Figure 48 - ^{13}C NMR spectrum of (4*E*)-4-(amino(phenyldiazenyl)methylene)-*N*5-(4-bromophenyl)-N^2,N^2-dimethyl-4*H*-imidazole-2,5-diamine (**5h**).

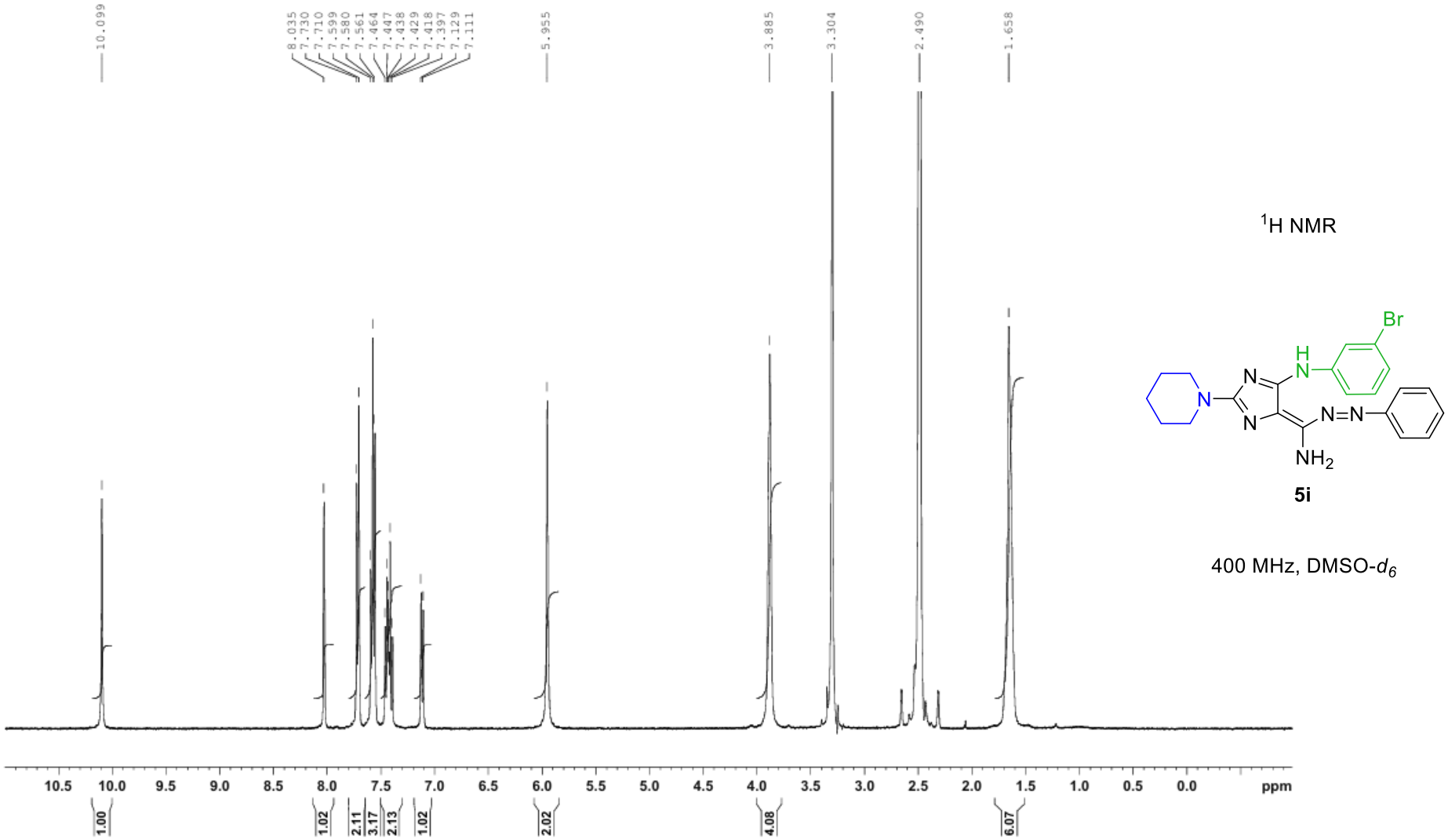

SI-Figure 49 - ^{1}H NMR spectrum of (4*E*)-4-(amino(phenyldiazenyl)methylene)-*N*-(3-bromophenyl)-2-(piperidin-1-yl)-4*H*-imidazol-5-amine (**5i**).

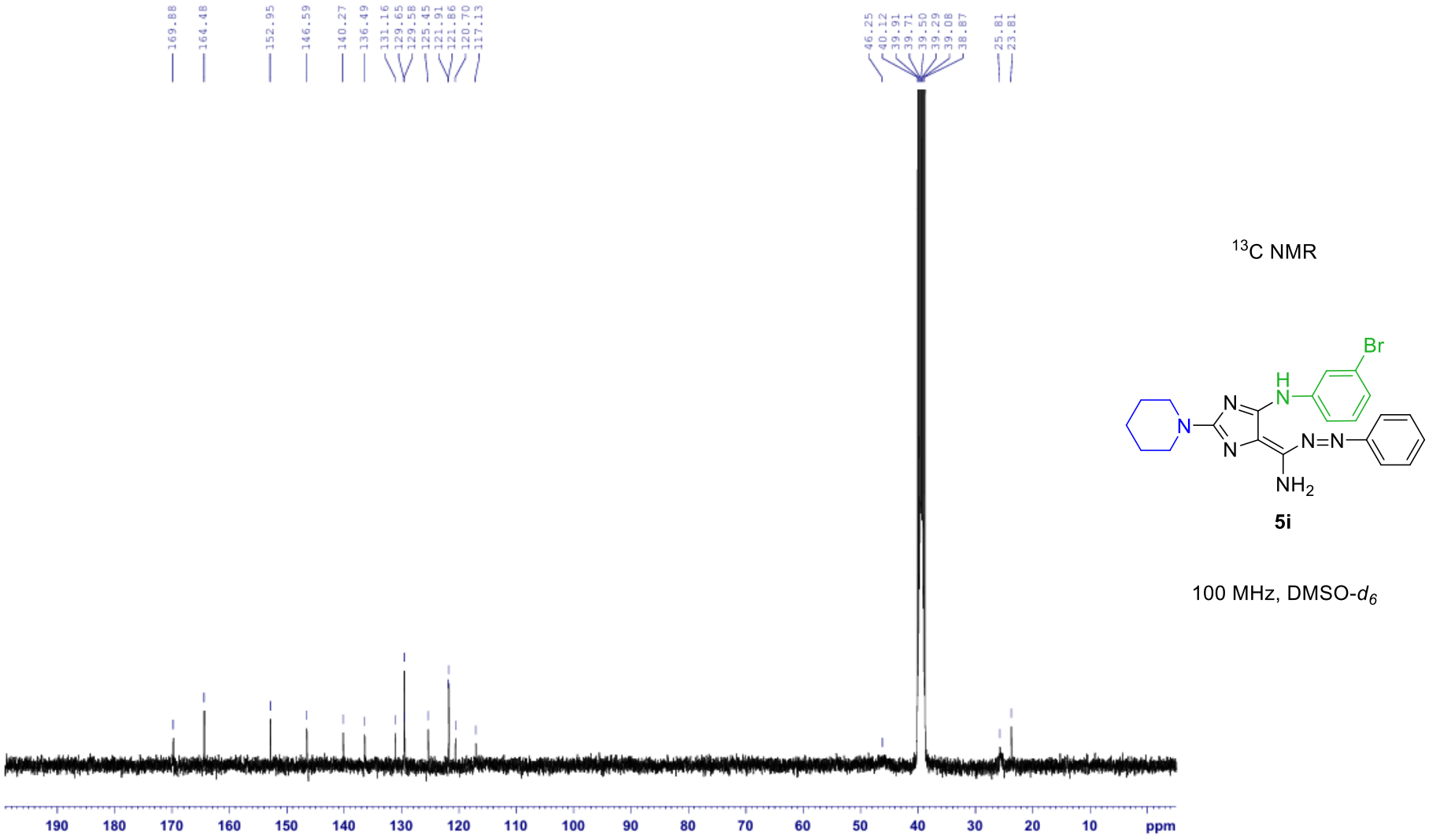

SI-Figure 50 - ^{13}C NMR spectrum of (4*E*)-4-(amino(phenyldiazenyl)methylene)-*N*-(3-bromophenyl)-2-(piperidin-1-yl)-4*H*-imidazol-5-amine (**5i**).

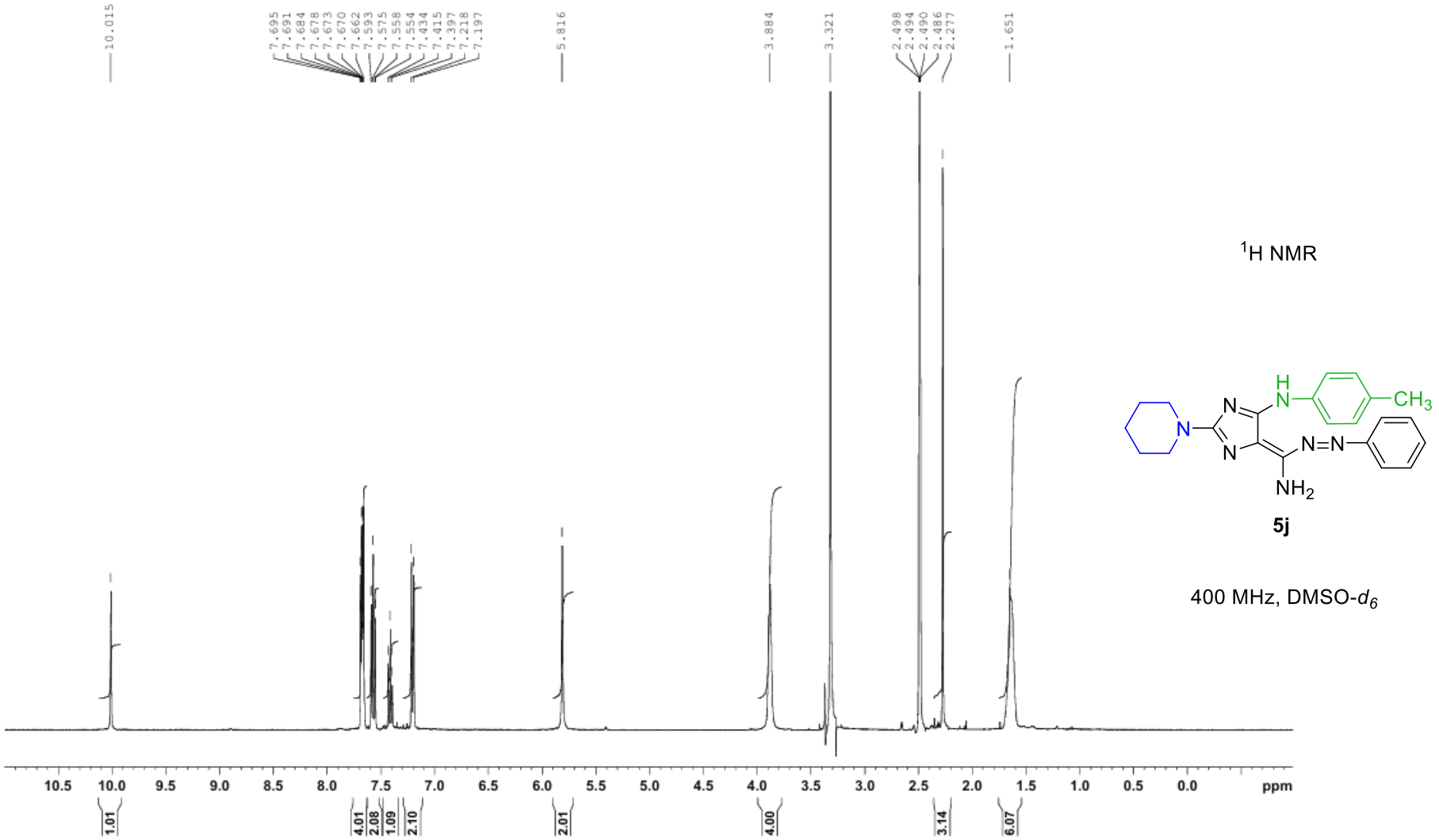

SI-Figure 51 - ^{1}H NMR spectrum of (4*E*)-4-(amino(phenyldiazenyl)methylene)-*N*-(*p*-tolyl)-2-(piperidin-1-yl)-4*H*-imidazol-5-amine (**5j**).

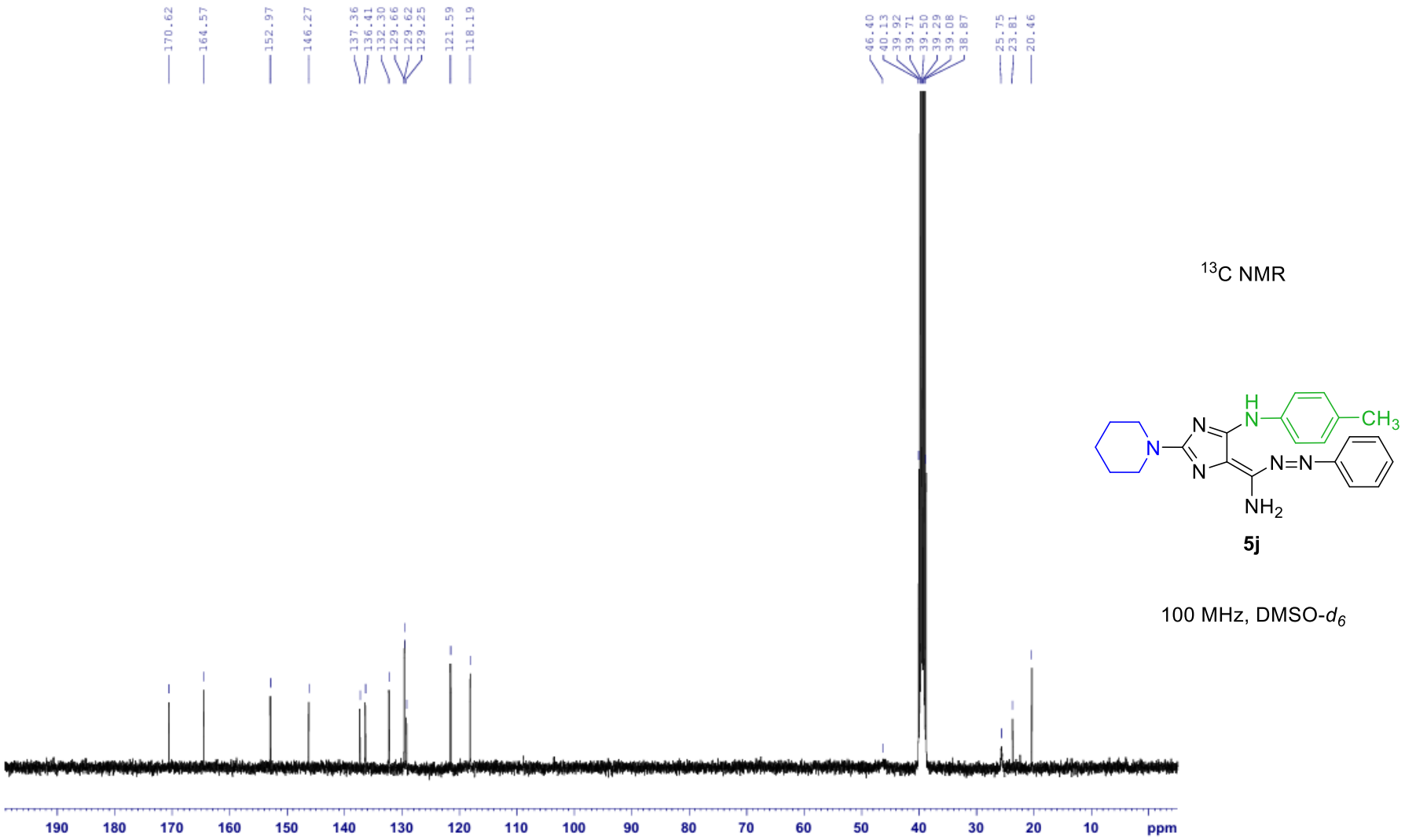

SI-Figure 52 - ^{13}C NMR spectrum of (4*E*)-4-(amino(phenyldiazenyl)methylene)-*N*-(*p*-tolyl)-2-(piperidin-1-yl)-4*H*-imidazol-5-amine (**5j**).

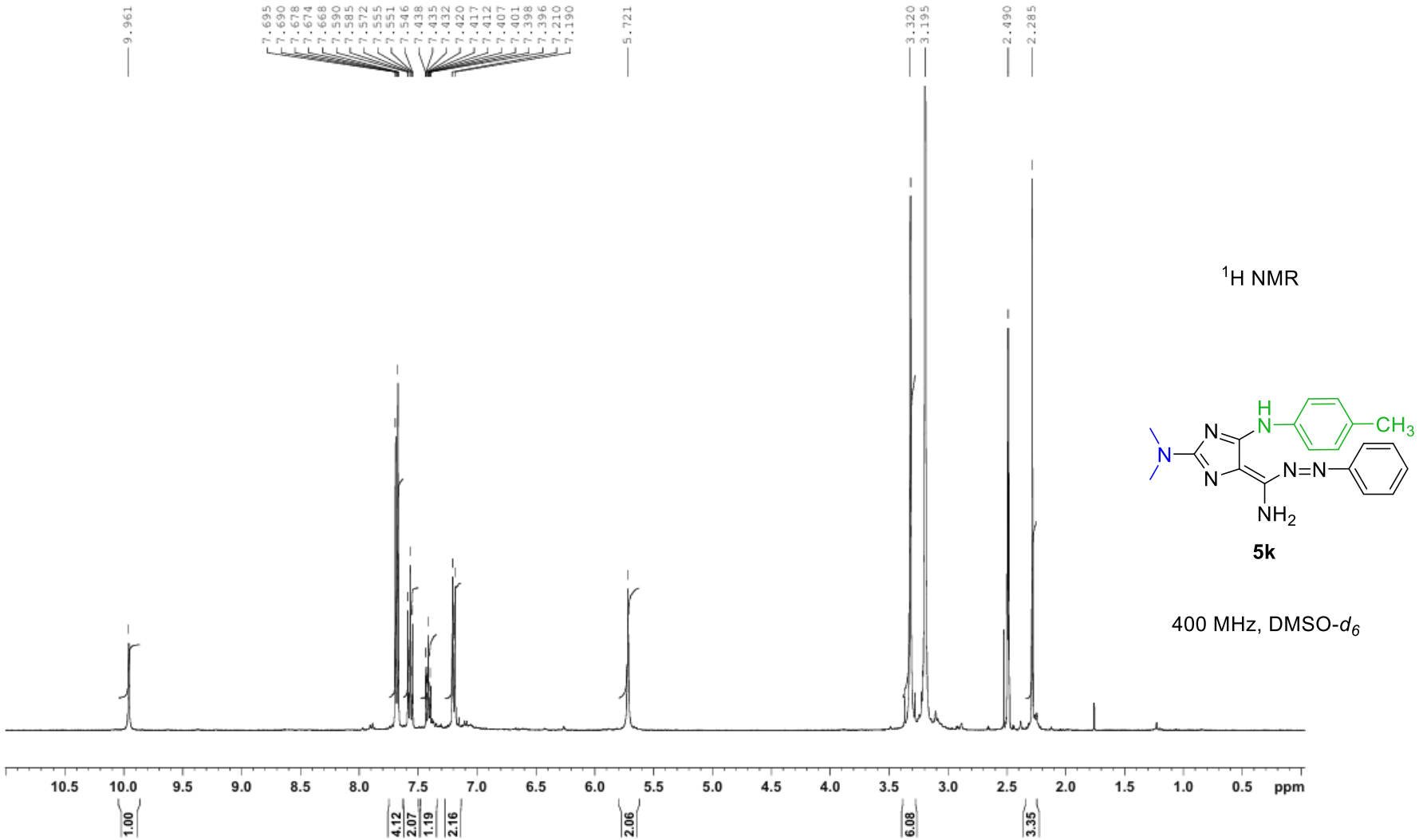

SI-Figure 53 - ^{1}H NMR spectrum of (4*E*)-4-(amino(phenyldiazenyl)methylene)-*N*5-(*p*-tolyl)-N^2,N^2-dimethyl-4*H*-imidazole-2,5-diamine (**5k**).

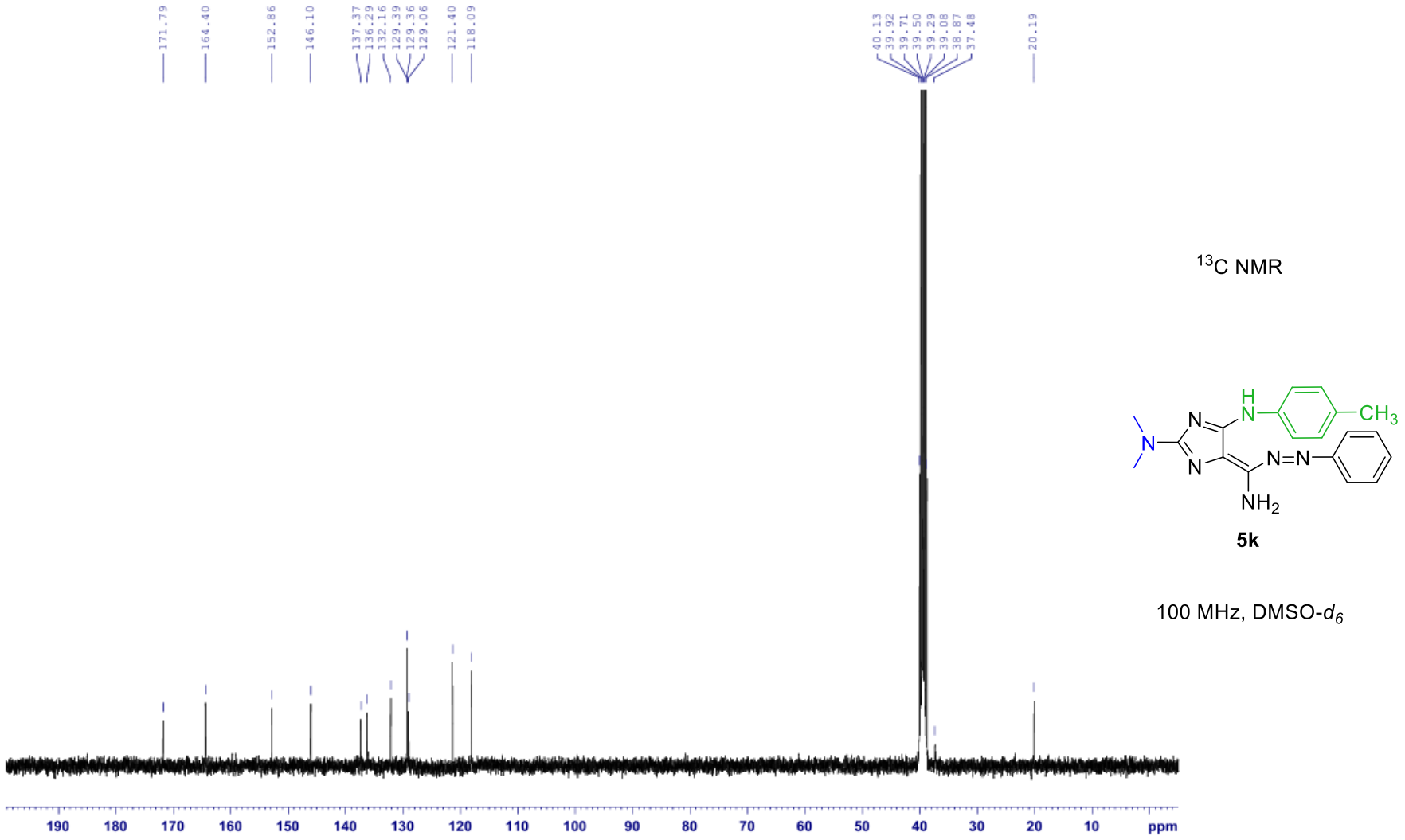

SI-Figure 54 - ^{13}C NMR spectrum of (4*E*)-4-(amino(phenyldiazenyl)methylene)-*N*5-(*p*-tolyl)-N^2,N^2-dimethyl-4*H*-imidazole-2,5-diamine (**5k**).

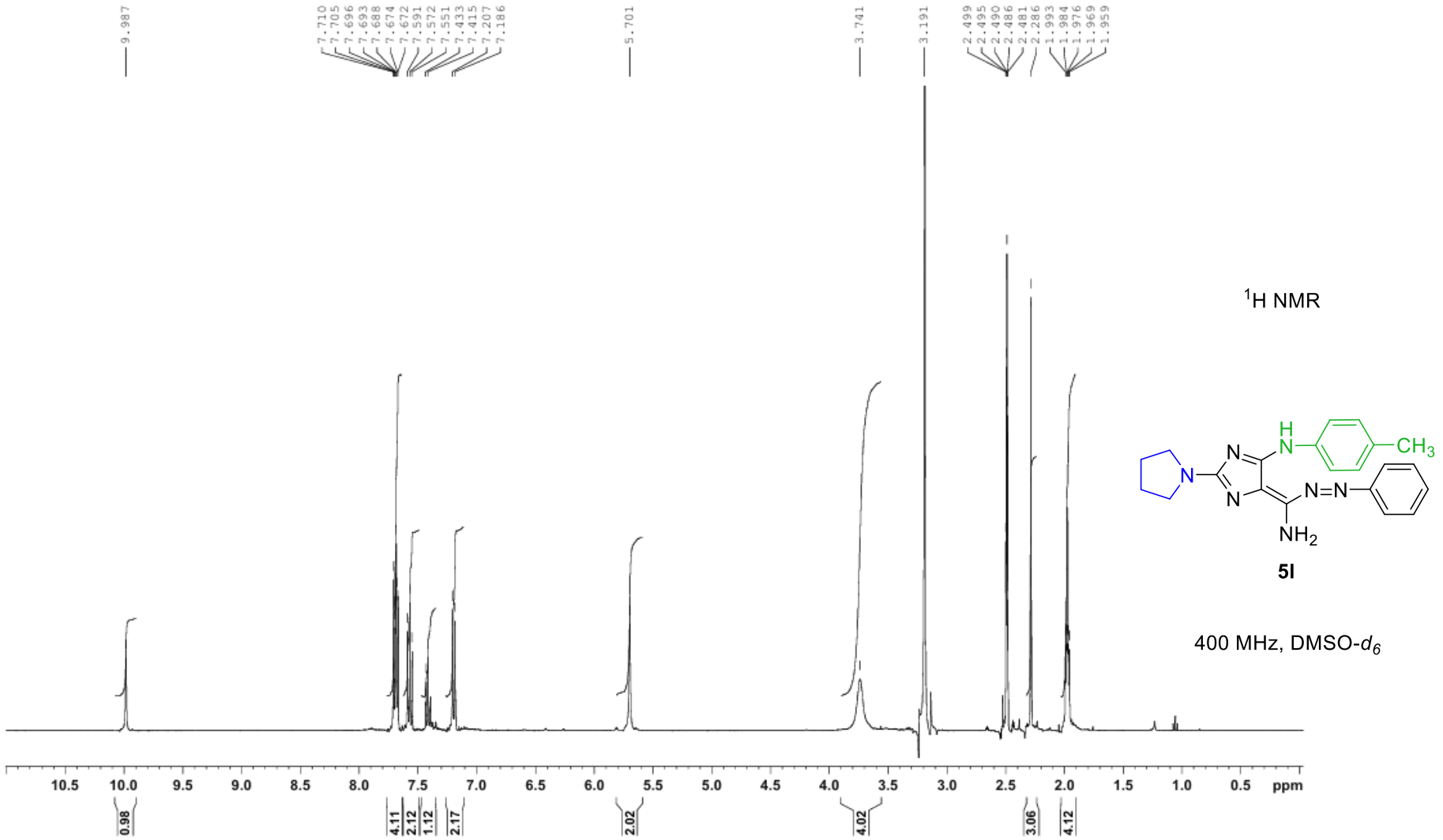

SI-Figure 55 - ^{1}H NMR spectrum of (4*E*)-4-(amino(phenyldiazenyl)methylene)-*N*-(*p*-tolyl)-2-(pyrrolidin-1-yl)-4*H*-imidazol-5-amine (**5l**).

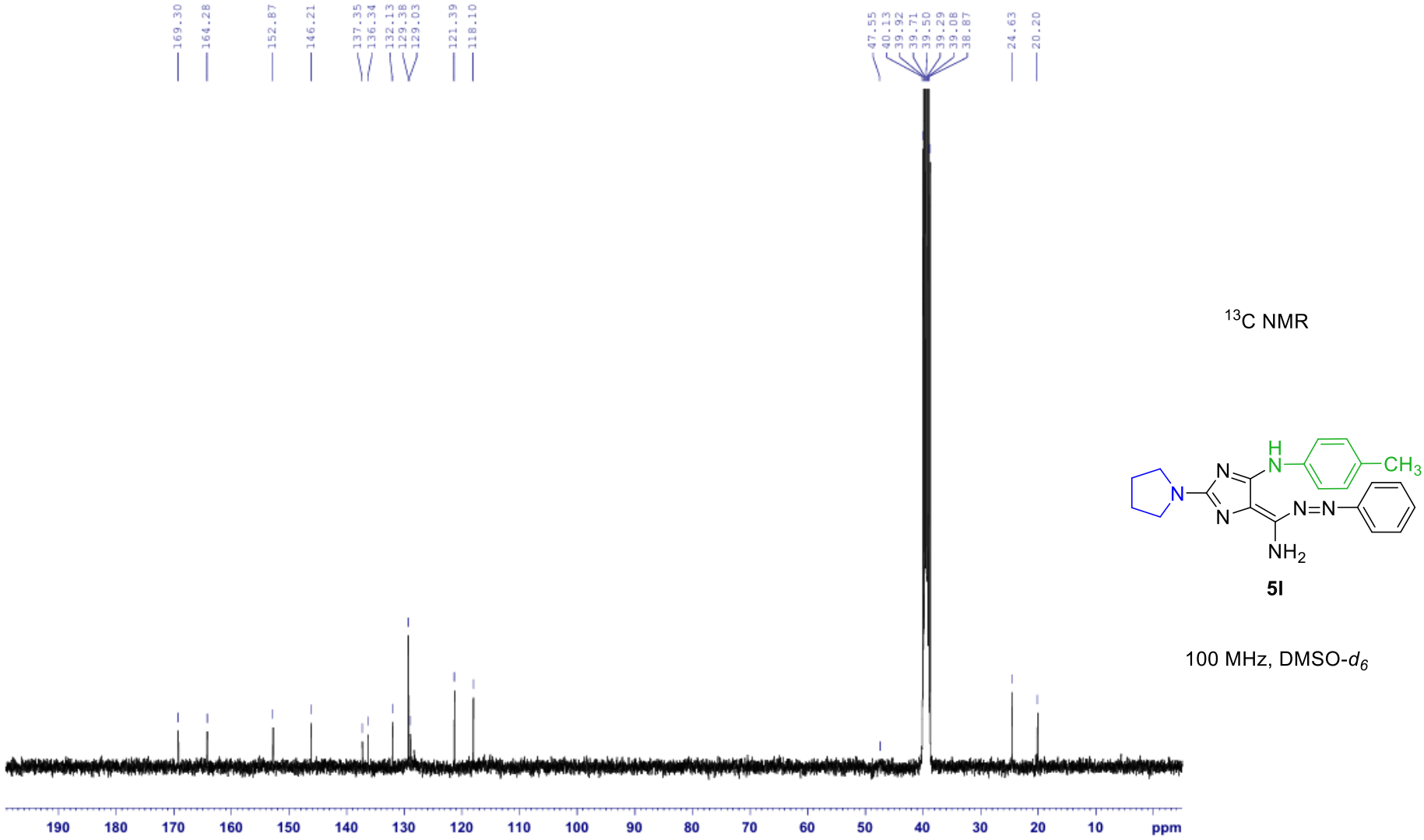

SI-Figure 56 - ^{13}C NMR spectrum of (4*E*)-4-(amino(phenyldiazenyl)methylene)-*N*-(*p*-tolyl)-2-(pyrrolidin-1-yl)-4*H*-imidazol-5-amine (**5l**).

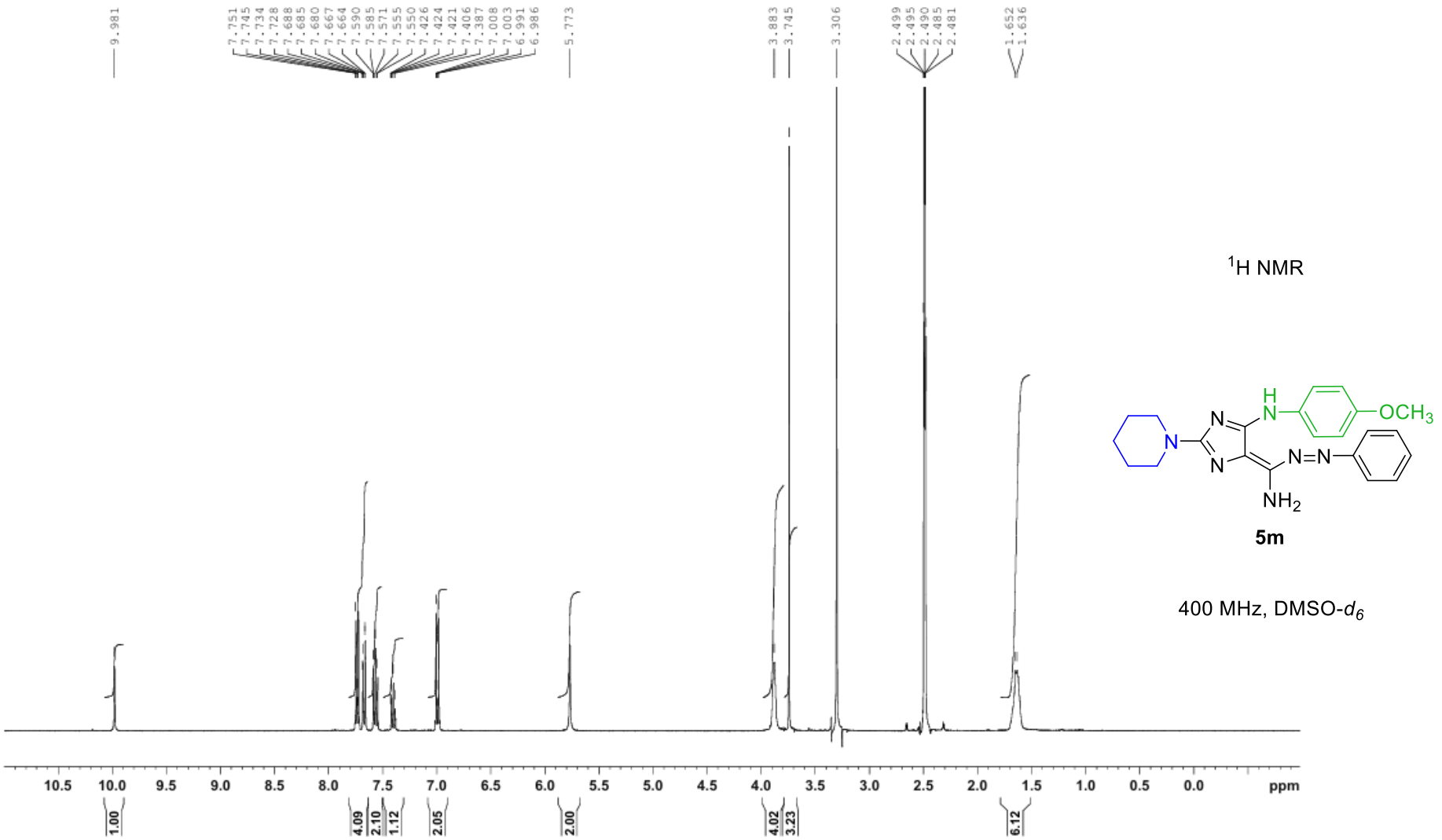

SI-Figure 57 - ^{1}H NMR spectrum of (4*E*)-4-(amino(phenyldiazenyl)methylene)-*N*-(4-methoxyphenyl)-2-(piperidin-1-yl)-4*H*-imidazol-5-amine (**5m**).

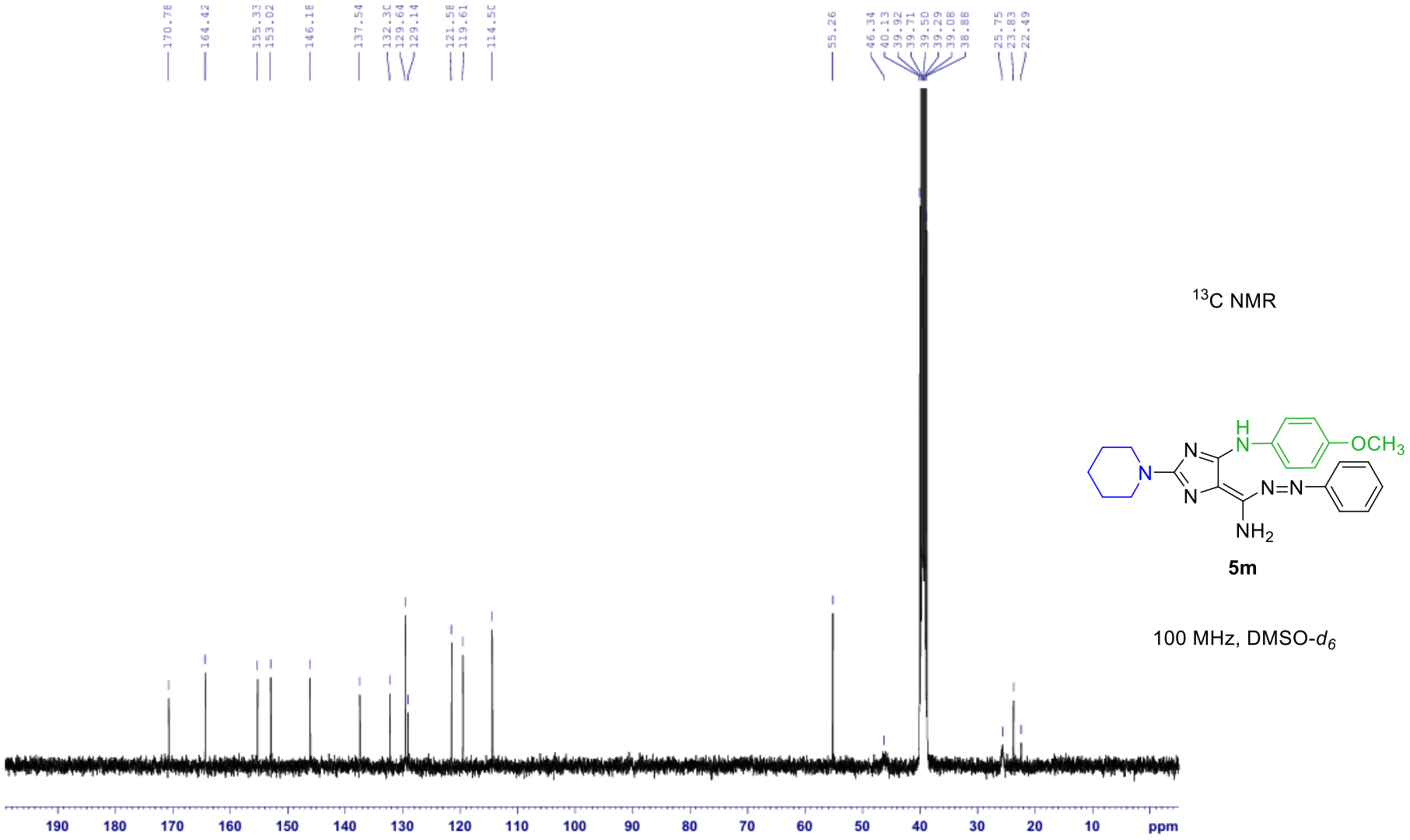

SI-Figure 58 – ^{13}C NMR spectrum of (4*E*)-4-(amino(phenyldiazenyl)methylene)-*N*-(4-methoxyphenyl)-2-(piperidin-1-yl)-4*H*-imidazol-5-amine (**5m**).

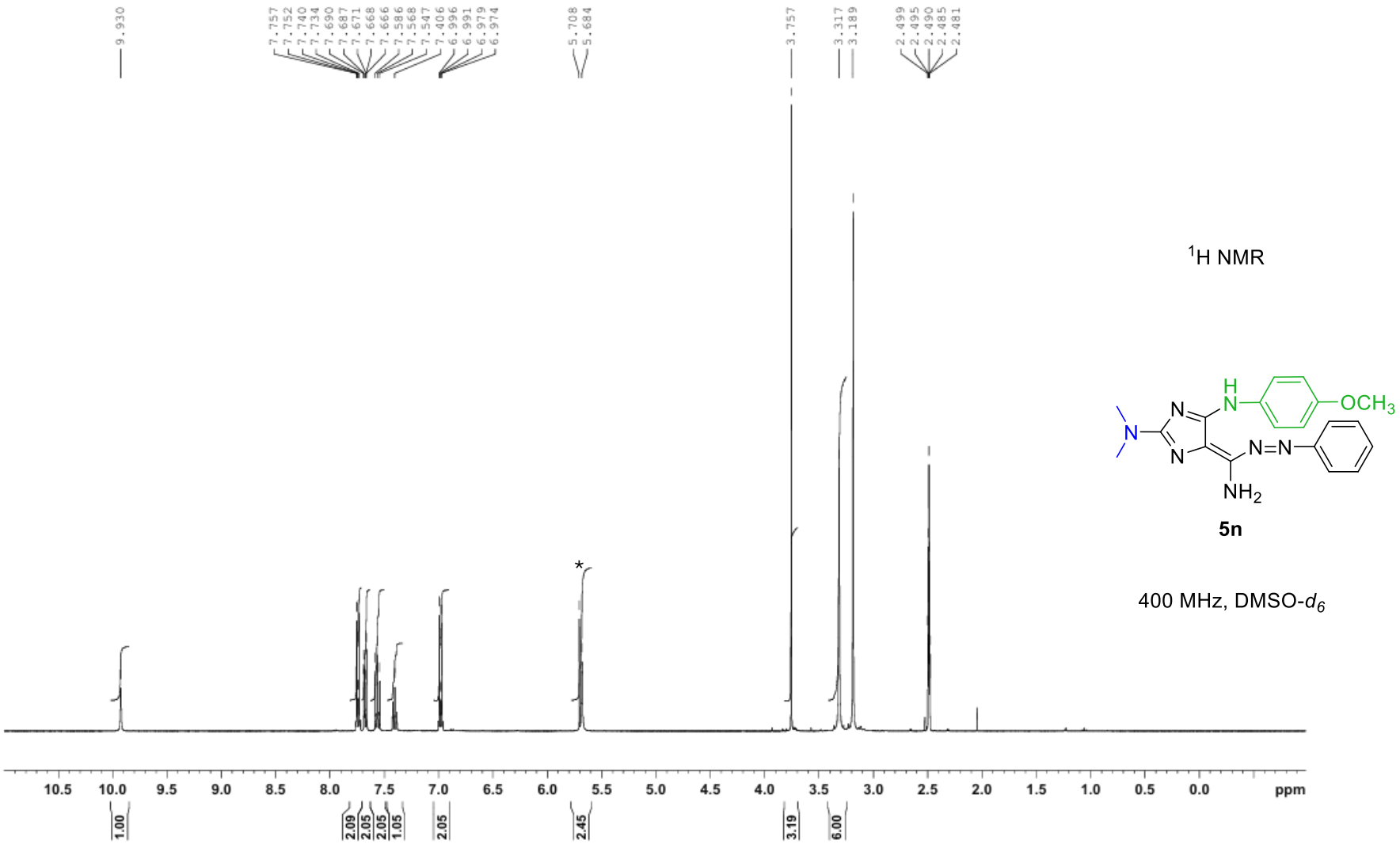

SI-Figure 59 - ^{1}H NMR spectrum of (4*E*)-4-(amino(phenyldiazenyl)methylene)-*N*5-(4-methoxyphenyl)-N^2,N^2-dimethyl-4*H*-imidazole-2,5-diamine (**5n**). *CH_2Cl_2 impurity

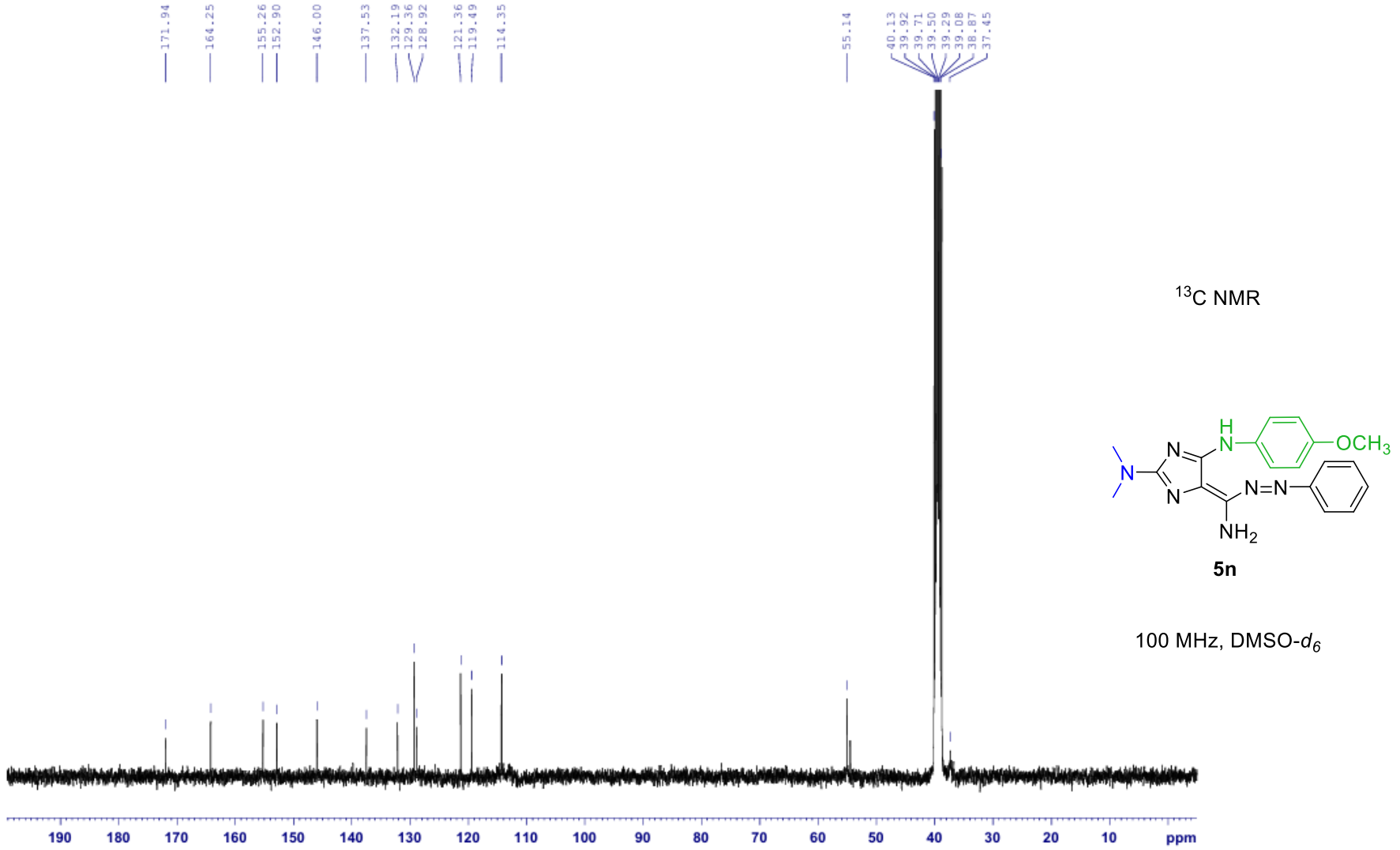

SI-Figure 60 - ^{13}C NMR spectrum of (4*E*)-4-(amino(phenyldiazenyl)methylene)-*N*5-(4-methoxyphenyl)-N^2,N^2-dimethyl-4*H*-imidazole-2,5-diamine (**5n**).

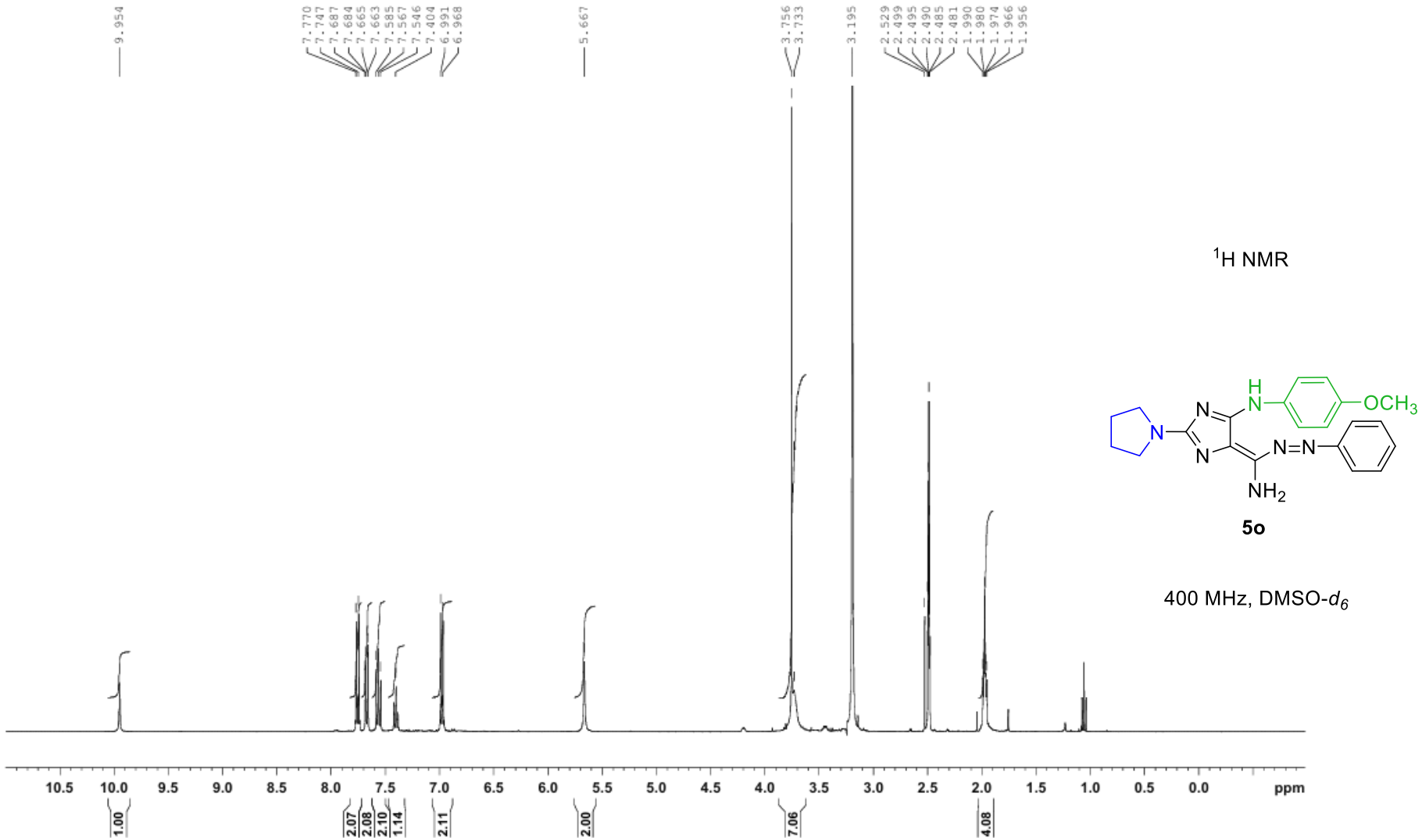

SI-Figure 61 - ^{1}H NMR spectrum of (4*E*)-4-(amino(phenyldiazenyl)methylene)-*N*-(4-methoxyphenyl)-2-(pyrrolidin-1-yl)-4*H*-imidazol-5-amine (**5o**).

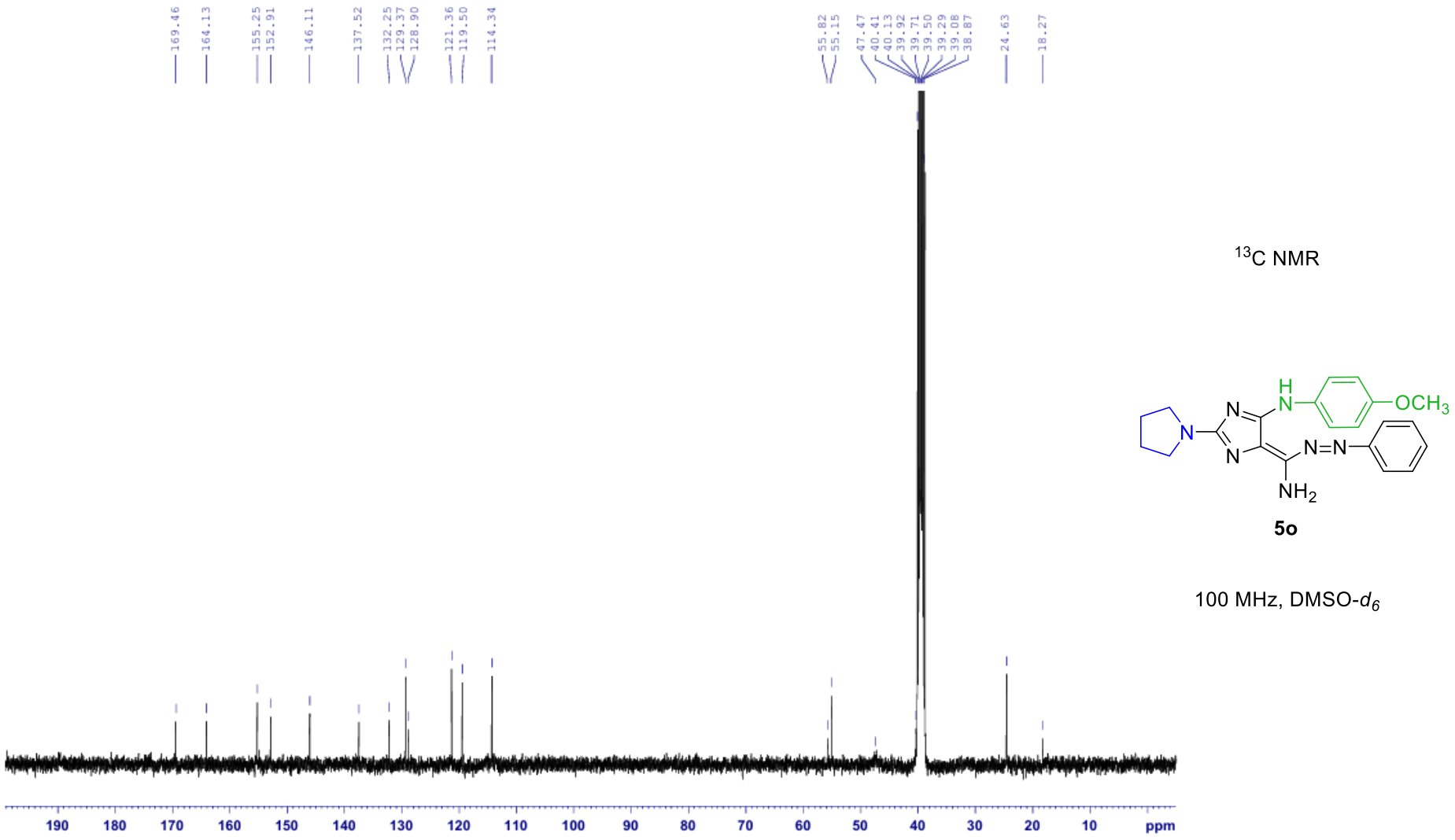

^{13}C NMR

5o

100 MHz, DMSO-d_6

SI-Figure 62 - ^{13}C NMR spectrum of (4*E*)-4-(amino(phenyldiazenyl)methylene)-*N*-(4-methoxyphenyl)-2-(pyrrolidin-1-yl)-4*H*-imidazol-5-amine (**5o**).

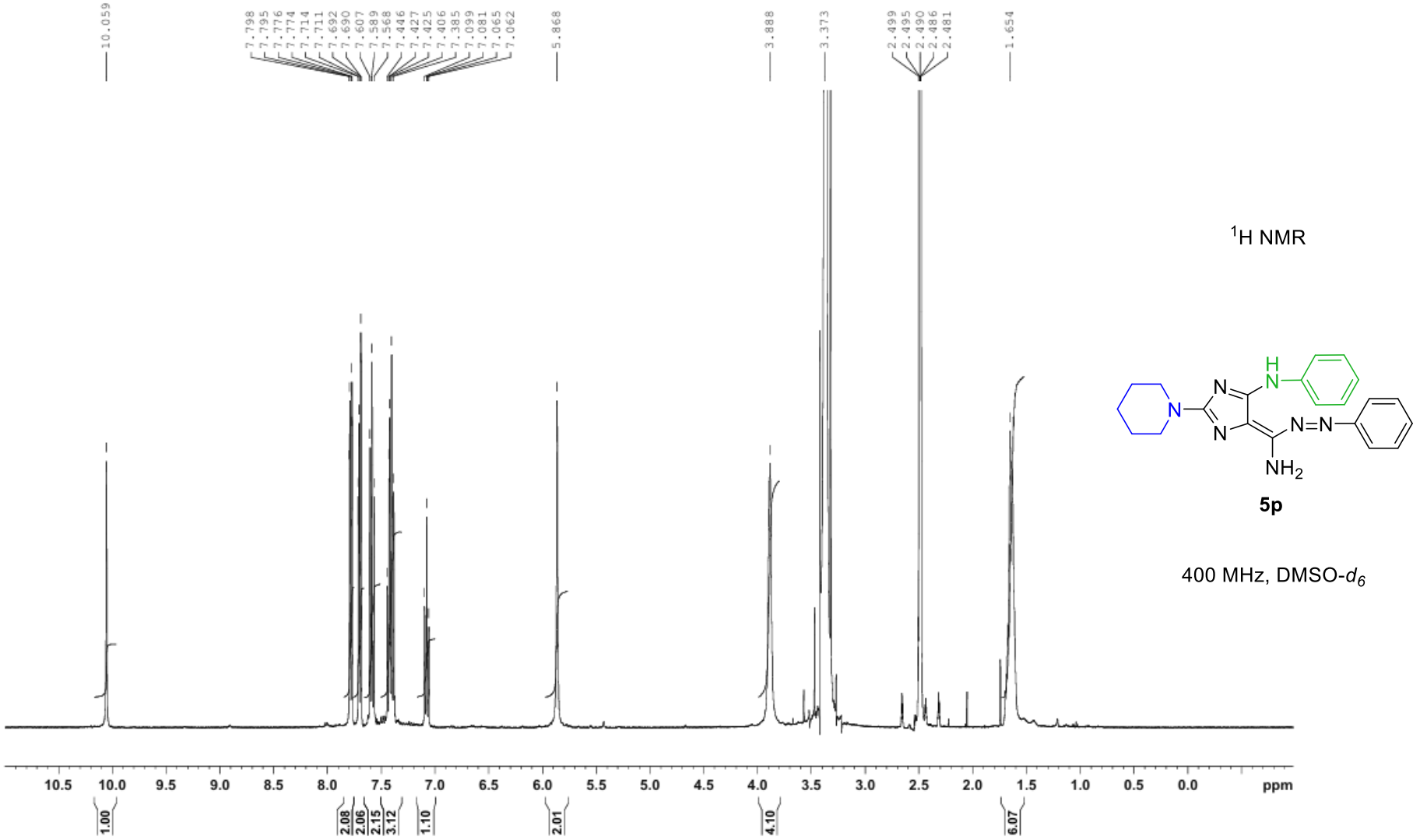

SI-Figure 63 - ^{1}H NMR spectrum of (4*E*)-4-(amino(phenyldiazenyl)methylene)-*N*-phenyl-2-(piperidin-1-yl)-4*H*-imidazol-5-amine (**5p**).

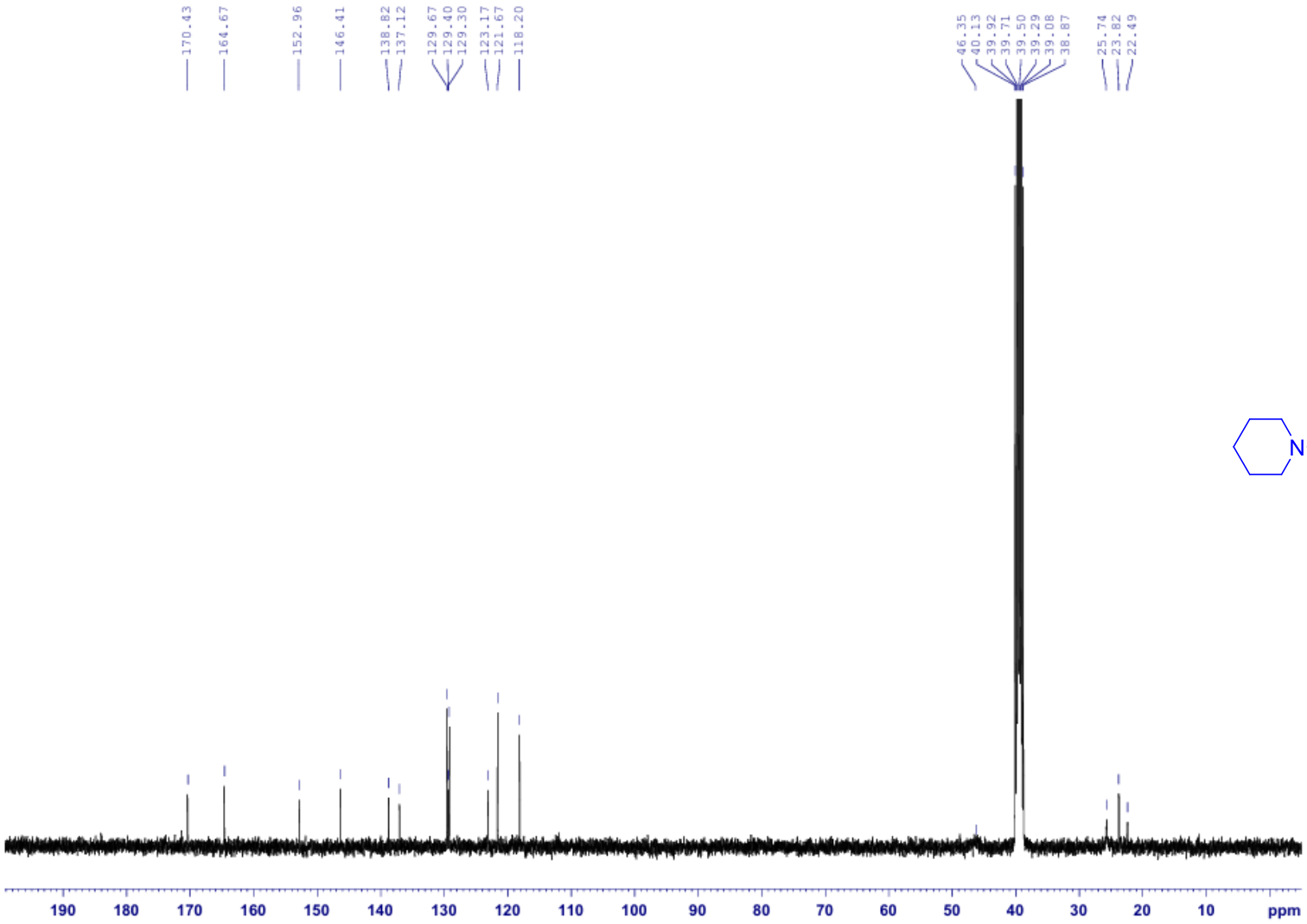

^{13}C NMR

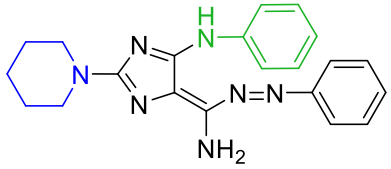

5p

100 MHz, DMSO-d_6

SI-Figure 64 - ^{13}C NMR spectrum of (4*E*)-4-(amino(phenyldiazenyl)methylene)-*N*-phenyl-2-(piperidin-1-yl)-4*H*-imidazol-5-amine (**5p**).

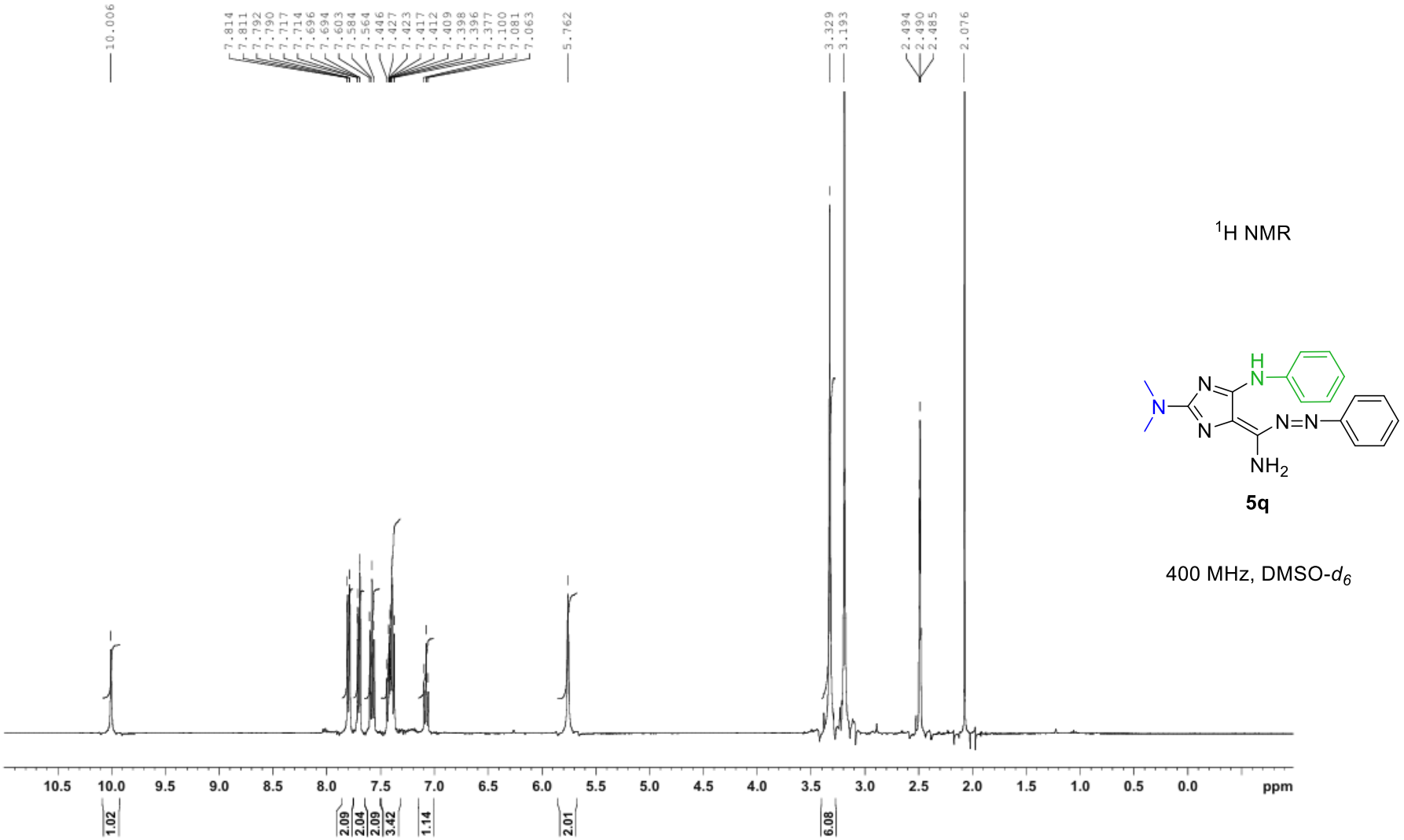

^{1}H NMR

5q

400 MHz, DMSO-d_6

SI-Figure 65 - ^{1}H NMR spectrum of (4*E*)-4-(amino(phenyldiazenyl)methylene)-N^2,N^2-dimethyl-*N*5-phenyl-4*H*-imidazole-2,5-diamine (**5q**).

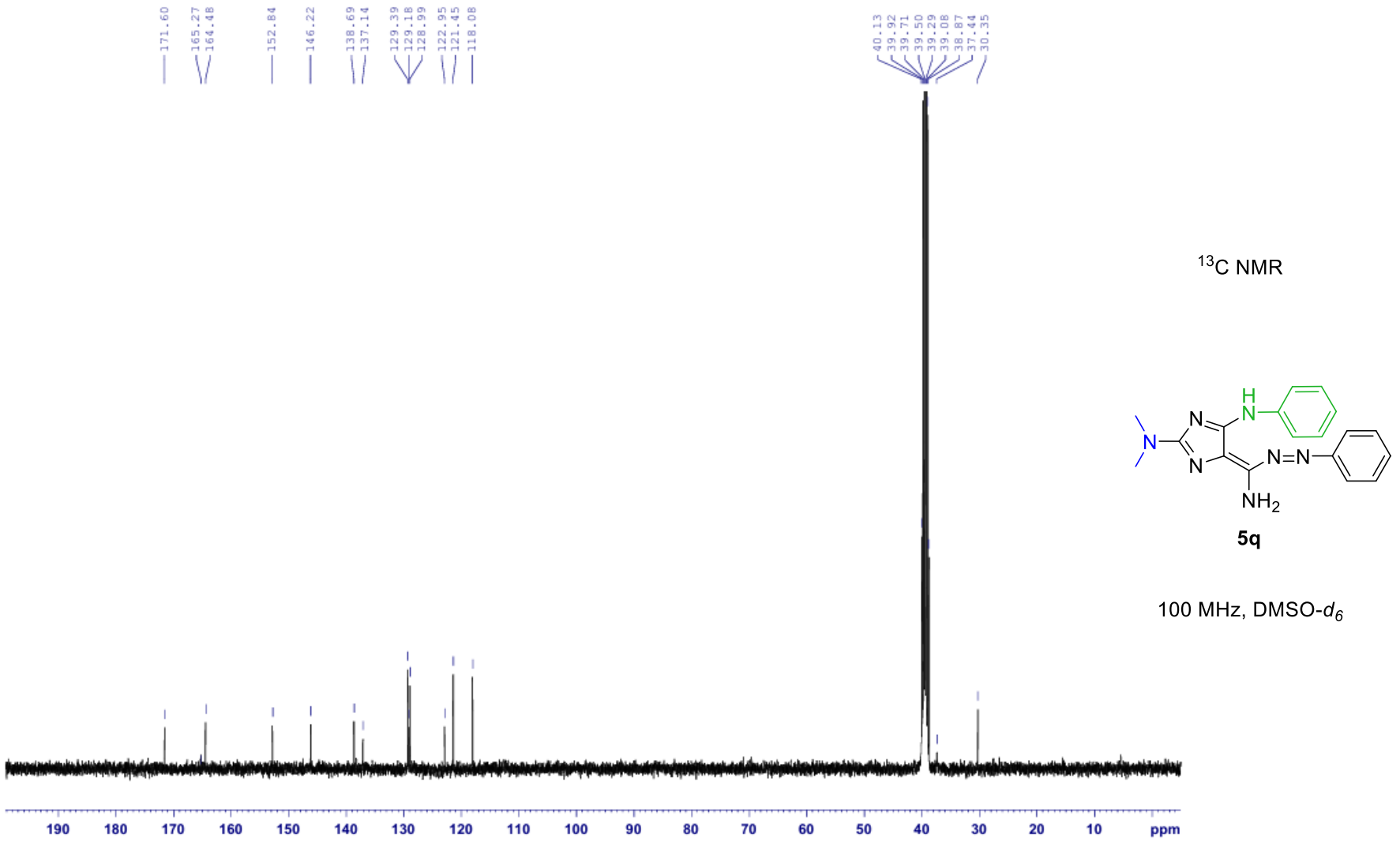

SI-Figure 66 - ^{13}C NMR spectrum of (4*E*)-4-(amino(phenyldiazenyl)methylene)-*N*^{2},*N*^{2}-dimethyl-*N*5-phenyl-4*H*-imidazole-2,5-diamine (**5q**).

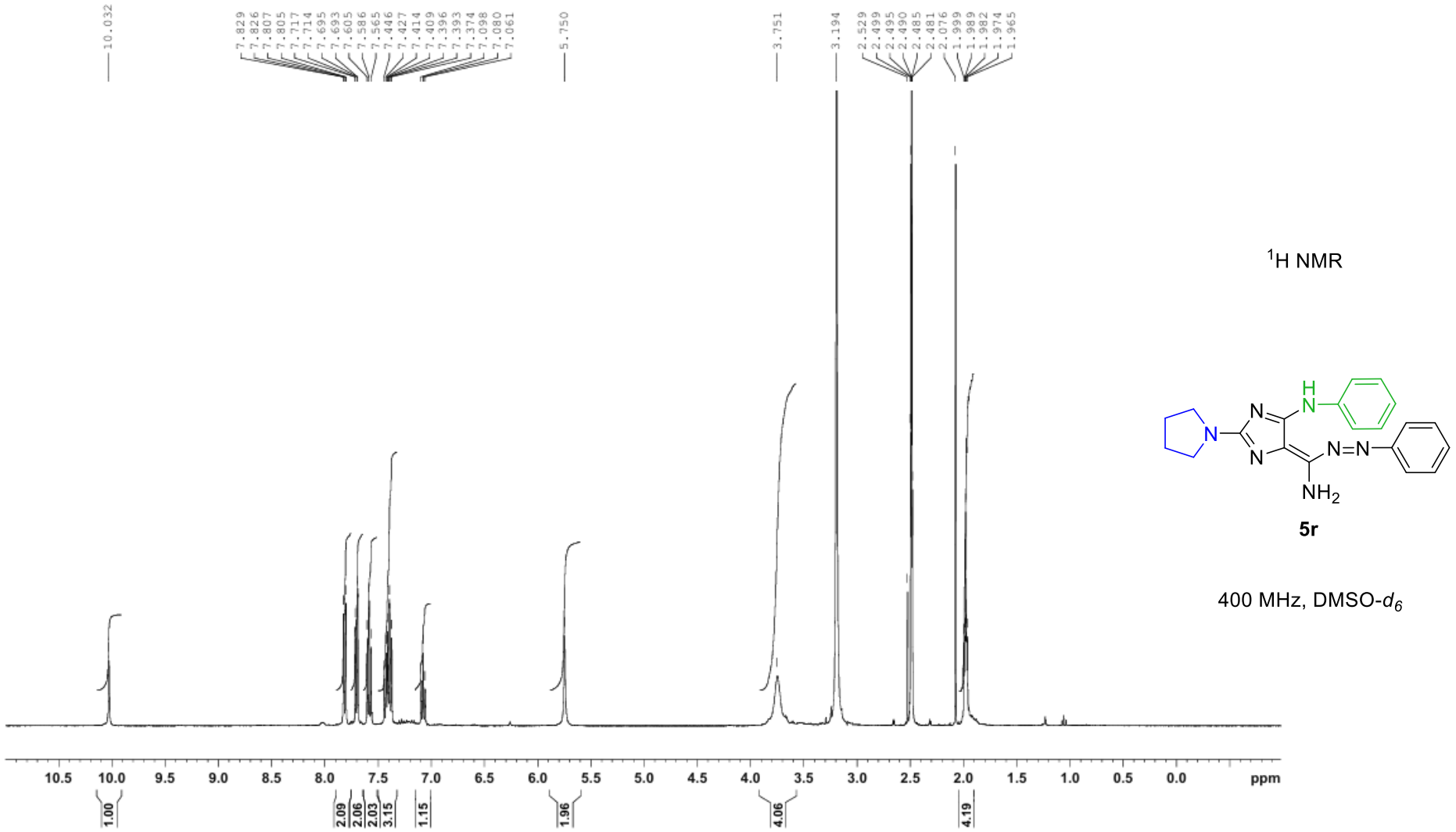

SI-Figure 67 - ^{1}H NMR spectrum of (4*E*)-4-(amino(phenyldiazenyl)methylene)-*N*-phenyl-2-(pyrrolidin-1-yl)-4*H*-imidazol-5-amine (**5r**).

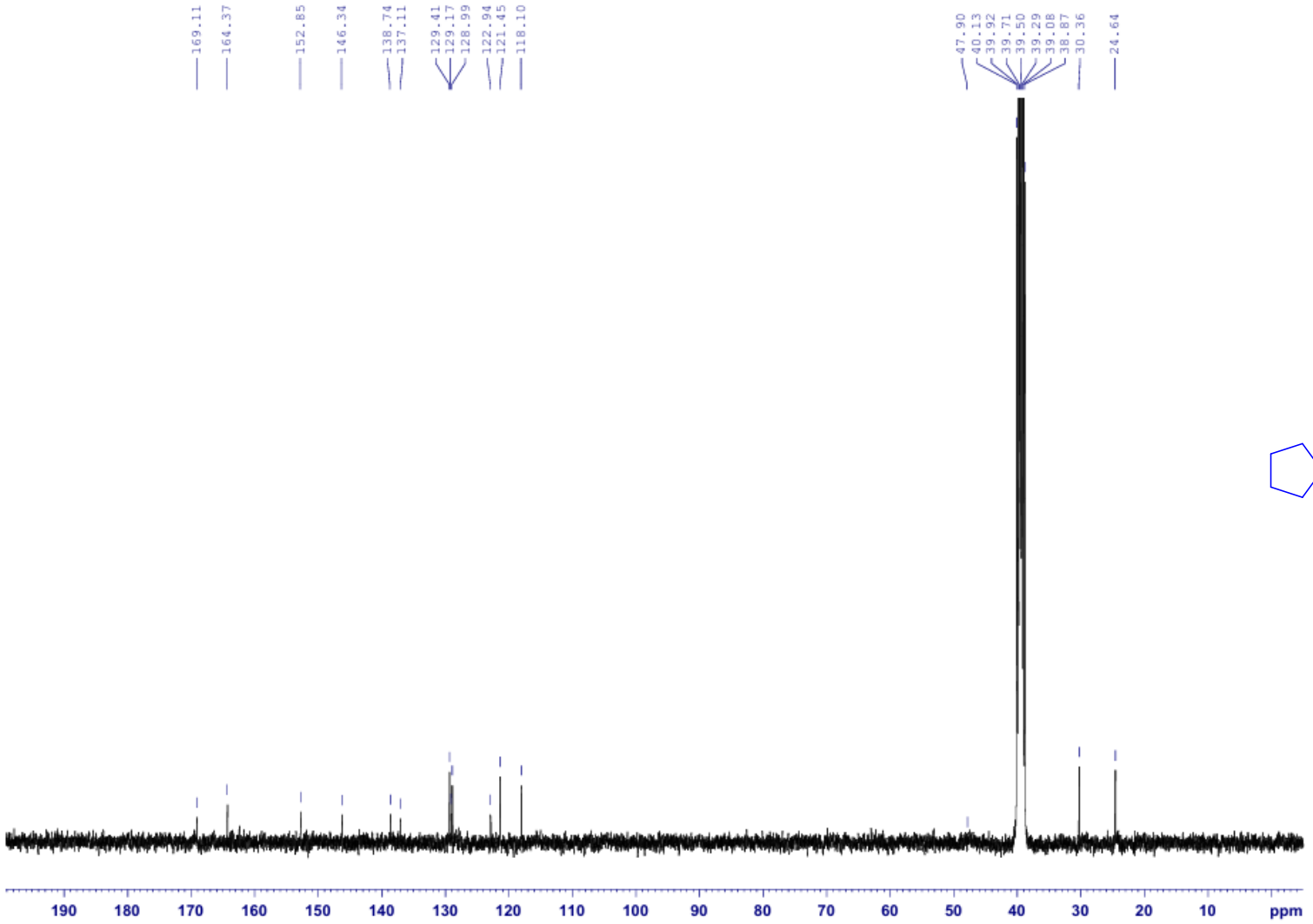

^{13}C NMR

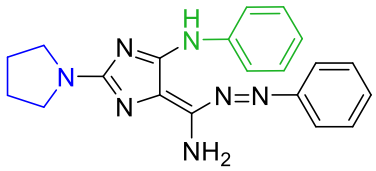

5r

100 MHz, DMSO-d_6

SI-Figure 68 - ^{13}C NMR spectrum of (4*E*)-4-(amino(phenyldiazenyl)methylene)-*N*-phenyl-2-(pyrrolidin-1-yl)-4*H*-imidazol-5-amine (**5r**).

4.2. HMBC and HSQC NMR spectra

4.2.1. (Z)-5-amino-N'-phenyl-1-(p-tolyl)-1H-imidazole-4-carbohydrazonamide (**1f**)

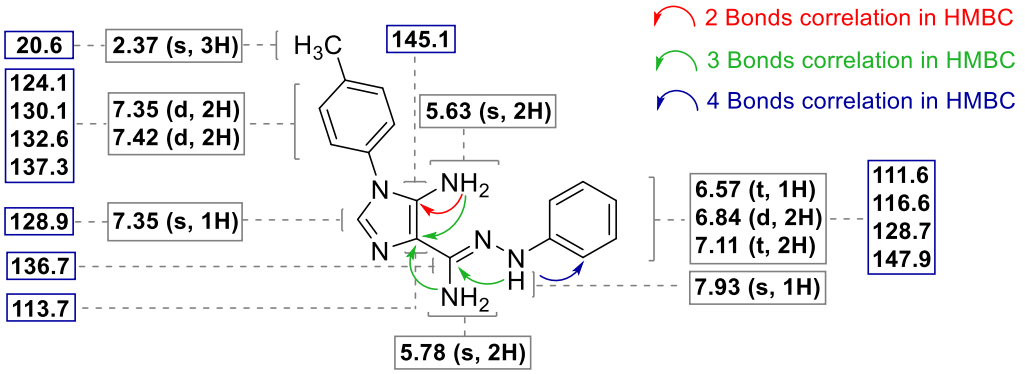

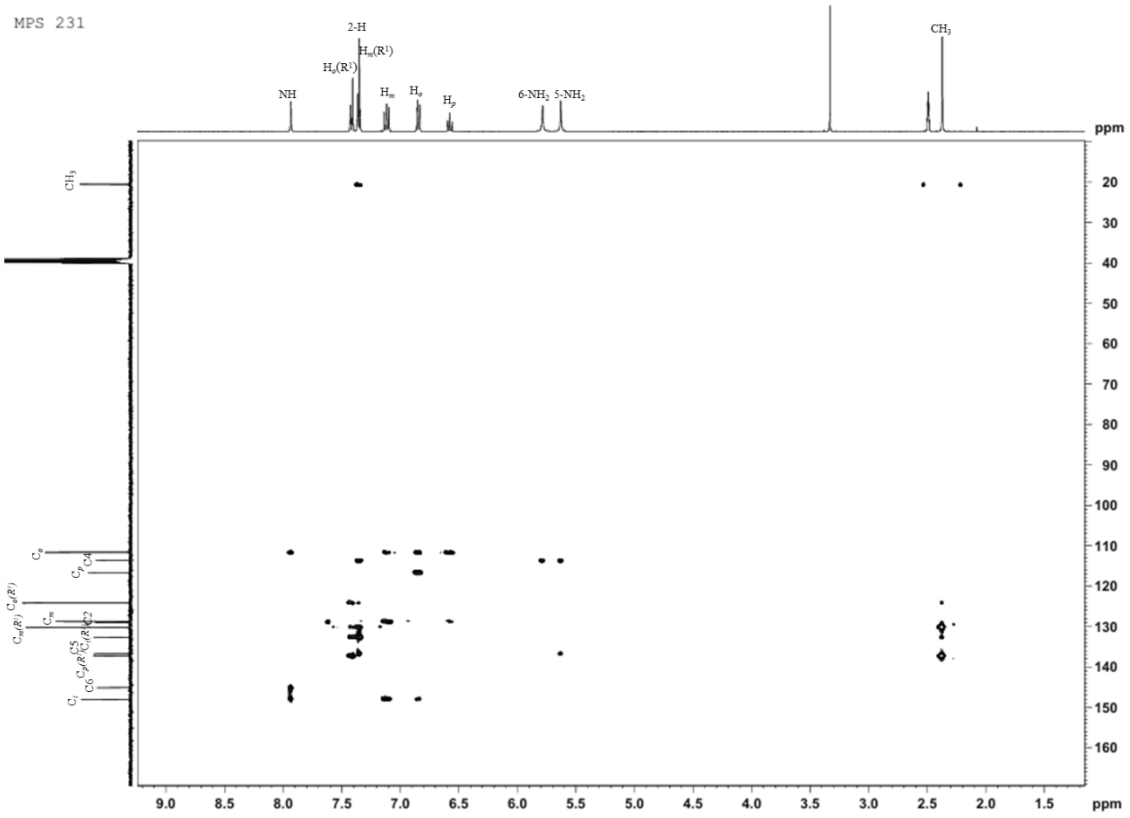

SI-Figure 69 – HMBC spectrum of (*Z*)-5-amino-1-(*p*-tolyl)-*N*'-phenyl-1*H*-imidazole-4-carbohydrazonamide (**1f**).

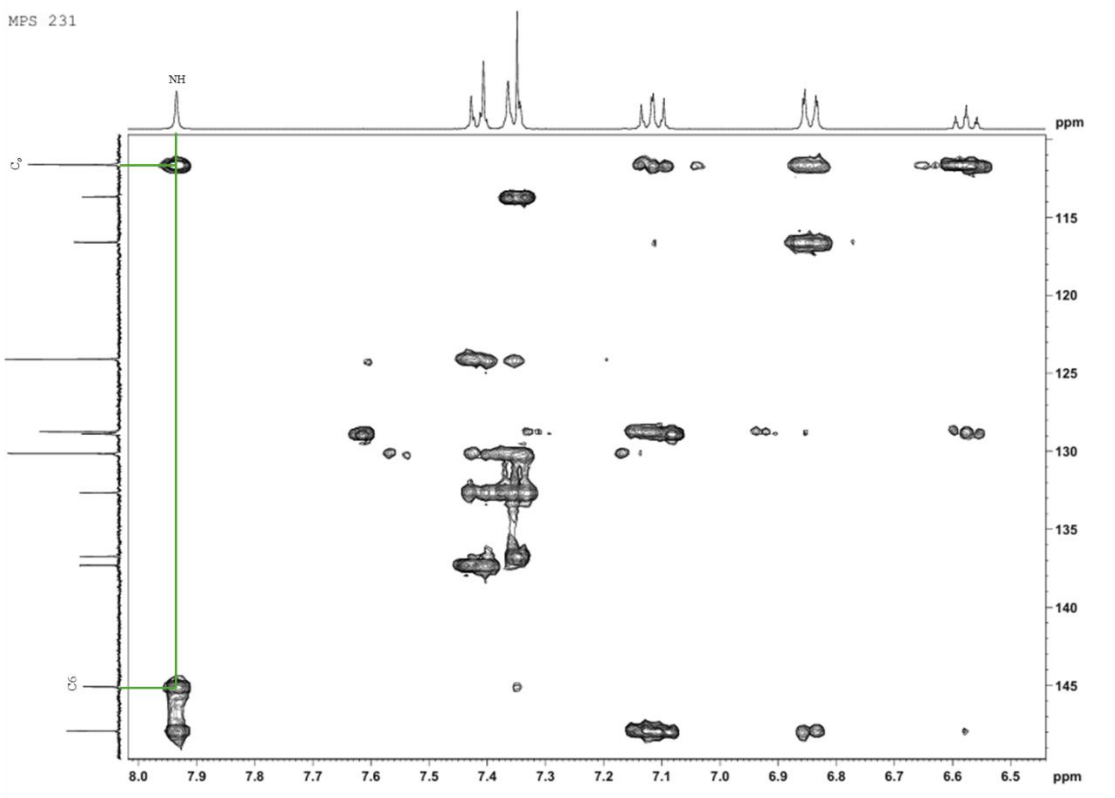

SI-Figure 70 – HMBC spectrum (expansion) of (*Z*)-5-amino-1-(*p*-tolyl)-*N*'-phenyl-1*H*-imidazole-4-carbohydrazonamide (**1f**).

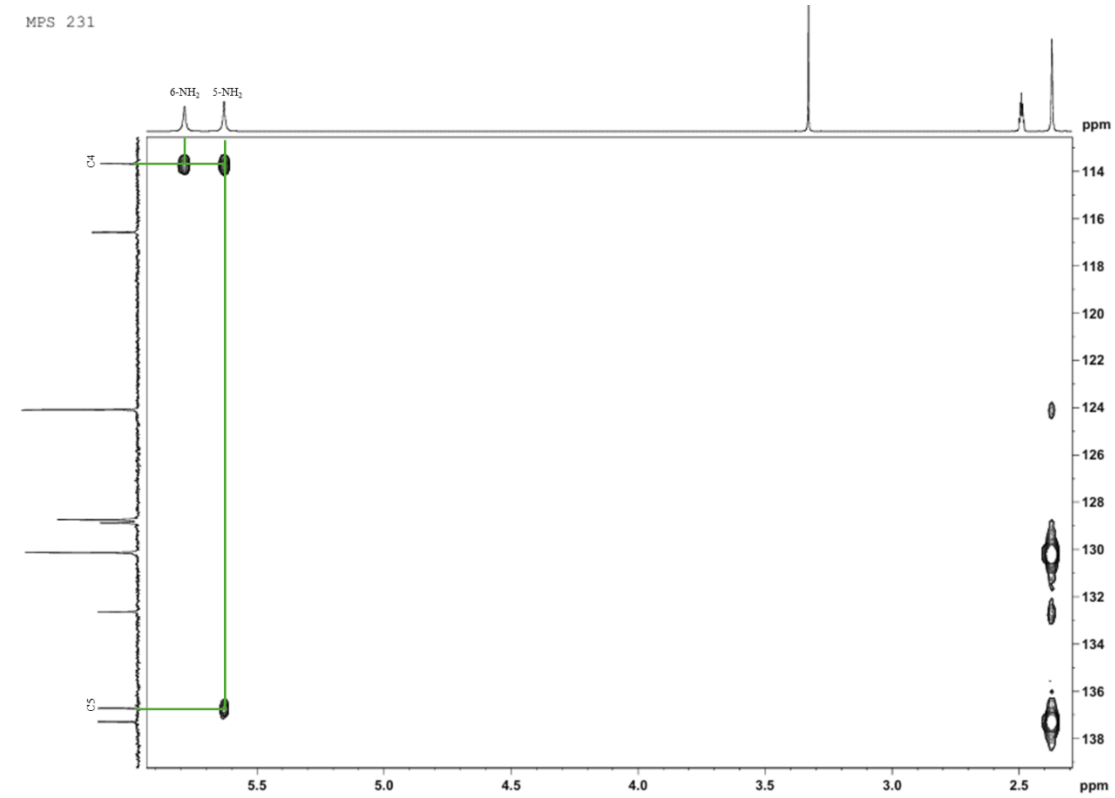

SI-Figure 71 - HMBC spectrum (expansion 2) of (*Z*)-5-amino-1-(*p*-tolyl)-*N*'-phenyl-1*H*-imidazole-4-carbohydrazonamide (**1f**).

*4.2.2.(E)-(1-(4-chlorophenyl)-5-imino-2-(piperidin-1-yl)imidazolidin-4-ylidene)((E)-phenyldiazenyl)methanamine (**4d_II**)*

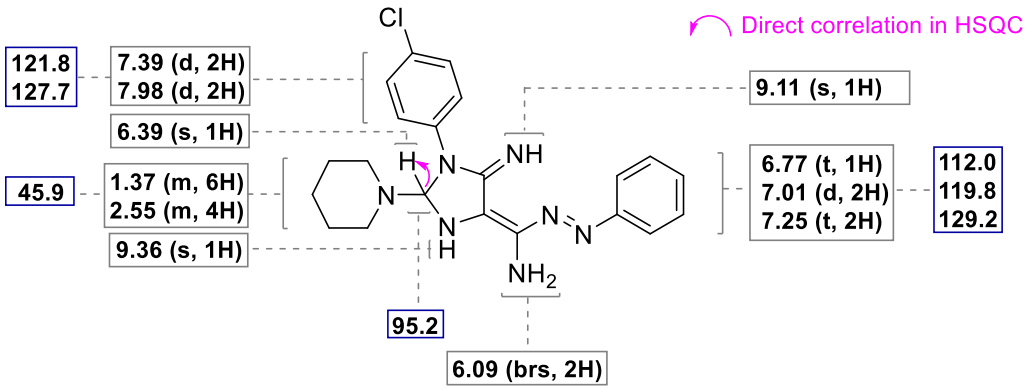

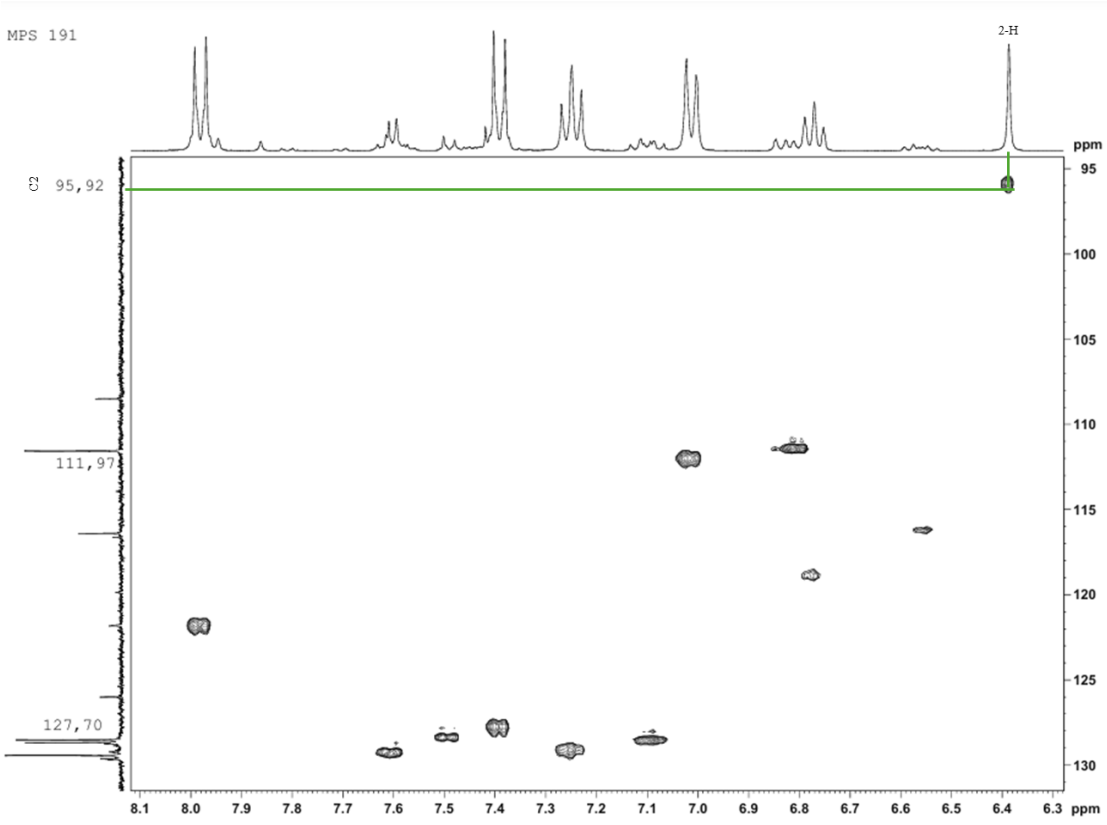

SI-Figure 72 – HSQC spectrum (expansion) of (*E*)-(1-(4-chlorophenyl)-5-imino-2-(piperidin-1-yl)imidazolidin-4-ylidene)((*E*)-phenyldiazenyl)methanamine (**4d_II**)

*4.2.3. (Z)-5-amino-N'-phenyl-2-(piperidin-1-yl)-1-(p-tolyl)-1H-imidazole-4-carbohydrazonamide (**4j_I**).*

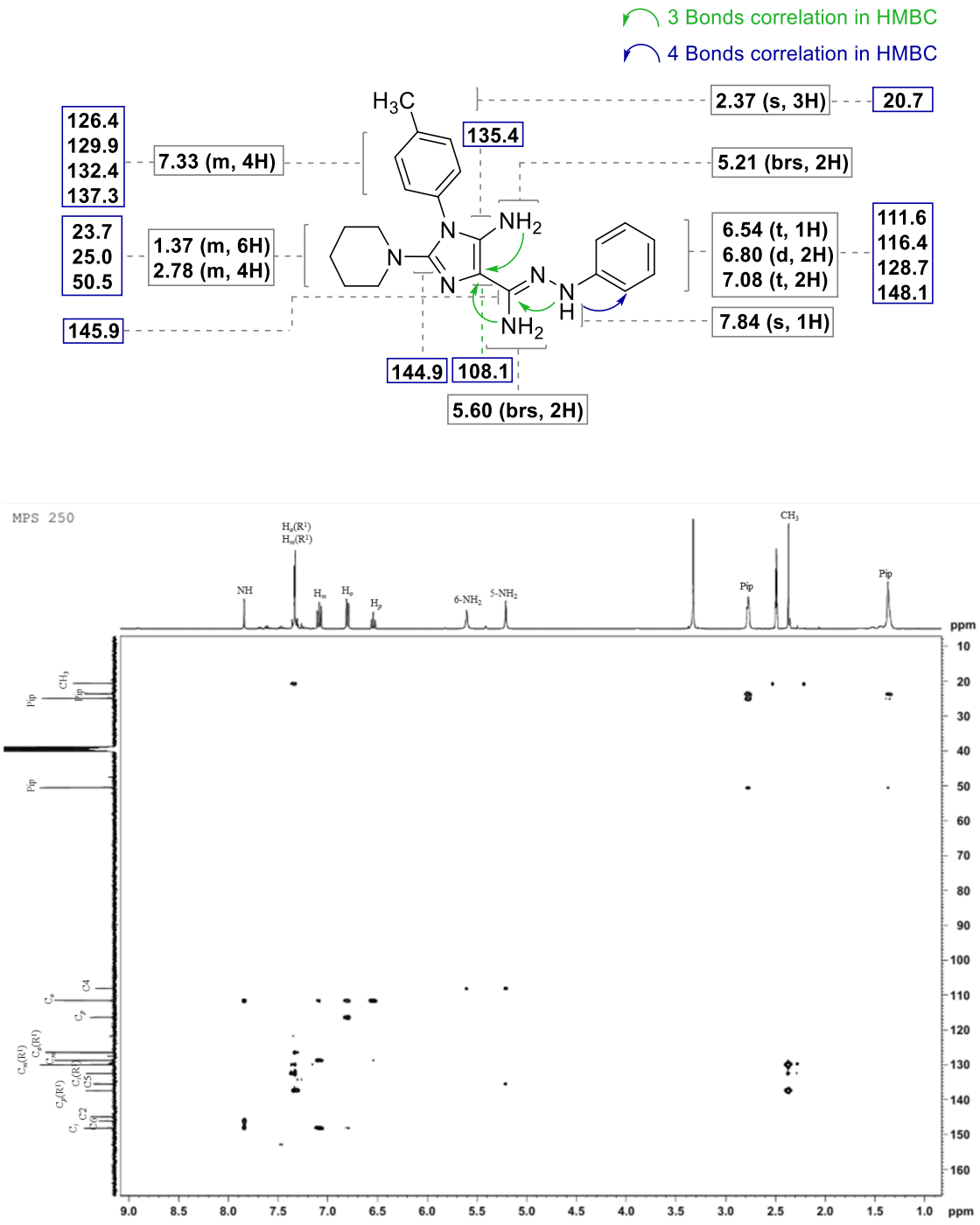

SI-Figure 73 – HMBC spectrum of (*Z*)-5-amino-*N*'-phenyl-2-(piperidin-1-yl)-1-(*p*-tolyl)-1*H*-imidazole-4-carbohydrazonamide (**4j_I**).

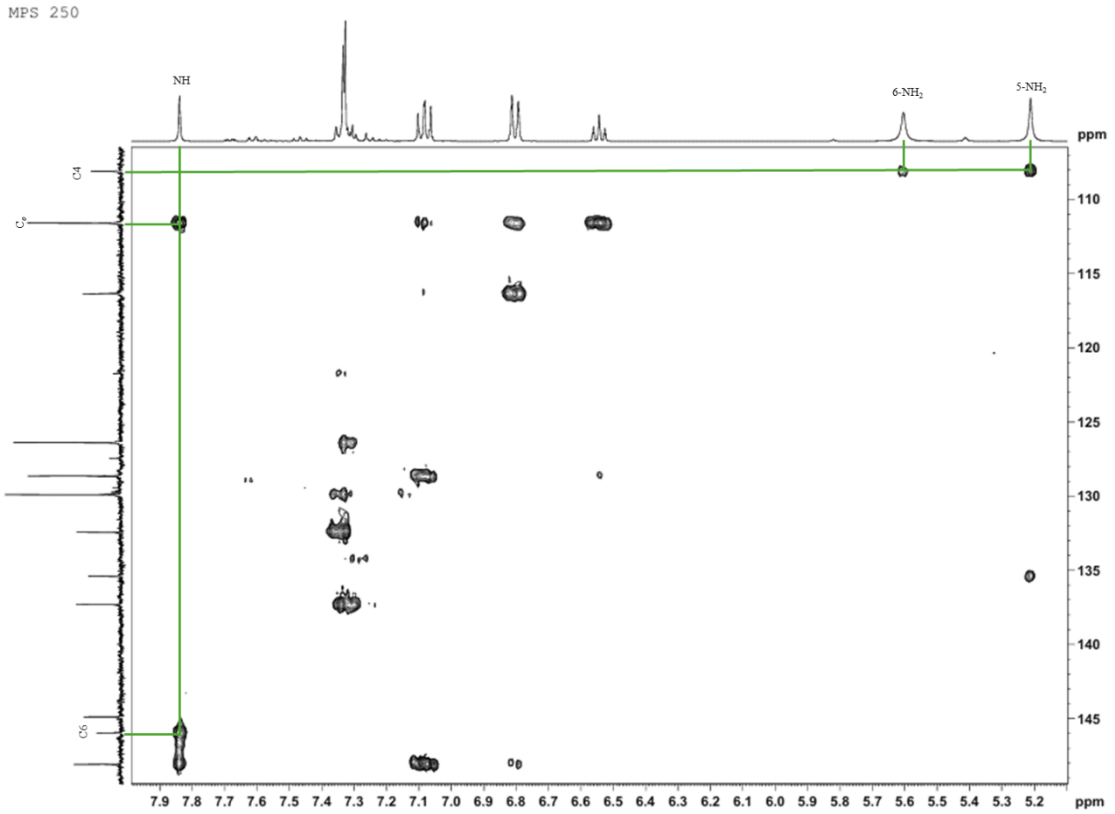

SI-Figure 74 - HMBC spectrum (expansion) of (*Z*)-5-amino-*N*'-phenyl-2-(piperidin-1-yl)-1-(*p*-tolyl)-1*H*-imidazole-4-carbohydrazonamide (**4j_I**).

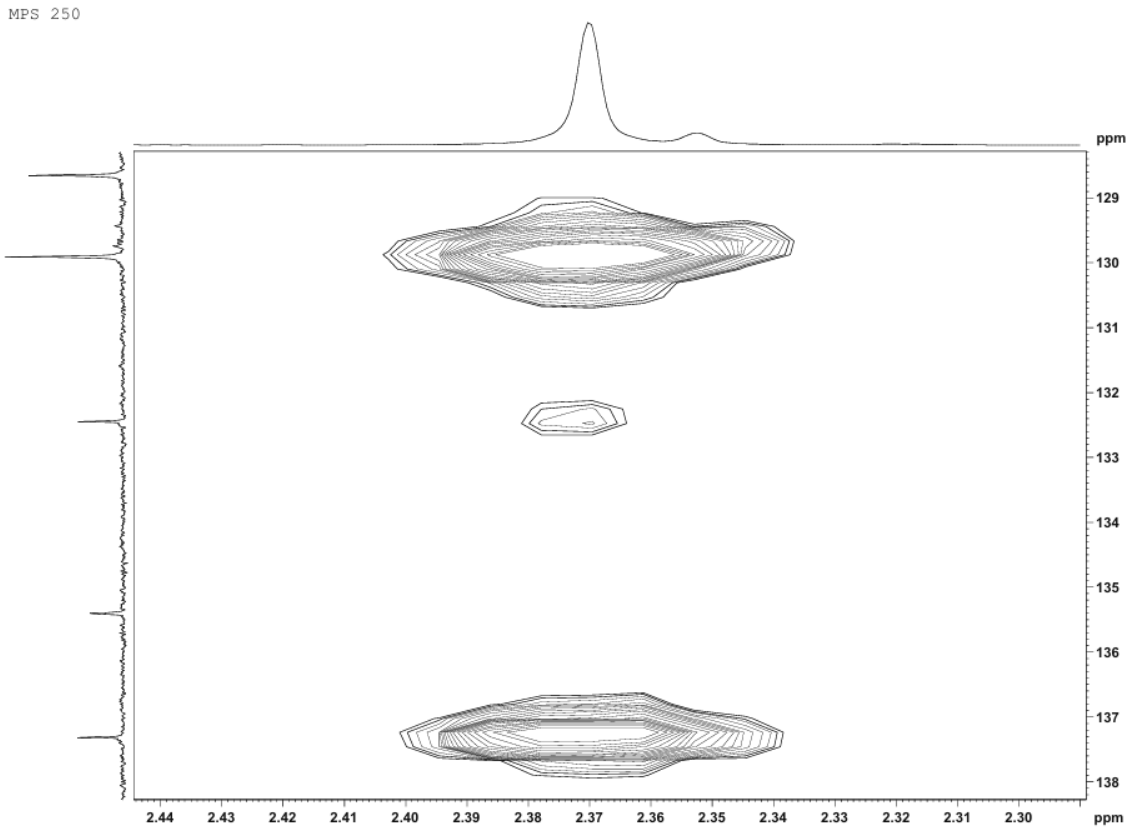

SI-Figure 75 - HMBC spectrum (expansion 2) of (*Z*)-5-amino-*N*'-phenyl-2-(piperidin-1-yl)-1-(*p*-tolyl)-1*H*-imidazole-4-carbohydrazonamide (**4j_I**).

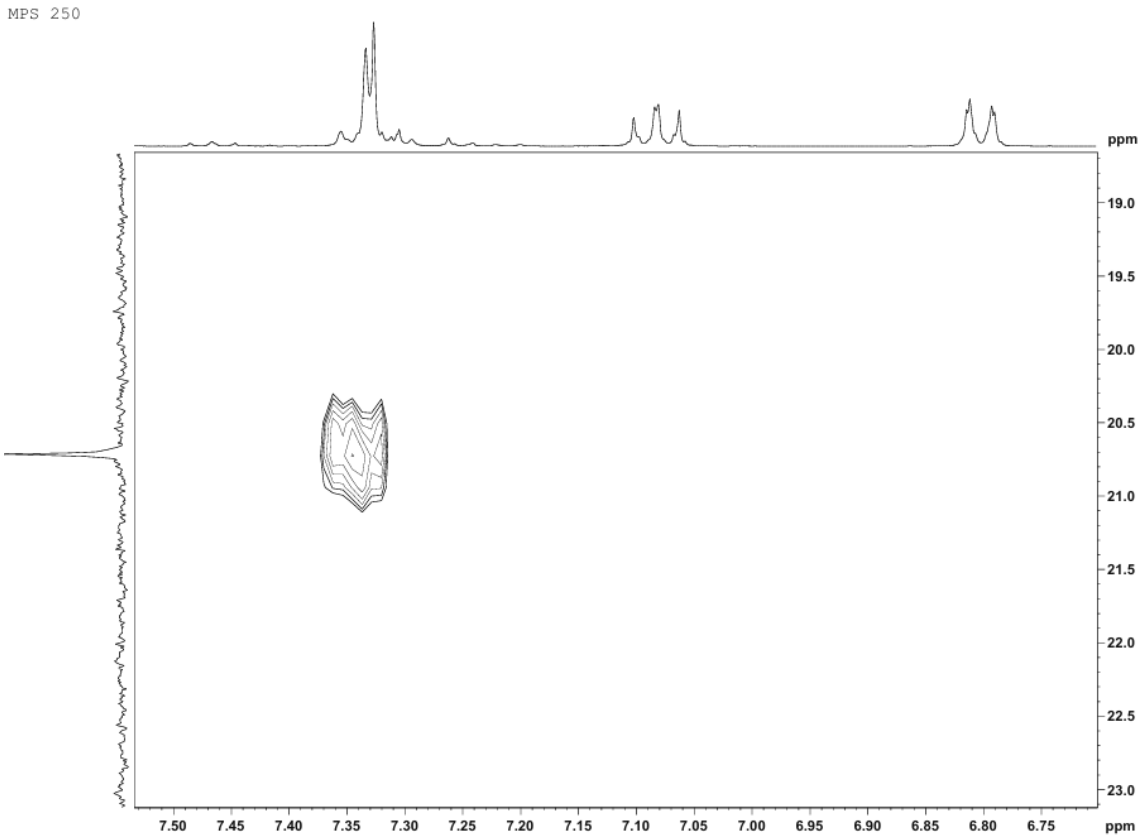

SI-Figure 76 - HMBC spectrum (expansion 3) of (*Z*)-5-amino-*N*'-phenyl-2-(piperidin-1-yl)-1-(*p*-tolyl)-1*H*-imidazole-4-carbohydrazonamide (**4j_I**).

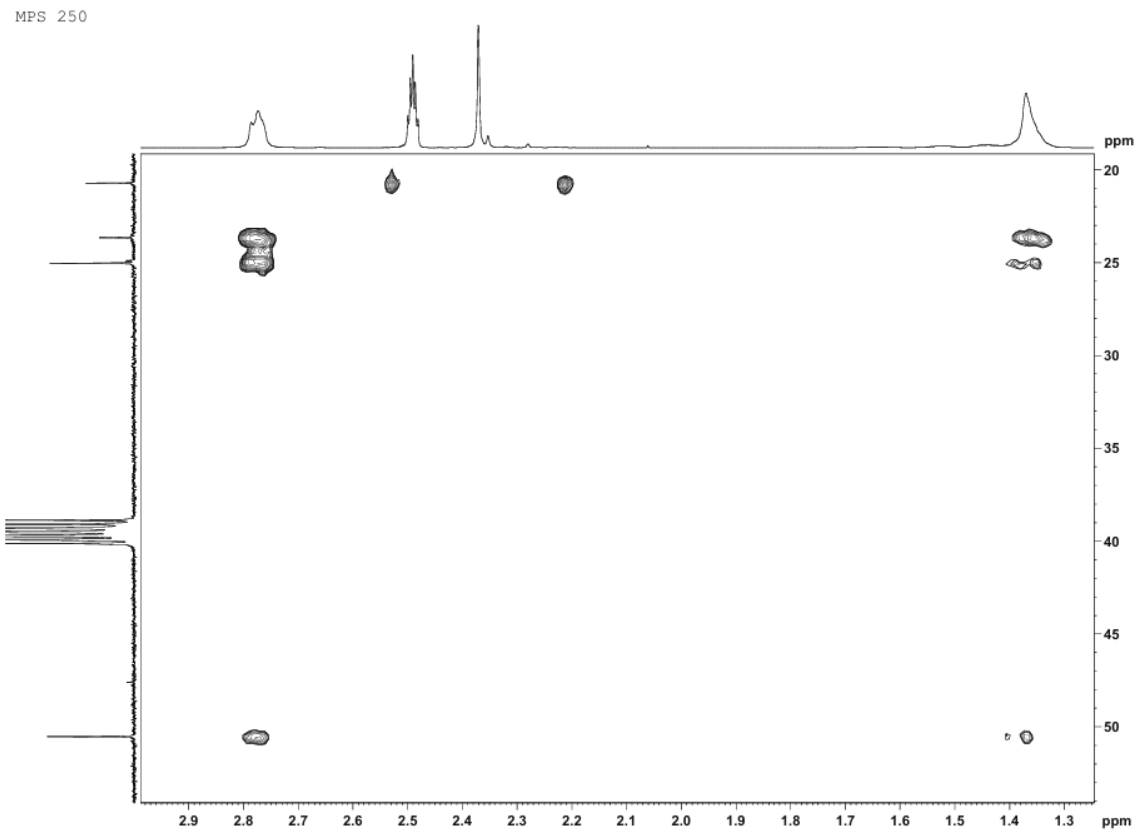

SI-Figure 77 - HMBC spectrum (expansion 4) of (*Z*)-5-amino-*N*'-phenyl-2-(piperidin-1-yl)-1-(*p*-tolyl)-1*H*-imidazole-4-carbohydrazonamide (**4j_I**).

*4.2.4. (4E)-4-(amino(phenyldiazenyl)methylene)-2-(piperidin-1-yl)-N-(p-tolyl)-4H-imidazol-5-amine (**5j**).*

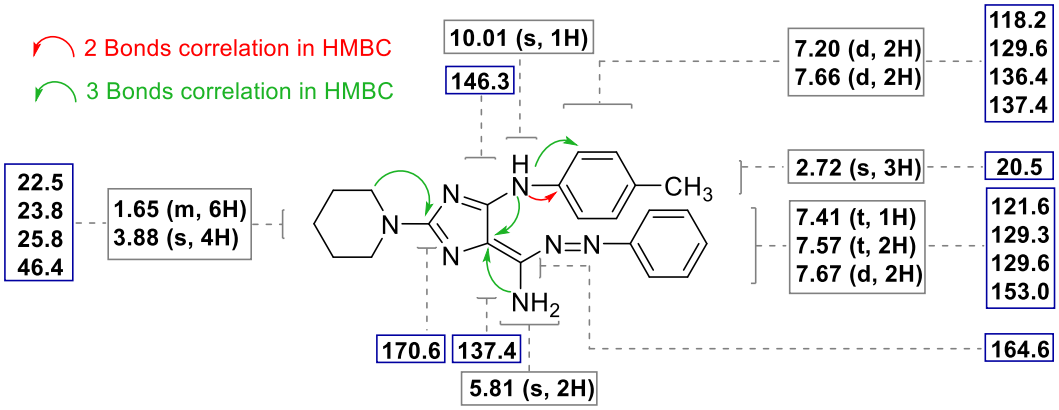

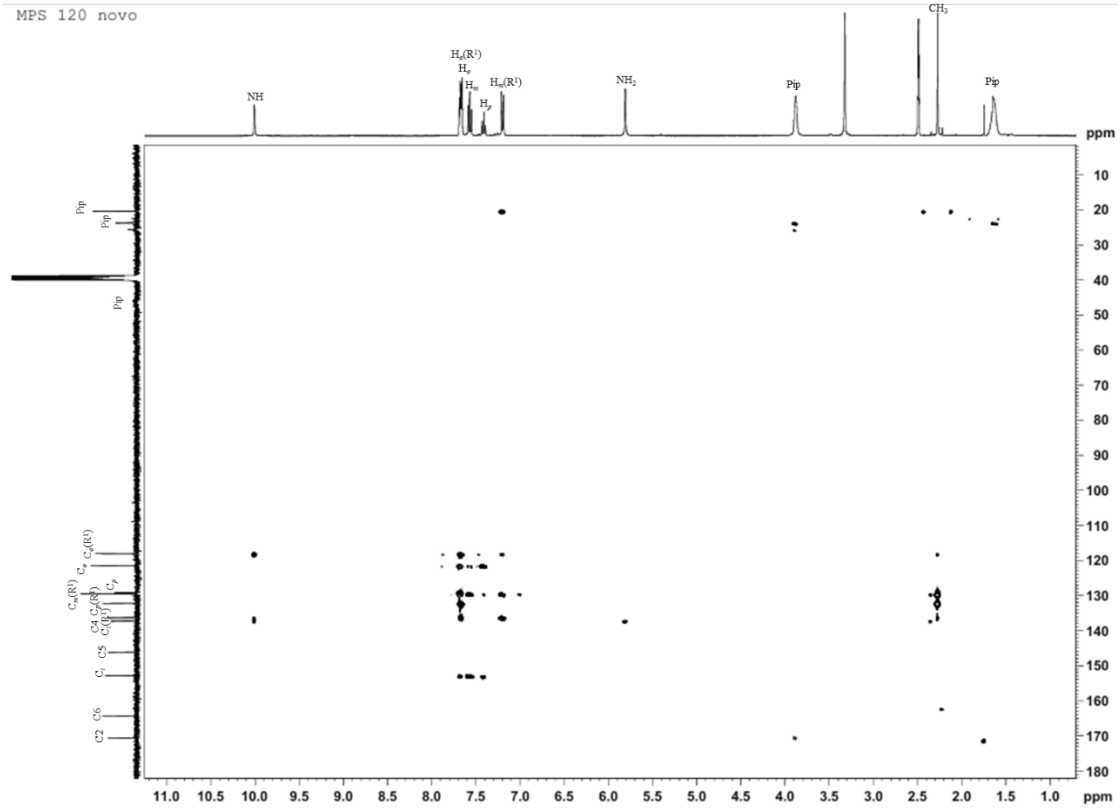

SI-Figure 78 - HMBC spectrum of (4*E*)-4-(amino(phenyldiazenyl)methylene)-2-(piperidin-1-yl)-*N*-(*p*-tolyl)-4*H*-imidazol-5-amine (**5j**).

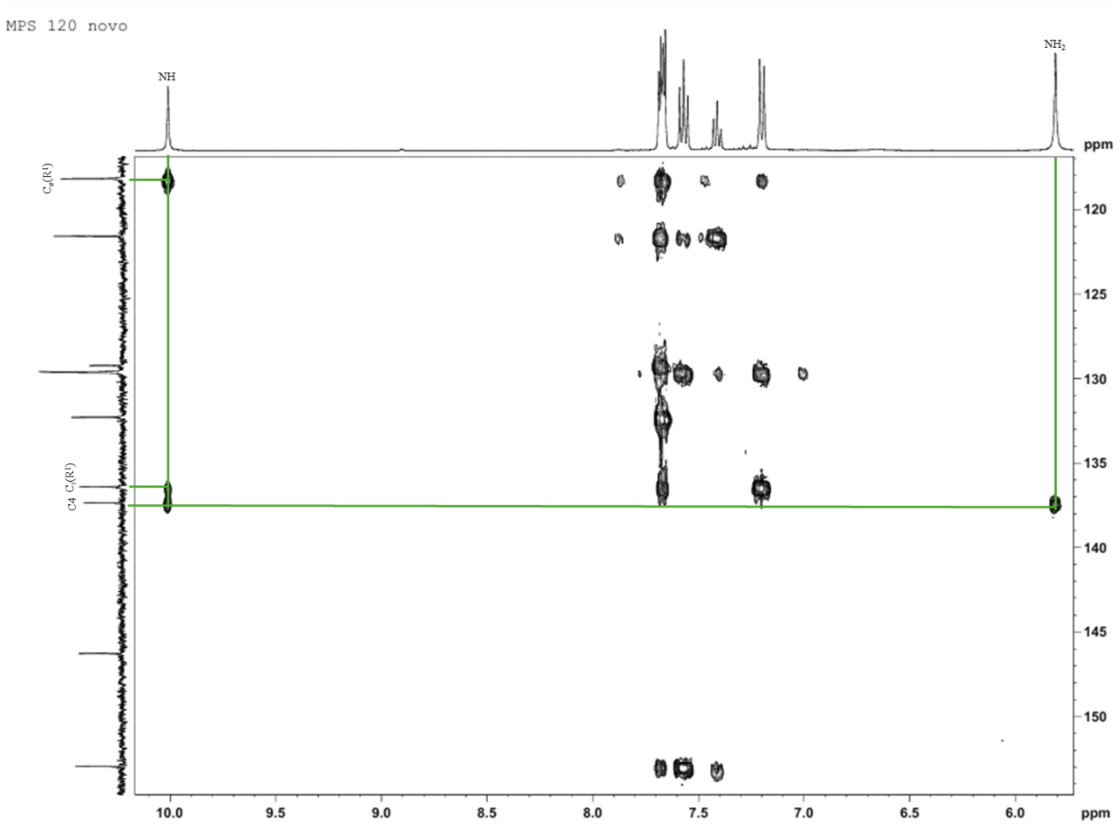

SI-Figure 79 - HMBC spectrum (expansion) of (4*E*)-4-(amino(phenyldiazenyl)methylene)-2-(piperidin-1-yl)-*N*-(*p*-tolyl)-4*H*-imidazol-5-amine (**5j**).

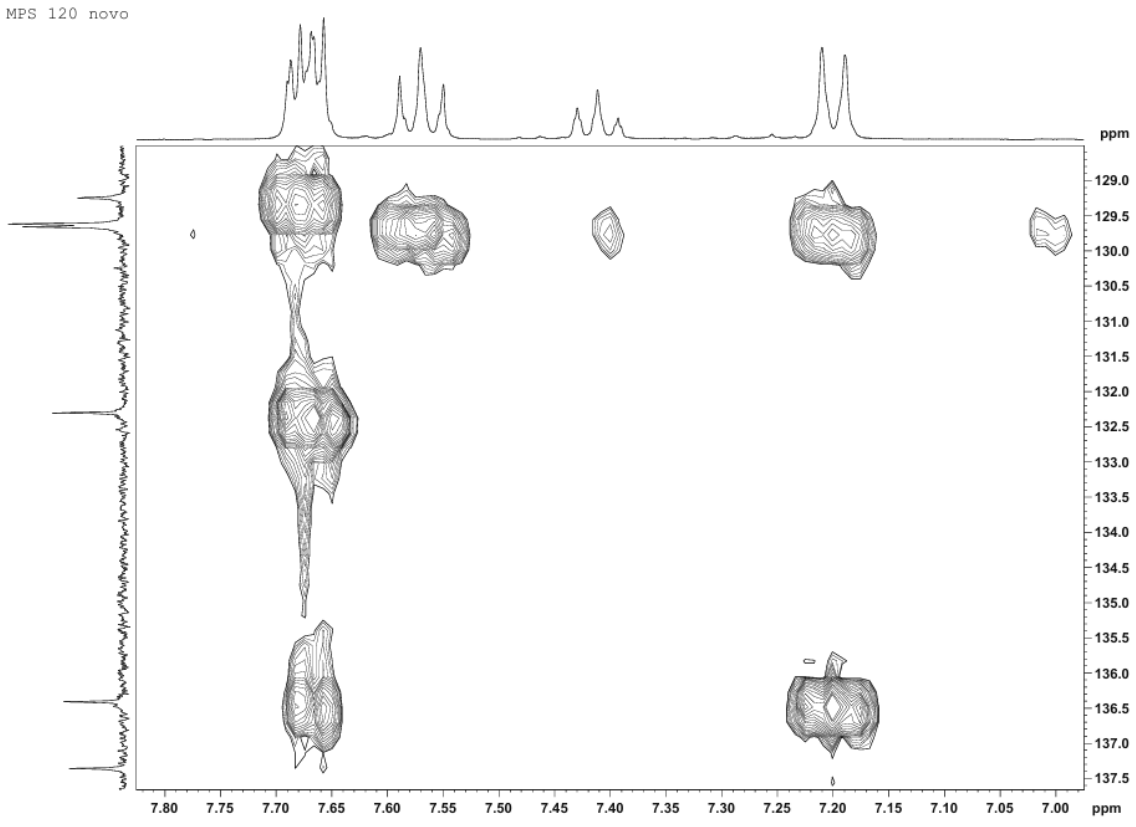

SI-Figure 80 - HMBC spectrum (expansion 2) of (4*E*)-4-(amino(phenyldiazenyl)methylene)-2-(piperidin-1-yl)-*N*-(*p*-tolyl)-4*H*-imidazol-5-amine (**5j**).

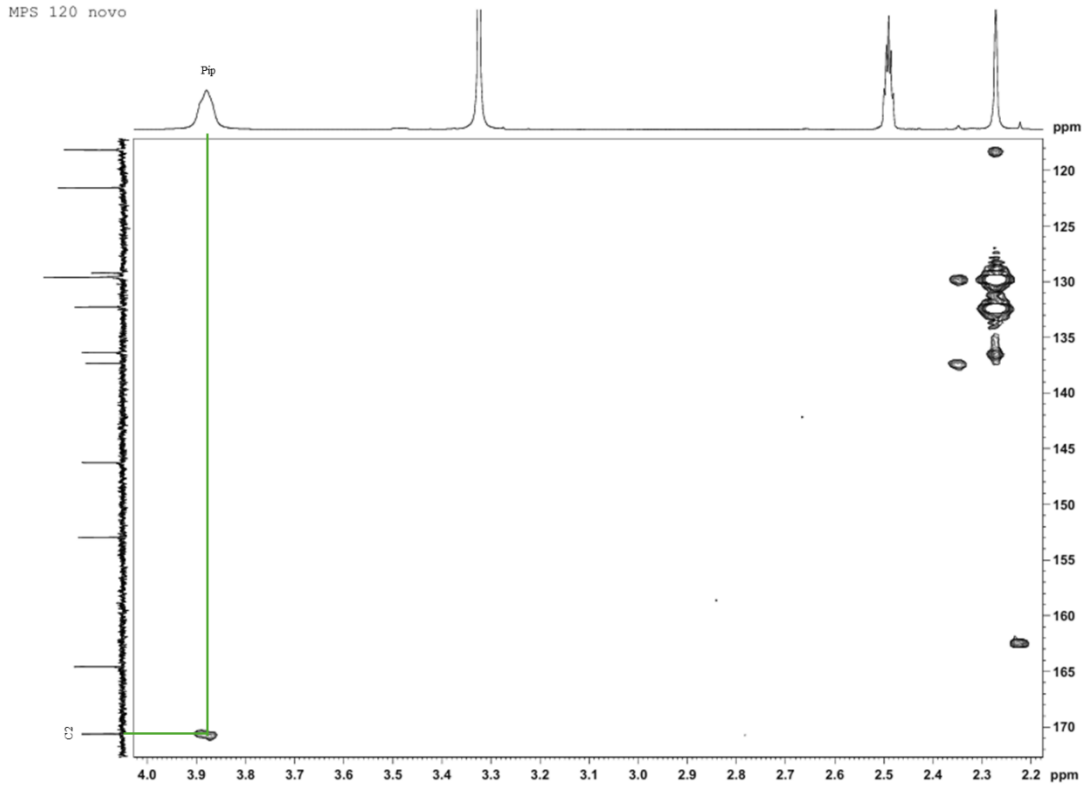

SI-Figure 81 - HMBC spectrum (expansion 3) of (4*E*)-4-(amino(phenyldiazenyl)methylene)-2-(piperidin-1-yl)-*N*-(*p*-tolyl)-4*H*-imidazol-5-amine (**5j**).

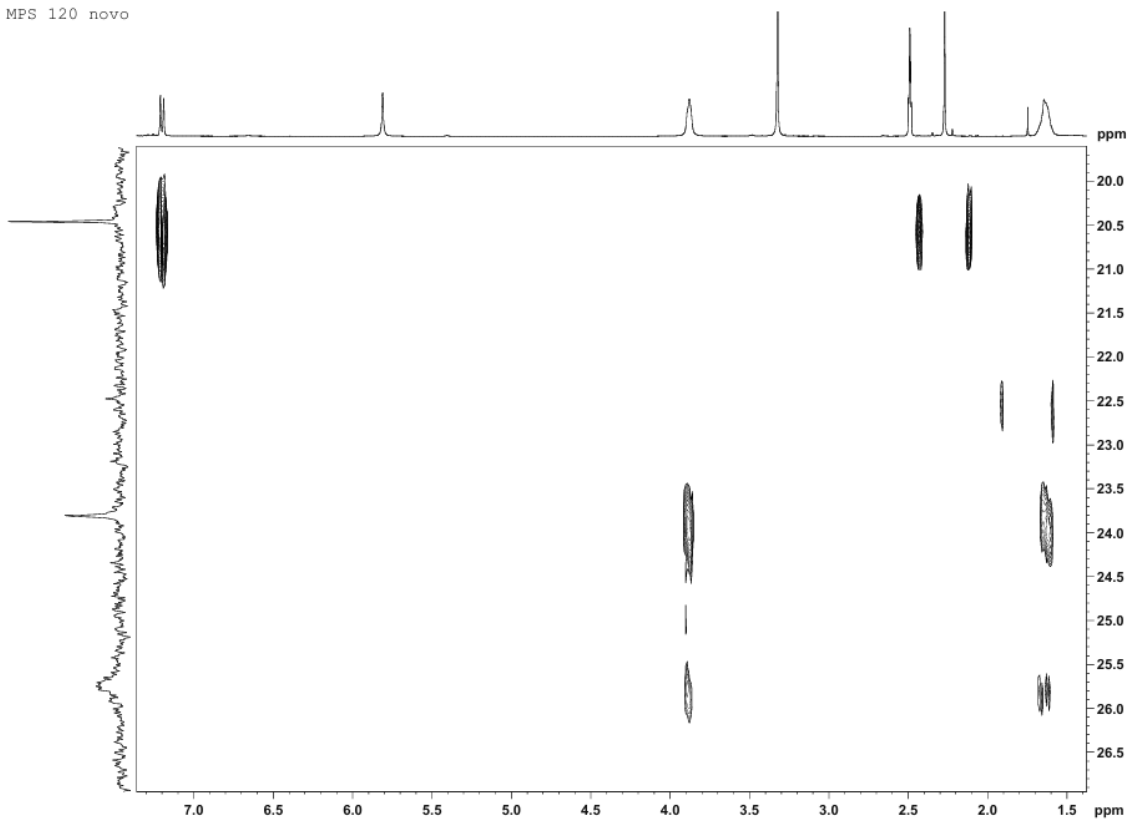

SI-Figure 82 - HMBC spectrum (expansion 4) of (4*E*)-4-(amino(phenyldiazenyl)methylene)-2-(piperidin-1-yl)-*N*-(*p*-tolyl)-4*H*-imidazol-5-amine (**5j**).

5. References

[1] Alves MJ, Booth BL, Proenç MFJRP. Synthesis of 5-amino-4-(cyanoformimidoyl)-1H-imidazole: a reactive intermediate for the synthesis of 6-carbamoyl-1,2-dihydropurines and 6-carbamoylpurines. J Chem Soc, Perkin Trans 1 1990:1705–12. https://doi.org/10.1039/P19900001705.

[2] Ribeiro AI, Gabriel C, Cerqueira F, Maia M, Pinto E, Sousa JC, et al. Synthesis and antimicrobial activity of novel 5-aminoimidazole-4-carboxamidrazones. Bioorg Med Chem Lett 2014;24:4699–702. https://doi.org/10.1016/j.bmcl.2014.08.025.

[3] Ossowski T, Goulart MOF, De Abreu FC, Euzébio A, Sant'ana G, Rogério P, et al. Determination of the pK a Values of some Biologically Active and Inactive Hydroxyquinones. vol. 19. 2008.

[4] Salgado LEV, Vargas-Hernández C. Spectrophotometric Determination of the pKa, Isosbestic Point and Equation of Absorbance vs. pH for a Universal pH Indicator. Am J Anal Chem 2014;05:1290–301. https://doi.org/10.4236/ajac.2014.517135.